



Review

New Advances and Future Possibilities in Forming Technology of Hybrid Metal–Polymer Composites Used in Aerospace Applications

Tomasz Trzepieciński ^{1,*} , Sherwan Mohammed Najm ^{2,3} , Manel Sbayti ⁴, Hedi Belhadjsalah ⁴, Marcin Szipnar ⁵ and Hirpa G. Lemu ⁶

- ¹ Department of Materials Forming and Processing, Rzeszow University of Technology, al. Powst. Warszawy 8, 35-959 Rzeszow, Poland
 - ² Department of Manufacturing Science and Engineering, Budapest University of Technology and Economics, Műgyetemrkp 3, H-1111 Budapest, Hungary; sherwan.mohammed@gpk.bme.hu
 - ³ Kirkuk Technical Institute, Northern Technical University, Kirkuk 41001, Iraq
 - ⁴ Laboratory of Mechanical Engineering (LGM), National Engineering School of Monastir (ENIM), University of Monastir, Av. Ibn El Jazzar, Monastir 5000, Tunisia; manelasbayti@gmail.com (M.S.); hedi.belhadjsalah@enim.rnu.tn (H.B.)
 - ⁵ Doctoral School of Engineering and Technical Sciences, Rzeszow University of Technology, al. Powst. Warszawy 12, 35-959 Rzeszów, Poland; d547@stud.prz.edu.pl
 - ⁶ Department of Mechanical and Structural Engineering, University of Stavanger, N-4036 Stavanger, Norway; hirpa.g.lemu@uis.no
- * Correspondence: tomtr@prz.edu.pl



Citation: Trzepieciński, T.; Najm, S.M.; Sbayti, M.; Belhadjsalah, H.; Szipnar, M.; Lemu, H.G. New Advances and Future Possibilities in Forming Technology of Hybrid Metal–Polymer Composites Used in Aerospace Applications. *J. Compos. Sci.* **2021**, *5*, 217. <https://doi.org/10.3390/jcs5080217>

Academic Editor: Konda Gokuldoss Prashanth

Received: 24 July 2021

Accepted: 11 August 2021

Published: 13 August 2021

Publisher's Note: MDPI stays neutral with regard to jurisdictional claims in published maps and institutional affiliations.



Copyright: © 2021 by the authors. Licensee MDPI, Basel, Switzerland. This article is an open access article distributed under the terms and conditions of the Creative Commons Attribution (CC BY) license (<https://creativecommons.org/licenses/by/4.0/>).

Abstract: Fibre metal laminates, hybrid composite materials built up from interlaced layers of thin metals and fibre reinforced adhesives, are future-proof materials used in the production of passenger aircraft, yachts, sailplanes, racing cars, and sports equipment. The most commercially available fibre–metal laminates are carbon reinforced aluminium laminates, aramid reinforced aluminium laminates, and glass reinforced aluminium laminates. This review emphasises the developing technologies for forming hybrid metal–polymer composites (HMPC). New advances and future possibilities in the forming technology for this group of materials is discussed. A brief classification of the currently available types of FMLs and details of their methods of fabrication are also presented. Particular emphasis was placed on the methods of shaping FMLs using plastic working techniques, i.e., incremental sheet forming, shot peening forming, press brake bending, electro-magnetic forming, hydroforming, and stamping. Current progress and the future directions of research on HMPCs are summarised and presented.

Keywords: die forming; fibre metal laminates; FML; GLARE; hybrid metal-polymer composites; hydroforming; incremental sheet forming; lay-up; stamping

1. Introduction

In recent years, polymer matrix composites reinforced with continuous fibres have become one of the basic and most promising groups of materials in many engineering sectors, especially in the automotive and aerospace industries. Fibre metal laminates (FMLs) were developed due to the limitations of metals, which relate primarily to their large weight, and the limited use of classic composites. These consist of alternating layers of metal and a polymer composite reinforced with fibres [1–3]. The first FMLs were developed in the laboratory in the mid-20th century. Among these, we distinguish two groups. The first group consists of composites based on aluminium, while the second group consists of composites in which other metals are used, such as magnesium [4–6], titanium [7,8], or steel [9–11]. The most commercially available FMLs are glass reinforced aluminium laminates (GLARE), aramid reinforced aluminium laminate (ARALL), and

carbon reinforced aluminium laminate (CARALL). The first generation FML, ARALL, was developed in 1978 at Delft University of Technology [12]. There are four grades of ARALL composites, differing mainly in the grade of the base material (ARALL: 1-7075-T6; 2-2024-T3; 3-7075-T76; 4-2024-T8). ARALLs have not been widely used due to their low strength and durability on the metal–composite interface, low strength of the fibre–matrix connection, and high production costs [13–15]. CARALL is a laminate made of layers of a polymer composite reinforced with carbon fibres preimpregnated with epoxy resin and layers of aluminium [16–18]. CARALL exhibits good fatigue properties under high cycle loading [19]. This property of FMLs is one of the main concerns for aerospace applications, especially during the service life of aircraft structures [20]. GLARE laminates consist of composite layers reinforced with high strength glass fibres (GFs) in an epoxy resin matrix and metal layers made of 2024-T3 aluminium alloy (GLARE 2 through GLARE 6) and 7475-T761 (Glare 1) [21,22]. The industrially produced varieties of GLARE differ in the number of composite layers and the angular orientation of the reinforcing fibres [23]. FMLs are widely used in aviation. The Boeing 787 was the first commercial aircraft to be 80% constructed of composites by volume [24,25]. Each Boeing 787 aircraft contains approximately 32,000 kg of carbon fibre reinforced polymer (CFRP) composites. Now, each A380 contains 440 m² of FMLs in vertical stabiliser leading edges and fuselage panels [26].

The Boeing 787, Bombardier C-Series, and Airbus A350 aircraft are fabricated with FRP composites with 50%, 47%, and 53% by weight of composites, respectively [24,27,28]. In the aircraft industry, FMLs are often used in upper fuselage skin panel structures, and CFRPs are used in the aircraft wing boxes, wing panels, and stabilisers [29]. Drones and unmanned aerial vehicles (UAVs) are currently being fabricated using fibre reinforced polymer (FRP) composites [30,31]. It is clear from Figure 1 that the importance of composite materials in passenger aviation is increasing exponentially.

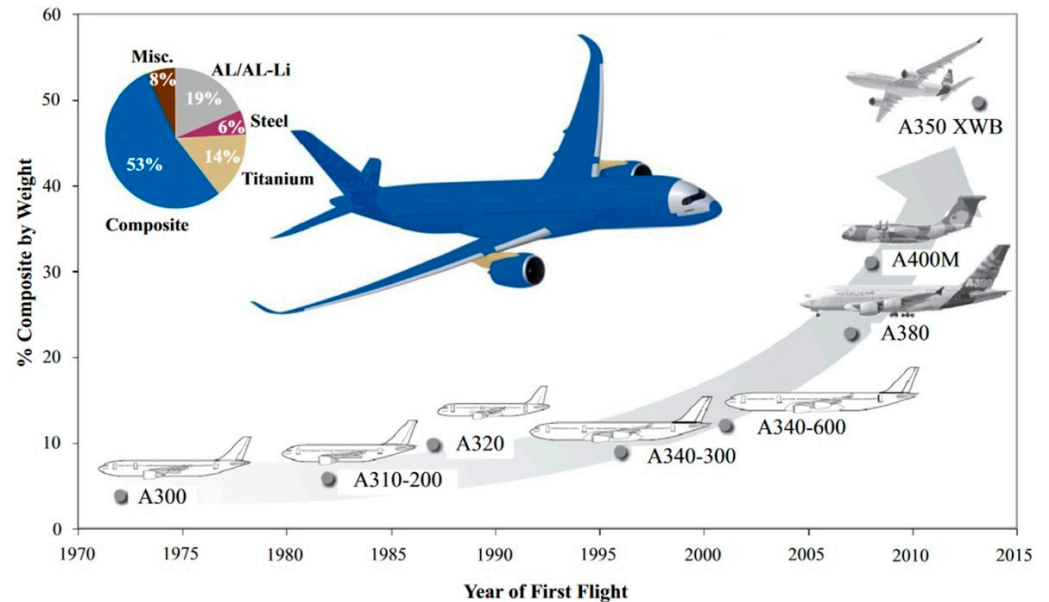


Figure 1. Trends in the use of composite materials in Airbus aircraft (reprinted with permission from [32]; copyright© 2021, Springer International Publishing AG, part of Springer Nature).

The properties of FMLs are clearly more desirable than those of the constituent elements. By using various combinations and numbers of metal layers as well as fibre reinforced polymer composites, the properties of FMLs can be controlled to give a practically unlimited range. FMLs exhibit very high strength in relation to their weight [33–35]. These properties derive from the properties of the individual components and depend on the properties and orientation of the reinforcing fibres, the kind of metal layer and its thickness [36–38]. The orientation of the fibres in relation to the successive layers of the

FML determines the anisotropy or isotropy of the resultant composite [39,40]. Fibres used for their production can be continuous or discontinuous (staple fibres, whiskers) [41,42]. Numerous products made of single fibres, such as fabrics, mats, rovings, or preimpregnates [43,44], can also be used as reinforcement.

The FML production process uses various production methods, which depend mainly on the type of matrix (thermosetting or thermoplastic) due to significant differences in the properties of the polymers used [45,46]. The most common methods of manufacturing composites using thermosetting polymers include hand lay-up, forming with the use of a flexible vacuum bag or autoclave, infusion methods, low and high pressure pressing, and automated fibre placement (AFP). Composite materials consisting of thermoplastics are mainly produced by the method of “hot” pressuring in presses using chilled moulds, AFP, and methods of continuous pultrusion [47]. In terms of the mechanical strength of FMLs, the most advantageous method of producing FMLs is the autoclave method, which uses the simultaneous action of pressure, vacuum, and temperature [15,48].

The main advantage of autoclave technology is the obtaining of a laminate of very high quality in terms of the degree of porosity and metal–composite adhesion. The adhesive bonding of metal and composite layers and hardening of the preimpregnate take place in the autoclave process; however, this method requires a long cycle time and complex tool set. Therefore, directly formed FMLs are gaining more attention. The most common FML forming methods include press brake bending, lay-up technique, shot peening forming, incremental sheet forming, and die forming (stamping, hydroforming, and electromagnetic forming).

The research work currently being conducted is focused on new types of metal–fibre laminates for specific applications, such as use underwater [49,50], and techniques for their production [51,52]. The development priorities of FMLs in industrial use are titanium/CFRP hybrid laminates [53] and composites with a thermoplastic polyether ether ketone (PEEK) matrix reinforced with carbon fibres [54,55]. Currently, there is an intensification of research on the use of thermoplastic preimpregnates in the production of FMLs [56,57] due to their high resistance to dynamic loads [58,59].

In order to reduce the environmental impact without compromising the strength requirements, there is a growing interest in the production of FMLs reinforced with carbon, sugar palm, and flax fibres [60]. The environmental concerns lead to the development of FMLs containing natural fibre composites [61,62]. Hussain et al. [63] developed novel 3D jute reinforced natural fibre aluminium laminates (JuRALs). Mohammed et al. [64] tested compression, tensile, and flexural strengths of FMLs made from natural/synthetic fibre composites. The compressive and tensile strengths obtained showed that the carbon and flax fibre reinforced aluminium alloy (CAFRALL) composite had superior properties over the carbon and kenaf fibre reinforced aluminium alloy (CAKRALL) composite. It was also found that both composites can be used as materials in the fire-designated zone. At the same time, investigations have been conducted on various nanofillers, including clay nanoparticles, graphene nanoplatelets, oxide nanoparticles, and carbon nanotubes, to improve the properties of FMLs [65–67].

Due to the growing interest in hybrid metal–polymer composites (HMPC) and the emergence of a rapidly growing number of publications in this field, this paper presents a systematic review according to the PRISMA guidelines [68] on the new advances in and future potential of forming technology for HMPCs. A brief classification of the currently available types of FMLs and details of their methods of fabrication are also presented, with particular emphasis on research carried out in recent years. Review articles found in the literature are mainly devoted to production methods and methods of surface preparation of materials intended for the production of FMLs. Meanwhile, this article places particular emphasis on the methods of forming FMLs using plastic working, incremental sheet forming, shot peening forming, press brake bending, electromagnetic forming, hydroforming, and stamping. The article ends with a summary and conclusions.

2. Classification of FMLs

Over the past decade, most industrial demands, especially in the aircraft and automotive industries, have emphasised the use of high-performance, high strength, and lightweight structures. The hybrid material concept has been suggested to meet these kinds of demands and to overcome the disadvantages of lightweight materials. This has spurred the development of different FMLs. Fibre–metal laminates can be considered a family of hybrid materials [69] that can exhibit the advantages of both metals and composites. Ding et al. [52] presented the development of FMLs chronologically, starting with the metal bonding technology in the 1940s and ending with a new approach utilised by the LEIKA project in 2010. ALCOA and AKZO have produced the first generation of FMLs [70]. In 1971 and 1972, fibre–metal laminates were presented by embedding laminates of titanium and layers of fibres as part of a performance study in the space department of Fokker, a contractor to NASA, together with a department in Schliekelmann and in the Philips laboratory [71]. In 1978, the first tests were carried out on carbon and aramid fibre reinforced laminates with flight simulation [72]. Later, the demand was for FMLs with high strength characteristics together with much stiffer laminates, and CARALL was investigated and developed from ARALL [73]. In the 1980s, ARALL was developed by Delft University and used as a panel in the lower skin of the Fokker F-27 wing structure. ARALL is made from layers of aluminium and aramid fibre reinforced epoxy [74,75]. GLARE is a unique material for aircraft applications [76] and, nowadays, is mostly used for the fuselage structure of modern aircraft. GLARE was also developed at Delft in 1987, and the first tests were on the Airbus A380 super-jumbo on 16th May 2001 [71]. To find promising properties and applications, different FMLs have been investigated and developed since the 1990s using different materials and fibres. There are two main classical ways of bonding the layers of metals with fibre reinforced laminate, which are mechanical and adhesive, and the commercially available types of FML that have been most extensively used are ARALL, GLARE, and CARALL based on aramid fibres, high strength glass fibres, and carbon fibres, respectively [17,77]. A review paper has been presented by Sinke [78], which describes the manufacturing principles of FMLs. Overall, in view of all that has been mentioned in the brief literature survey presented here, this explains that FMLs are made of different metals as base materials and reinforced by different fibres. Moreover, FMLs can be fabricated using an alternating laminate of thin metal sheets and thin composite layers [79]. Therefore, the classification of FMLs is important and is needed for the performance requirements and manufacturing considerations of different applications. FMLs may be classified based on the structural arrangements of the different layers or by the materials of which it is composed. In terms of structural arrangements, FMLs may be divided into asymmetric, sandwich, and multi-stack [52]. As an alternative to the classification based on the structural arrangement, the constituent materials can be used as a more accepted classification of FMLs. Constituent materials can, in theory, be used and mixed freely to fabricate FMLs [80]. To this end, Table 1 lists the FMLs based on their constituents, and the reader should bear in mind that the classification does not consider the different treatment of the materials.

Table 1. Classifications of fibre–metal laminates.

Base Material	Alloy	Fibre Reinforced	References
Aluminum	Al 2024	glass fibre reinforced/epoxy	[41,48,81–100]
		carbon fibre reinforced/epoxy	[91,94,101–103]
		glass fibre reinforced polypropylene (GFRP)	[104–107]
		polypropylene fibre reinforced polypropylene (PP/PP)	[108]
		thermoplastic nylon LFT with glass fibre reinforced	[109]
		Nanoclay reinforced polypropylene and glass fibre	[110]
		self-reinforced polypropylene (SRPP)	[106,111,112]
Al 8090	Al 7075	glass fibre reinforced/epoxy	[113]
		aramid fibre reinforced/epoxy	[114]
			[115]

Table 1. Cont.

Base Material	Alloy	Fibre Reinforced	References
	Al 1100	aramid fibre reinforced polypropylene	[116]
	Al 5052	carbon fibre reinforced/epoxy	[117,118]
	Al 5005	self-reinforced polypropylene (SRPP)	[119,120]
	Al 6061	glass fibre reinforced/epoxy	[121]
	commercial aluminium	carbon fibre reinforced/epoxy	[122]
	Al 7475		[123]
	Al 5083		[114,124]
	Al 6082		[125]
	Al 1060		[126]
	Al 1050	Nanoclay reinforced polypropylene and glass fibre	[127]
	LY12M	glass fibre reinforced/J272	[130,131]
	Al 5182	carbon fibre reinforced/J272	[132]
		glass fibre reinforced (PA6)	[133]
Aluminium–lithium	Aluminium–lithium		[134]
	V-1469	glass fibre reinforced/epoxy	[135–138]
	2060		[139]
			[140]
Magnesium	AZ31 alloy	carbon fibre reinforced/epoxy	[5,141]
		glass fibre reinforced polypropylene (GFPP)	[5]
		glass fibre reinforced/epoxy	[6,100,142,143]
	Magnesium	self-reinforced polypropylene (SRPP)	[111]
		silicon carbide fibre reinforced	[144]
Titanium	Ti 15-3-3-3	carbon fibre reinforced polyetheretherketone (PEEK)	[145]
	β -titanium alloy	glass fibre reinforced PEKK (GF/PEEK)	[146]
	grade-2 alloy	glass fibre reinforced polymer (GFRP)	[147]
	TA2	carbon fibre reinforced/epoxy	[33,148]
			[149]
	Ti-6Al-4V	glass fibre reinforced/epoxy	[7,150]
		graphite fibre reinforced	[151]
		graphite-fibre/epoxy and boron fibre/aluminum	[152]
		thermoplastic fibre reinforced polymer	[153]
Steel	TS275	glass fibre reinforced (PA6)	[134]
	galvanized steel		[154]
	galvanized steel	glass fibre reinforced polypropylene (GFPP)	[9]
	AISI 304	glass fibre reinforced/epoxy	[155]
	steel		[156]
	galvanized steel	carbon fibre reinforced/epoxy	[157–159]
	DC03		[160]
	steel	self-reinforced polypropylene (SRPP)	[161]
	HC220Y	carbon fibre reinforced (PA6)	[162]
	HC260LAD + Z100	glass or carbon fibre reinforced (PA6)	[163,164]
			[165]

Figures 2 and 3 can be derived from Table 1, showing that aluminium alloy is the most frequently used base material in the fabrication of FMLs, with a percentage use of 62%, as indicated in Figure 2. Figure 3 shows that glass is the reinforcement most commonly used in FMLs, with a percentage use of 36.89%.

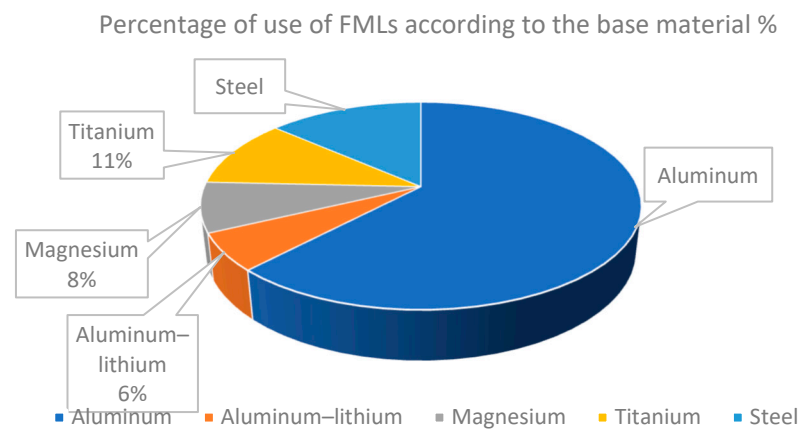


Figure 2. FMLs according to base material.

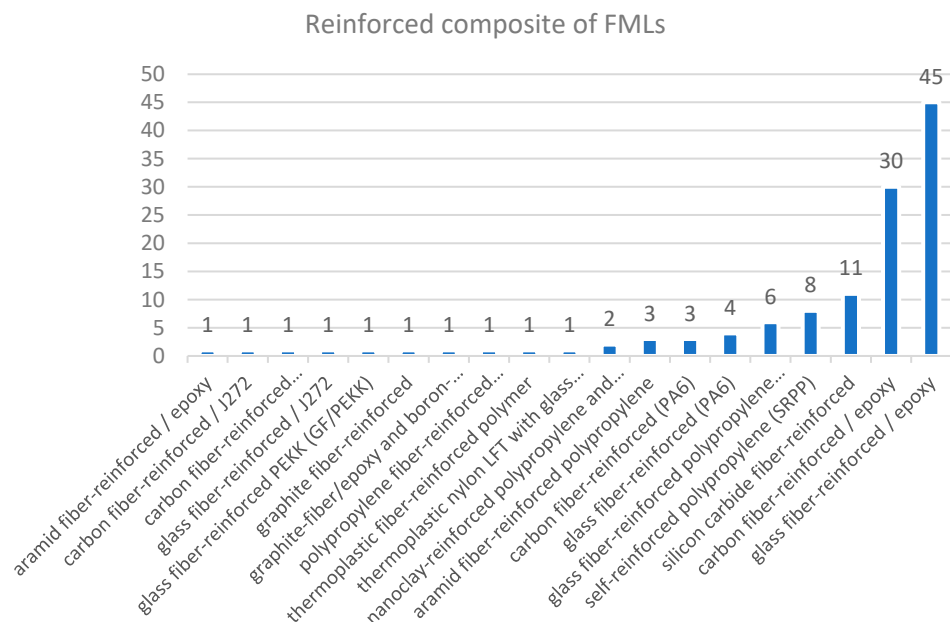


Figure 3. Reinforced composite used in FMLs.

3. Fabrication of FMLs

The procedure for preparing the surface of the layers of metal composites is similar to the procedure used for the adhesive bonding of materials. The surface preparation should help to obtain the strongest possible adhesive bonds. To meet this condition, it is necessary, [166–168], to remove impurities on the surface of the joined surfaces to obtain the appropriate surface roughness of the joined materials and to obtain the proper surface energy of the treated surface. There are three basic methods of surface treatment [17,169–171]:

- applying an adhesion promoter;
- mechanical treatment (e.g., grinding and sandblasting);
- the use of chemical or electrochemical treatment (e.g., etching with hydrofluoric acid and dry surface treatments).

Among the basic treatment methods, in addition to the methods mentioned above, there are special methods such as corona discharge, plasma treatment, laser treatment, flame treatment, electromagnetic radiation, and ozone oxidation. Examples of surface treatment methods used during the production of selected FML are listed in Table 2. All aluminium alloy sheets were initially degreased prior to further steps in the surface pretreatment.

Table 2. Review of surface treatments in the manufacture of fibre metal laminates.

Metal	Matrix	Metal Surface Treatment	Reference
aluminium (grade not specified)	self-reinforcing polypropylene	5% solution of sodium hydroxide for 5 min.	[172]
2024-T3 aluminium alloy	epoxy	etching with chromic–sulphuric acid	[173]
2024-T3 aluminium alloy	epoxy	anodising with phosphoric acid	[174]
2024-T3 aluminium alloy	epoxy	etching with chromic acid followed by anodising with phosphoric acid	[175]
35K cold-drawn steel	epoxy	5% etching solution for 10 min.	[176]
DP800 hot-dip galvanised steel	PA6	galvannealing	[154]
Ti-6Al-4V titanium alloy	epoxy	grit blasting	[177]
Ti-6Al-4V titanium alloy	polyimide	surface treatment with Pasa-Jell 107	[151]
β-titanium alloy	woven S-glass fibre reinforced PEKK	laser treatment	[146]
Ti-15–3–3–3 alloy	polyetheroimid	wiping with ethanol	[178]
Pure titanium TA2	polyimide	sand blasting	[179]
AZ31 magnesium alloy	glass fibre reinforced polypropylene	abrading with a 1200 sandpaper and cleaning with acetone	[5]
AZ31 magnesium alloy	epoxy	grit blasting	[180,181]
magnesium	epoxy	abrading and solvent wipe treatment	[182]

Mechanical treatment involves abrasive scrubbing of the substrate surface with sandpaper to introduce physico-chemical changes that modify the surface topography and yield a wettable surface [183]. The most commonly used chemical treatments are based on etching with a solution of potassium dichromate and sulphurous acid [184,185]. Acid etching is typically an intermediate step in production between degreasing, alkaline cleaning, and electrochemical treatment [186]. Three chemical etching methods have become the most popular: those using sulpho-ferric acid [17], Forest Product Laboratory [187], and chromic–sulphuric acid [17,188].

Electrochemical degreasing is one of the most effective methods of cleaning metal surfaces, but it requires strict adherence to the composition of the solutions used and strict operating parameters. The degreasing process is intensified by the emission of hydrogen (cathode cycle) or oxygen (anode cycle). It consists of emulsifying fats and oils with the help of gas bubbles emitted in the electrolysis process: hydrogen at the cathode and oxygen at the anode. Cathodic degreasing is more effective than anodic degreasing due to the evolution of twice as much gas. Too low a current density does not ensure complete degreasing, and too high a current density has a negative effect on the quality of the substrate. Anodic oxidation in chromic acid anodising (CAA) or phosphoric acid anodising (PAA) solutions is the preferred stabilising treatment for the structural adhesive bonding of high strength aluminium alloys in critical applications such as aircraft components [17]. Although the European aviation industry uses chromic acid anodising as its preferred stabilisation treatment, Boeing invented phosphoric acid anodising, which led to better joint durability [17,184,189].

Silane-based coatings are environmentally friendly multi-metal precoat that can be used on various metals, e.g., aluminium and its alloys [190]. Due to their environmental compatibility, these products can be used as substitutes for traditional pretreatment methods. Coupling agent treatment creates a permanent covalent bond between silane and the metal (oxide), which creates a layer with intermediate properties between the metal and the polymer [191].

To eliminate the use of non-ecological chemical treatment for the surface preparation of aluminium alloy sheets, dry surface treatments were developed: plasma-sprayed coating [192,193], excimer laser texturing [194,195], and ion beam enhanced deposition [188,196,197]. The plasma method consists of subjecting the outer layer of the modified material to the action of low temperature plasma, which is created because of high-frequency partial discharges taking place in a vacuum chamber. A review of the methods for treating metallic surfaces for the production of FMLs can be found in the papers by Sinmazçelik et al. [17] and Molitor et al. [198].

After the surface of the sheet and the fibre for the reinforced plastics have been prepared, they are stacked alternately, with the metal layers constituting the outer elements of the composite. Instead of producing FML from the metallic sheets and prepregs, metallic sheets can be combined with alternate layers of polymer films and fibres [199]. The suitably stacked materials are then bonded under pressure and temperature. In addition to conventional autoclave fabrication and hot press methods, out-of-autoclave methods are being developed [60,200,201]. Thermal treatment during the production of composites introduces residual stresses in the structure of the composite, which reduce the fatigue strength of FML components.

FMLs have a low density and a low rate of crack propagation in the layers of such hybrid materials. Additionally, FMLs, when compared with metallic materials, have increased:

- fatigue strength [99,176,202,203],
- fire resistance [204–206],
- resistance to electric (atmospheric) discharge [207],
- impact strength [114,208,209], and
- corrosion resistance [204,210,211].

Compared to polymer composites, FMLs show better strength, impact strength, and fracture toughness [46,64,212]. One of the major disadvantageous properties of FMLs is their susceptibility to delamination under unfavourable loads.

4. Press-Brake Bending

Single curvature FML components are formed by press-brake bending (PBB) in which a plastic deformation is created by clamping the material between the punch and the die (Figure 4a). This process takes place on a classic press brake and the degree of deformation of the material is limited by the properties of the composite, primarily by the low failure strain of the fibres of the matrix layer. Basic elements formed using PBB include single curvature sections (Figure 4b). Thin FMLs, where the distance of the deformed fibres from the neutral axis is small, do not cause problems during bending [213]. The most favourable bending conditions are for composites with 2/1 lay-up, in which the fibres are located near to the neutral axis. The basic parameter determining the possible degree of deformation of the composite sheet is the minimum bending radius, which is a function of the failure strain of the fibres [213]:

$$r_{min} \cong \frac{t}{2\epsilon} \quad (1)$$

where ϵ is the failure strain of the fibres and t is the distance of the outermost fibre layers to the neutral line.

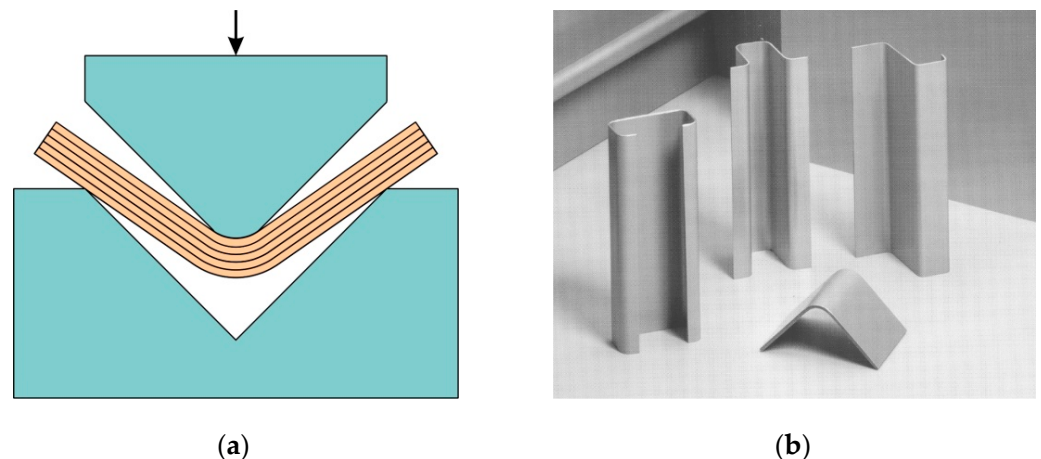


Figure 4. (a) schematic diagram of PBB and (b) examples of FML components produced by PBB (reproduced with permission from [213]; copyright© 2021 Woodhead Publishing Limited).

In a similar manner to the bending of metallic sheets, the minimum bending radius increases exponentially as the thickness of the composite increases. Apart from the failure strain of the fibres, the delamination of boundary layers outside the bending zone may occur when bending laminates with a thickness greater than approximately 1.5 mm. The greater the thickness, the more dominant is delamination as the destruction mechanism of FMLs. In general, the greater the thickness of the composite, the smaller the minimum bending radius [52,214]. Moreover, when the bending direction is parallel to the fibre direction, it enables smaller radius bending for GLARE [215].

The bending behaviour of CFRP and GFRP panels fabricated using the lay-up technique has been studied by Rajkumar et al. [202]. It was found that the interlaminar shear strength (ILSS), computed using Equation (2), decreased as strain rate increased.

$$ILSS \cong \frac{3F_{max}}{4wt} \quad (2)$$

where F_{max} is the maximum load, t is the FML thickness, and w is the specimen width.

Placing the carbon fibre layer exterior to the glass fibres will enhance the mechanical strength of FMLs. The good bonding strength between aluminium and CFRP leads to crack arresting in the flexural strength of 3/2 lay-up with stacking configuration Al/C/C/C/Al/C/C/C/Al (C—one layer of carbon fibre, Al—6061 aluminium alloy) [202].

The mechanical properties of composite materials depend on the adhesion between the fibre and the matrix and on the strength of the fibres. The basic strength tests for determining the adhesion of composite layers include inter alia and bending tests. The damage tolerance of the 2024-T3-based GLAREs and an aluminium roll-bonded laminate in the three-point bend test has been investigated by Cepeda-Jimiénez [103]. During the bend tests (Figure 5a), different fracture mechanisms of laminates were activated that depend on their interfaces and the constituent materials. There was clear debonding between fibres and the resin matrix in GLARE after bend testing (Figure 5b). Optical macrograph analysis of GLARE laminate has shown several delaminations and extensive plastic deformation of aluminium alloy layers.

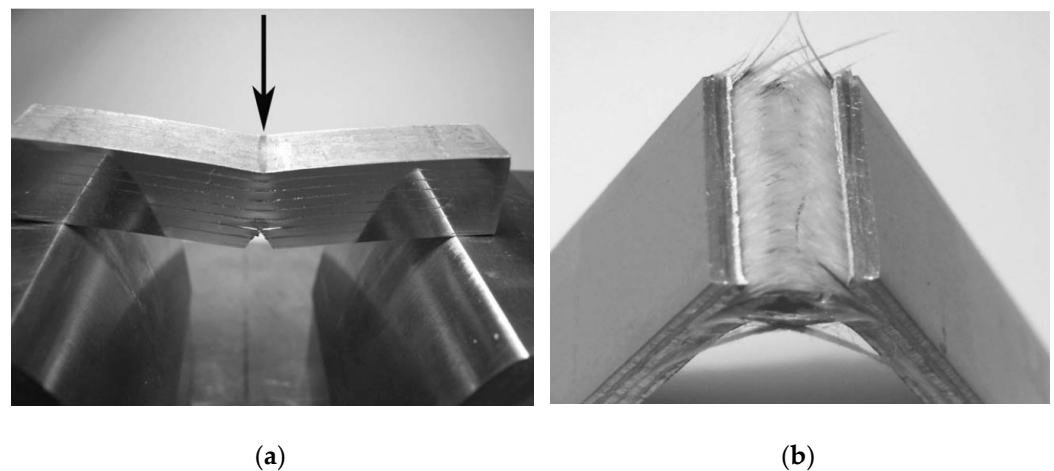


Figure 5. (a) Schematic view of test specimen and (b) fracture of GLARE specimen (reproduced with permission from [103]; copyright © 2021 Elsevier Ltd.).

Isiktas and Taskin [216] investigated the springback properties of 5754-H24/CFRP laminates prepared using adhesive. The effect of core thickness and bending angle on the springback behaviour of FMLs is studied using bending dies with different bending angles (Figure 6). They observed that (i) the amount of springback angle decreased as core thickness increased, and (ii) the amount of springback was higher at all bending angles when the thickness of the face sheet increased.

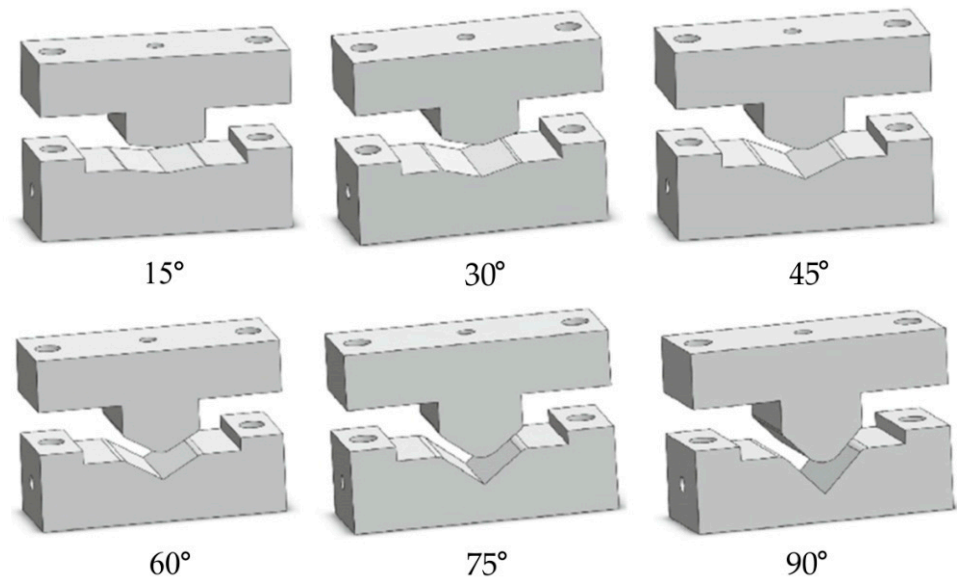


Figure 6. The punches and dies with different bending angles (reprinted with permission from [216]; copyright© 2021, King Fahd University of Petroleum & Minerals).

Impact and fatigue resistance of CARALLs was studied by Bellini et al. [217] in the three-point bending test. Two different interfaces were considered: one obtained with prepreg resin and the other with a structural adhesive. It was found that the laminate with only one metal sheet bonded with structural adhesive presented a higher ILSS than the laminate with the sheet metal bonded only with prepreg resin. In another paper, Bellini et al. [218] analysed the influence of both the adhesion interface between the CFRP layer and the aluminium sheets as well as the layer thickness. Four different laminates, bonded with prepreg resin or with structural adhesive alone and with one or two metal sheets (Figure 7), were investigated in the three-point bending test. It was found that the laminate with two metal sheets bonded with the adhesive had the lowest flexural strength, whilst the laminate with a single aluminium sheet bonded with just the prepreg resin resulted in a better solution. The effect of the stacking characteristics on the mechanical behaviour of the FML was the subject of many studies that have considered the thickness of the composite laminate [99,219,220] or worked with one standard thickness of the metal sheet [5,221].

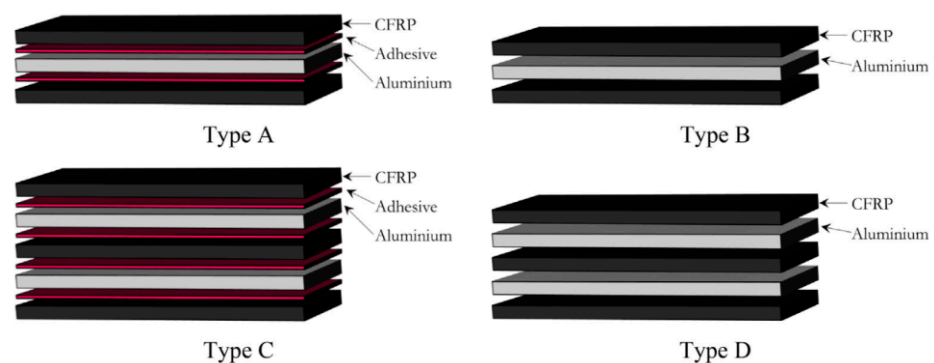


Figure 7. Stacking sequence of FMLs analysed by Bellini et al. [218] (reproduced with permission from [218]; copyright© 2021 Elsevier Ltd.).

Kim et al. [173] investigated the springback characteristics of GLARE 3 2/1-0.4 in the brake forming process. When the load is removed, most metallic materials exhibit springback as a result of the relaxation of the elastic part of the internal stress. After unloading, the material undergoes elastic deformation in the direction opposite to the

direction of the applied load (Figure 8a). The outer layers of the composite are subjected to tensile stress, and the inner layers are subjected to compressive stresses (Figure 8b). When the specimen was heated up to a temperature of 100 °C (limited by the degradation of the composite matrix), the springback was decreased by 19%, compared to that of the process at room temperature [173]. This is a result of the lower yield stress and elastic modulus of the aluminium alloy and the composite at elevated temperatures [222,223]. Springback characteristics are mainly influenced by the forming load [173].

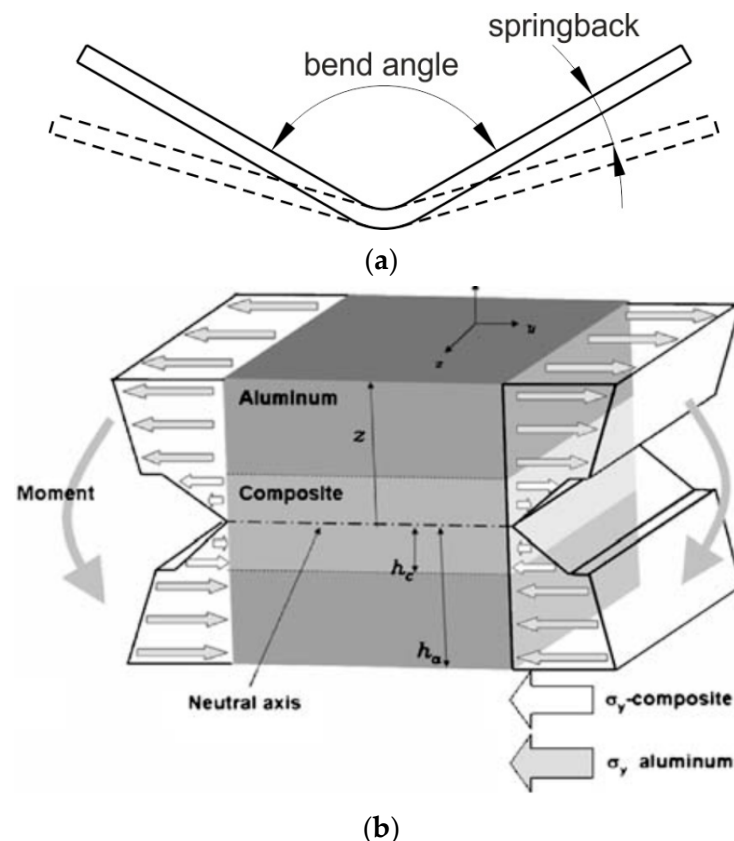


Figure 8. (a) The springback phenomenon and (b) the stress state in the bending of GLARE (reprinted with permission from [173]; copyright© 2021, Springer-Verlag London Limited).

Li et al. [224] analysed springback and failure modes of GLARE 2A-3/2-0.3, GLARE 3-3/2-0.3, and GLARE 2B-3/2-0.3 in the roll bending process, which is considered a cost-effective and efficient sheet forming process. Experimental and numerical results illustrated that springback depended strongly on the lay-up configurations of the laminates tested. GLARE laminates with different fibre orientations signified different resistance abilities to springback; the springback of GLARE 2B was at a minimum. Failures, including delamination, matrix cracking, and fibre fracture, occurred with increasing of the curvature of laminates after bending.

5. Shot Peening Forming

Shot peening forming (SPF) consists of the production of local deformation of the sheet as a result of interaction with hard balls. These balls impact with the surface of the FML at high speed, and the kinetic energy is transferred into a localised plastic strain in the material, which changes the curvature of the entire panel. The characteristics of the influence of the balls on the workpiece surface is elastic–plastic. In aviation, the SPF technique was originally used to form metallic sheets. Kulkarni et al. [225] used SPF to generate curvatures in thin 7075-T6 aluminium alloy sheets for the forming of airplane wing skins to controlled contours. Later, Friese et al. [226] re-shaped laser-welded fuselage panels

for the Airbus A380 using SPF. These had varying thicknesses and geometries of stringers and skin. The method that was developed provided design flexibility combined with a high level of automation. After much positive research, the use of SPF to manufacture metal components has focused on forming FMLs [227].

Another effective non-destructive method to detect material defects and to monitor the complete manufacturing process “in-situ” is X-ray computed tomography (XCT) [228]. XCT, due to its high spatial resolution and very short acquisition time, is successfully applied to determine the process parameters in aerospace composite manufacturing techniques (Figure 9). Naresh et al. [229] reviewed the application of XCT to assess the autoclave and out-of-autoclave manufacturing processes. He concluded that current aerospace manufacturing processes, combined with advanced modelling approaches using XCT, show great potential as tools for the design of better manufacturing processes for the next generation of composite aerospace parts.

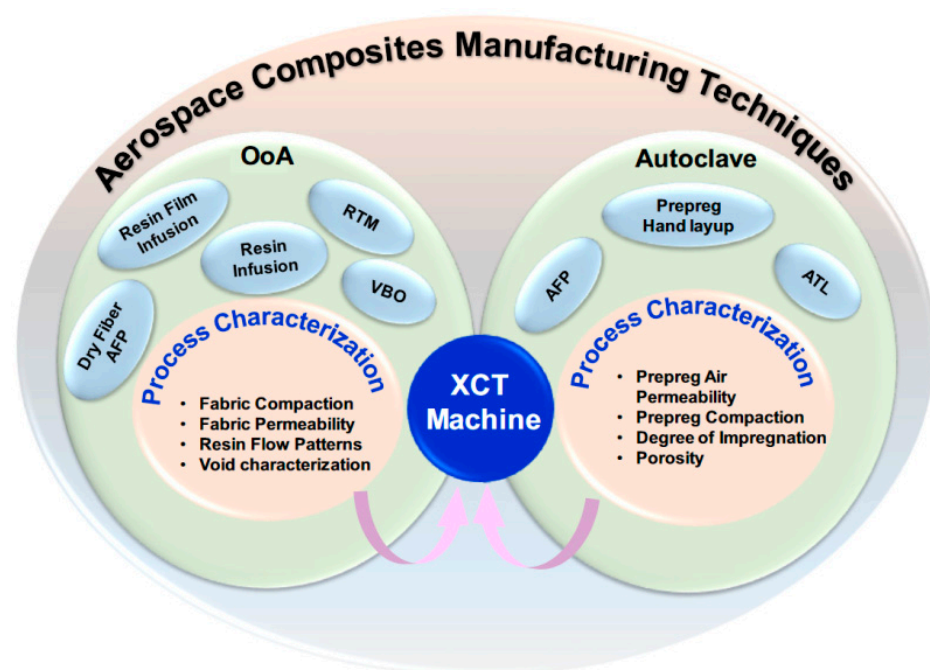


Figure 9. Potential application of XCT in aerospace composite manufacturing techniques (reproduced with permission from [229]; copyright© 2021 The Authors. Published by Elsevier Ltd.).

The results of the application of SPF to form an aluminium–lithium alloy indicated that shot peening caused non-negligible work hardening in the external metal layers, which increased the tensile strength of laminates consisting of 2060 aluminium alloy sheets and S4-glass/epoxy prepregs used as a fibre layer [140]. The compressive stresses introduced by SPF (Figure 10) effectively improved the fatigue crack growth properties of FMLs. Li et al. [140] also found that the failure was mainly dominated by the limitation of fibre failure strain. In another paper, Li et al. [138] studied the deformation behaviour of novel fibre metal laminates (NFMLs) (Figure 11) based on metal sheets from the Al–Cu–Li family, with a Cu/Li ratio of 5.29 after SPF.

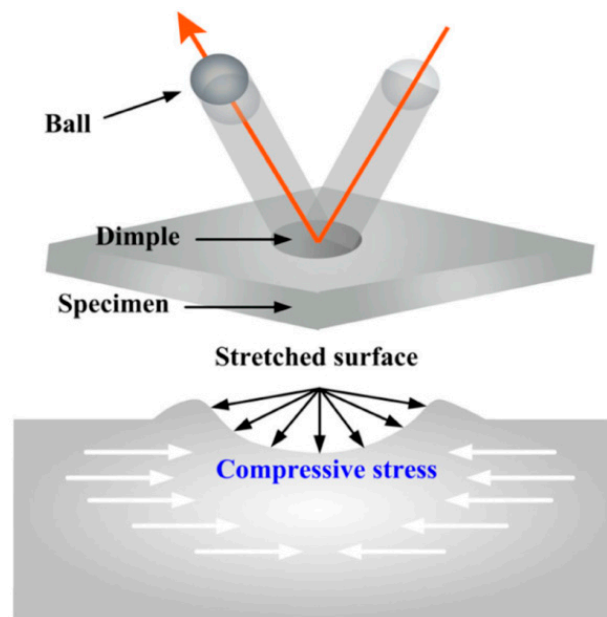


Figure 10. SPF principle of metallic sheets (reprinted with permission from [136]; copyright© 2021, Springer-Verlag London Ltd., part of Springer Nature).

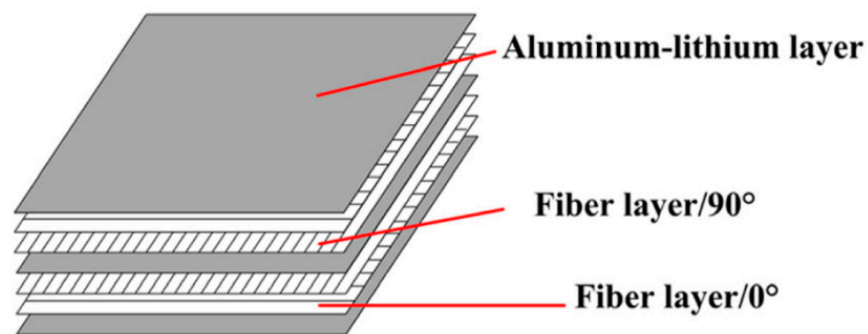


Figure 11. The laminating design of novel fibre–metal laminates (reprinted with permission from [136]; copyright© 2021, Springer-Verlag London Ltd., part of Springer Nature).

The curvature radius of NFML strips decreases when the upper metal layers are etched, indicating that the processed upper layer experiences a compressive state of stress [45]. It was found that the decreased curvature radius is only achieved for NFMLs after etching the lower metal layer (Figure 12). This proves that a state of tensile stress exists in the lower layer. The residual stresses vary at the fibre–metal and 0° –fibre– 90° interface due to the different material modulus of each component (Figure 13). The change in stresses at the interphase boundaries results from a rapid change in the deformation behaviour of the layers. Undoubtedly, due to the layered structure of FMLs, the residual stresses are distributed in a more complex manner than in homogeneous metals.

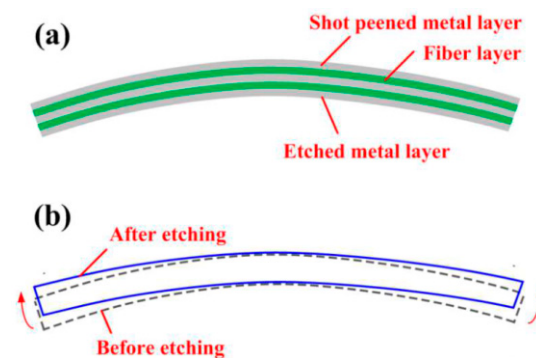


Figure 12. Deformation of shot peened NFMLs after etching: (a) schematic diagram of layer removal and (b) deformation after etching (reproduced with permission from [138]; copyright© 2021 Elsevier Ltd. All rights reserved).

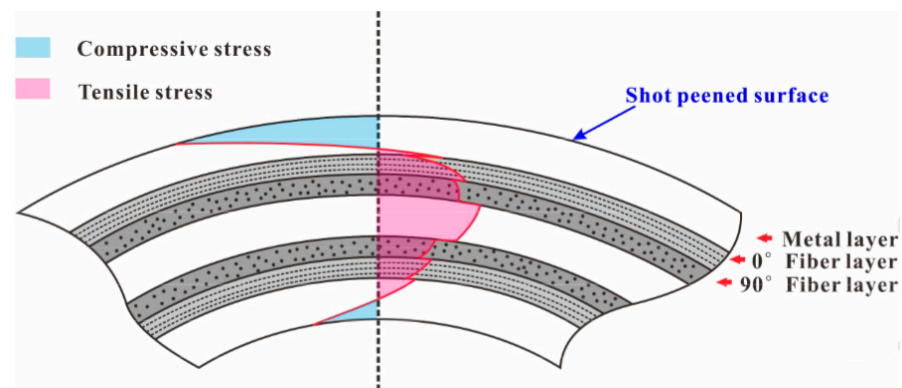


Figure 13. Distribution of residual stresses in shot peened NFML (reproduced with permission from [138]; copyright© 2021 Elsevier Ltd. All rights reserved).

The previous paper by Li et al. [136] on the failure behaviour of shot peened NFMLs shows that the failure mode of NFMLs after SPF mainly included fibre breakage around the shot peened surface and metal–fibre interface delamination. C-scan ultrasonic testing results indicated that ball size significantly affected the curvature of formed NFMLs due to the complex effects of fibre layers on the forming behaviour.

Effects of SPF parameters on the forming characteristics of Ti–CF–Polyimide and Ti–CF–PEEK laminates were investigated by Hu et al. [230]. They observed that the interfaces between the metal layers and the prepreg layers after SPF are continuous and well preserved. SPF did not generate visible micro-cracks and delaminations. Moreover, interfacial bonding within the laminate was not damaged after the forming process. The powerful compressive stresses in the shot peened surface make FML cracking, caused by tensile stresses, difficult. In this way, the mechanical properties of the outer metal layers of FMLs [231] are improved.

Russig et al. [232] developed the Rotary Peening Forming (RPF) process as a new shot peening forming process in which the shot is moved on a circular trajectory held by a flexible connection. GLARE-3 5/4, GLARE-2 3/2, and GLARE-1 3/2 were used as the test materials. It was found that the curvature obtained by RPF is less than that obtained using conventional SPF.

RPF is an evolution of the flap peening process [233], which uses elastic flaps with embedded shot topeen part surfaces. Compared to conventional SPF, the RPF does not require particle recirculation, and, consequently, the machine can be made more compact. RPH induces a similar stress state as SPF, but also involves tangential components that can create shear deformation in the deformed layer.

Wang et al. [234] improved the fatigue strength of CFRP laminate by application of shot peening onto the surfaces of welded flange plates (Figure 14) of high strength low alloy steel. They found that shot peening significantly increases roughness and hardness, in contrast to those samples without treatment. Moreover, an improvement in fatigue life of 20% to 30% and an enhancement in fatigue strength were observed in shot peened specimens.

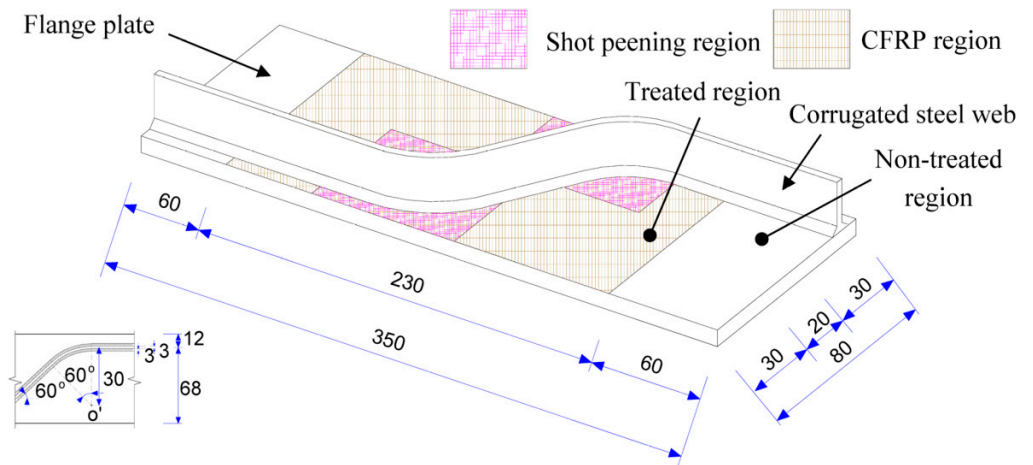


Figure 14. Geometry of a typical test specimen [234] (this is an open access article distributed under the Creative Commons Attribution License which permits unrestricted use, distribution, and reproduction in any medium, provided the original work is properly cited).

6. Incremental Sheet Forming

6.1. Background

Single-point incremental forming (SPIF) is known as the simplest process variant within the incremental sheet forming technologies. It has been studied intensively, which has led to its progressive development since the 2000s [235]. In SPIF, there is no need for dedicated dies; a simple clamping rig alone is used to support the blank edge. The sheet is incrementally formed into the desired shape using a hemispherical end tool following a predefined toolpath [236,237]. The process works as illustrated in Figure 15.

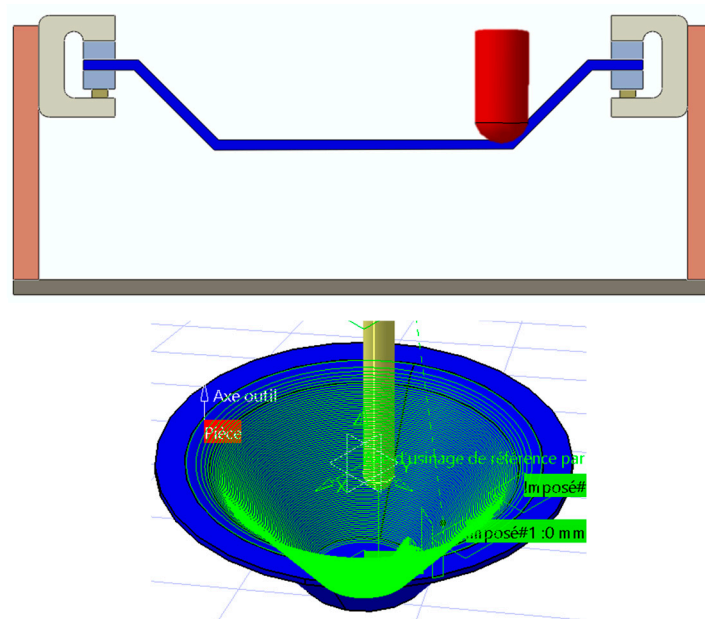


Figure 15. Schematic illustration of the SPIF principle.

Due to its high degree of flexibility, low cost, ability to process complex shapes, high formability, as well as low-forming forces, compared to conventional sheet forming processes, SPIF has mainly proven itself for small batch and rapid prototype production [238–240].

Some examples of SPIF applications are given in [241,242]. The potential markets for this technology are the medical sector [243–246], architecture [247,248], aircraft [249–251], and the automotive industry in particular [252,253].

Furthermore, the suitability of SPIF and the accuracy of the products thus formed are enormously influenced by numerous factors: in particular, the sheet material, tool path strategy, technological parameters (punch diameter, punch rotational speed, tool-path strategy, step size, friction), and design parameters (initial sheet thickness, target geometry) [254–256].

On the other hand, single-point incremental forming originated as a technique for forming metallic materials [257–259]. Some research has, however, been carried out in order to produce components made of non-metallic material, such as:

- bimetal composite [260,261],
- polymers [262,263],
- bilayer polymeric sheets [264],
- polymer-based composite materials [265–271].

Recently, there has been increased attention on possible applications of SPIF for hybrid metal–polymer composites (sandwich panels, FMLs, GLAREs) (Figure 16), which is proving a promising research field [272].

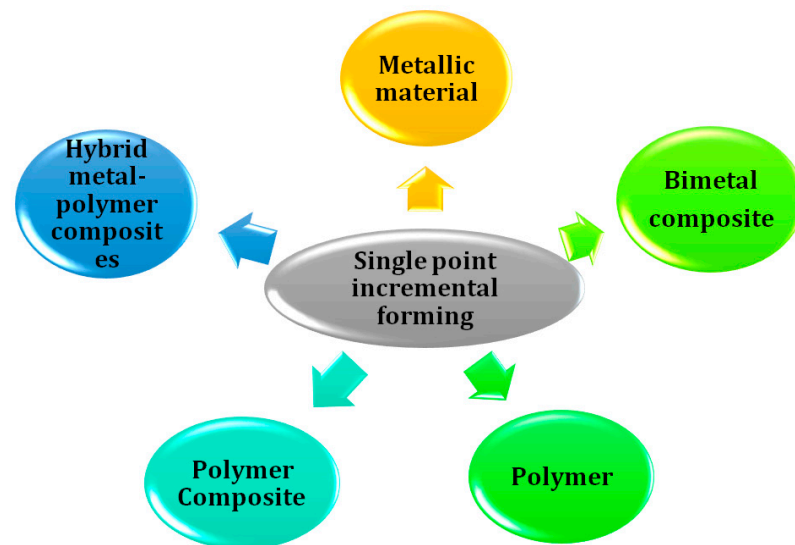


Figure 16. Materials used in the SPIF process.

6.2. Application of SPIF to Hybrid Metal–Polymer Composites

Up to now, research on the use of the SPIF process for hybrid metal–polymer composites is very limited. In this context, Jackson et al. [272] demonstrated the mechanical viability of SPIF for two panels with metal faceplates and polymer cores: mild steel–polypropylene–mild steel (MS/PP/MS, Sollight®) and aluminium–polypropylene–aluminium (Al/PP/Al, Hylite®). As illustrated in Figure 17, four failure modes have been observed in SPIF of composites: faceplate fracture, core shear, local indentation, and delamination. In order to avoid indentation, panels must be ductile and have an incompressible core and faceplates.

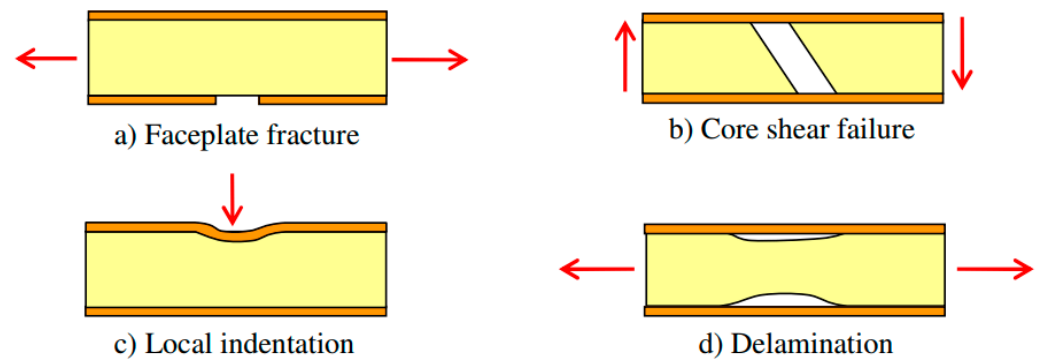


Figure 17. Failure modes of sandwich panels in SPIF (reproduced with permission from [272]; copyright© 2021 Elsevier B.V.).

It was shown that similar results are noted concerning the effect of step size and tool radius, the accuracy of the sine law, and the trends of forces on both sandwich panels and monolithic sheet metal. However, a reduction of 50% in the magnitude of the vertical force was noted for the composite, which is advantageous in process design. Moreover, for a step size of 0.5 mm and a punch radius of 10 mm, the maximum formable wall angles (a widely used parameter for assessing formability) are about 50° and 40° for MS/PP/MS and Al/PP/Al, respectively. It is noted that the limiting failure mechanism in both cases is faceplate fracture (Figure 18). Accordingly, these results revealed that, with these materials, the range of geometric shapes that can be formed is slightly more limited than that of sheet metals, for which the maximum achievable wall angle can reach 78° (2.1 mm of AA 3003-O), as reported by Jeswiet et al. [235].

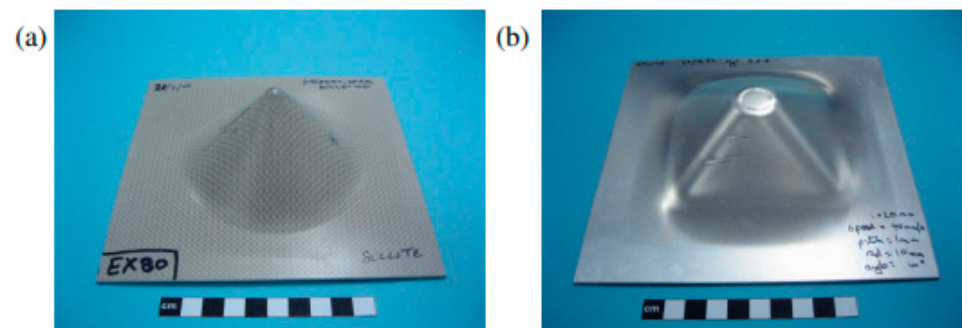


Figure 18. Sandwich panels formed using SPIF: (a) MS/PP/MS (45° angle without failure) and (b) Al/PP/Al (40° angle showing faceplate fracture) (reproduced with permission from [272]; copyright© 2021 Elsevier B.V.).

Nevertheless, it cannot be assumed that these are the forming limits of the sandwich panels with SPIF in general due to the various process conditions that can be considered later. As is well known, a different combination of process parameters [245,273–275] will certainly lead to different conclusions.

Fiorotto et al. [265] evaluated the feasibility of producing complex geometry panels from two aluminium plates and a composite core in a cost- and time-effective manner. Composite laminates consist of two woven kevlar fabrics. During FML forming, circumferential cracking and the generation of wrinkles along the wall of the part have been noted (Figure 19). By contrast, by excluding the composite core, two aluminium plates were simultaneously formed without defects.



Figure 19. Mechanical failure on formed FML (reprinted with permission from [265]; copyright© 2021, Springer-Verlag France).

The effect of initial sheet thickness on the formability of laminated materials, Al/PP/Al (Hylite[®]), has been investigated by Girjob et al. [276]. This material has exceptional properties, such as flexural stiffness and very low density. It was found that a non-uniform thickness distribution occurred throughout the circumference of the formed workpiece. Obviously, it is known that a proper selection of SPIF process parameters has, in fact, a great influence on the production of components with satisfactory structural and dimensional characteristics. Thus, further experimental tests should be performed to reach more accurate conclusions.

In this framework, Davarpanah et al. [277] examined the effect of some of the process parameters, i.e., step down Δz (0.2 mm and 0.4 mm), metal thickness t_{Al} (0.8 mm and 1.0 mm), and polymer thickness t_{PA} (0.79, 1.19, 1.58, 1.98 and 2.38 mm), on the formability and failure modes during incremental forming of adhesively bonded AA5052 aluminium–polyamide laminate sheets. The observed failure modes for the laminates are delamination, metal tearing, and galling, as shown in Figure 20.

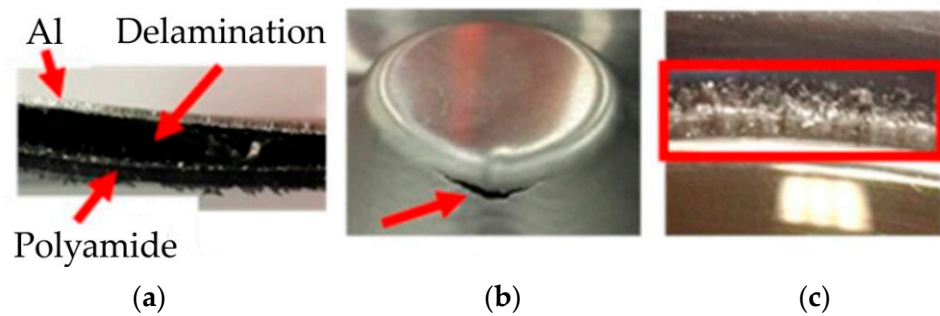


Figure 20. Types of failure: (a) delamination, (b) metal tearing, and (c) galling (reproduced with permission from [277]; copyright© 2021 The Author(s). Published by Elsevier B.V.).

The series of experiments and conclusions are summarised in Table 3. It has been noted that, at low polymer thicknesses, the composite undergoes delamination between the layers. Increasing polymer thickness improves formability because the tendency to delamination decreases until the transition thickness is attained. Thus, the mode of failure shifts from delamination to metal tearing, resulting in maximum formability. In addition, this critical t_{PA} value increases with greater Δz when the metal thickness is constant. In laminates with a thinner metal sheet (0.8 mm), only two types of failure appear: delamination and metal tearing. However, a small increase in the AA5052 thickness (1 mm), at $t_{PA} > t_{PA-critical}$, results in galling of the polymer before fracture.

Table 3. Summary of the experimental tests performed by Davarpanah et al. [277].

t_{PA} (mm)	t_{Al} (mm)	Δz (mm)	Failure Mode	Formability
<1.58	0.8	0.2	delamination	increases
1.58			metal tearing	maximum
>1.58			metal tearing	slightly reduced
<1.98	0.4	0.4	delamination	increases
1.98			metal tearing	maximum
>1.98			metal tearing	slightly reduced
<1.58	1	0.2	delamination	increases
1.58			metal tearing	maximum
>1.58			galling	slightly reduced
<1.98	0.4	0.4	delamination	increases
1.98			metal tearing	maximum
2.38			galling	slightly reduced

However, more research is needed to reveal the effects of other parameters, such as adhesive strength and forming speed (rotation and feed rate).

Harhash et al. [278] conducted several experimental tests to prove that, like metal sheets, steel–polymer–steel sandwich composites can be formed successfully by SPIF, subject to different forming limits. It was found that shaping the SPS sheets is possible and similar to steel sheets, but with an earlier fracture at angles of more than 30%. Thus, the formability of the SPS is much lower than the uniform sheet in terms of the limiting wall angle and cracking height.

Additionally, after cutting the shaped conical part, delamination was observed in the unsupported SPS laminate regions (Figure 21a). Owing to the tool step down ($\Delta z = 0.5$ mm) and the friction, the inner side of the formed part shows galling marks, whereas the outer skin sheet is subject to failure by cracking (Figure 21b). The high ductility of the core layer (>200% elongation at failure) prevents it from cracking.

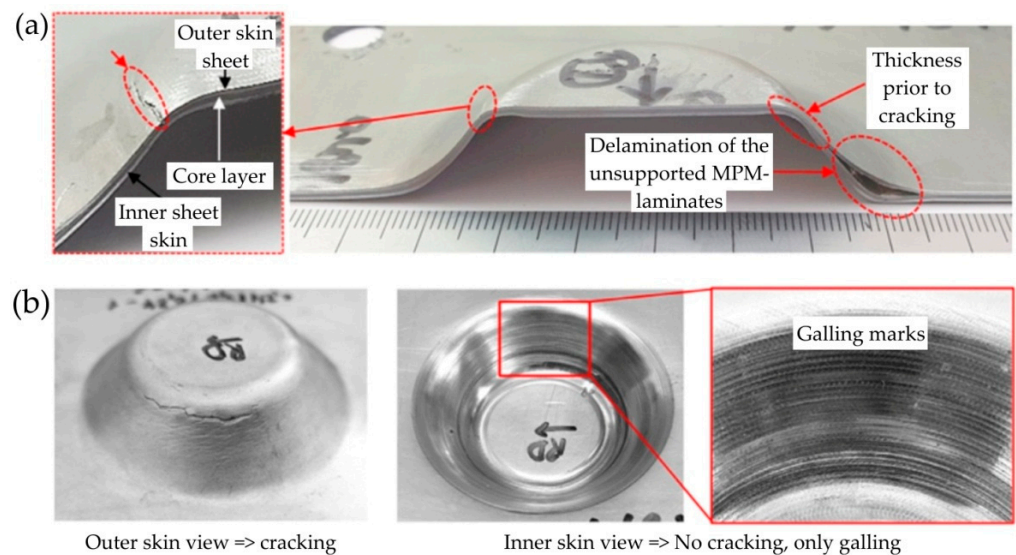


Figure 21. Defects during SPIF of metal–polymer–metal (MPM) sandwich sheets: (a) delamination and (b) cracking of the outer skin sheet and galling marks in the inner surface of the formed part, reproduced from [278] (this is an open access article distributed under the terms of the Creative Commons CC-BY license, which permits unrestricted use, distribution, and reproduction in any medium, provided the original work is properly cited).

As a means of extending these SPIF limits for the metal–polymer–metal sheets, multi-stage forming was examined in the same paper [278]. It was concluded that two-stage SPIF improves the part height at cracking, in comparison with direct SPIF (Figure 22). This

is explained by the fact that the direct SPIF forming was under plane strain conditions until failure.

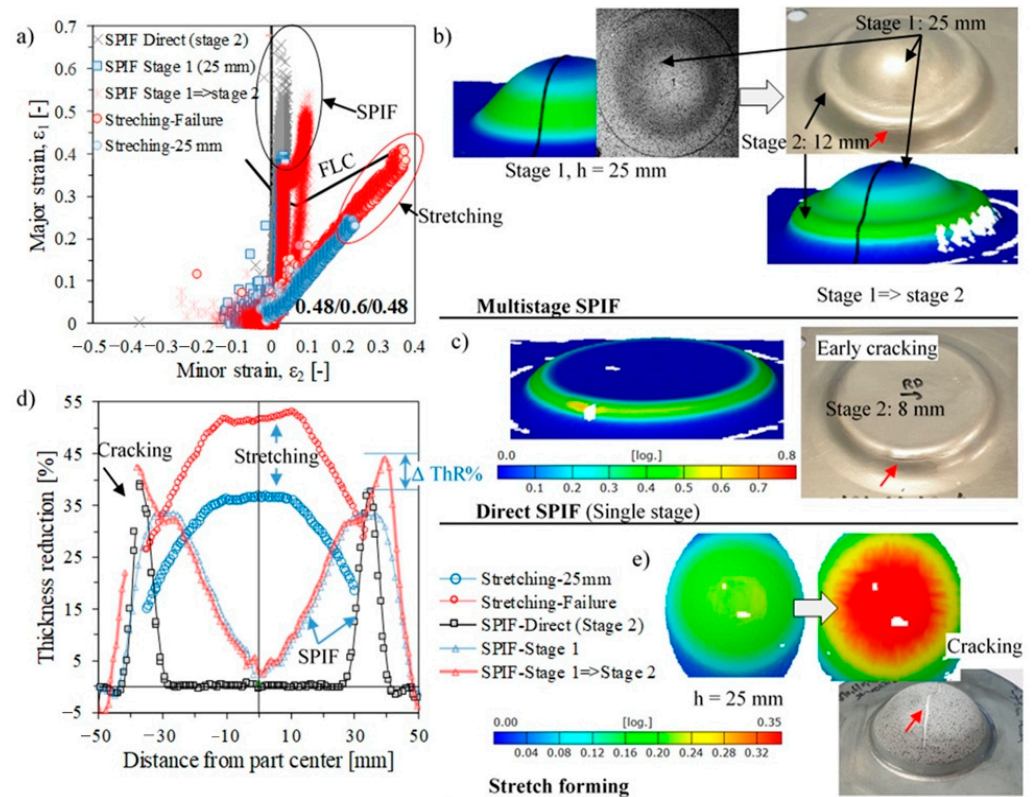


Figure 22. Evaluation of semi-spherical parts formed by direct, multi-stage, as well as conventional stretch forming in terms of: (a) minor–major strain distribution and (d) thickness reduction distribution determined by Digital Image Correlation of (b) the multi-stage and (c) direct SPIF compared to (e) stretch forming of Ø75 mm semi-spherical parts. Red arrows indicate cracking of the outer skin sheet, reproduced from [278] (this is an open access article distributed under the terms of the Creative Commons CC-BY license, which permits unrestricted use, distribution, and reproduction in any medium, provided the original work is properly cited).

On the other hand, a comparison of two-stage SPIF with stretch forming proves that both could produce a dome of 25 mm depth in the first stage, but with entirely different thinning behaviour (Figure 22b,d,e). In stretch forming, the thinning rate is more significant in the centre (at the bottom of the sample). As a result, cracking occurs in this zone (Figure 22e), while it appears in the wall area with SPIF.

Although promising results are obtained with multi-stage SPIF, the depth achieved in stretch forming is greater. Therefore, the authors recommended increasing the number of the sequential stages with an angle interval of ~5°.

The results of the previously cited investigations confirm the applicability of SPIF; however, the presence of some different failure types and limits was observed when compared to metal sheets. These defects are generally due to the non-uniform thickness properties and relatively insufficient metal/polymer adhesion strength. Forming at elevated temperature becomes, accordingly, the most suitable and promising solution to overcome the current process limitations, especially for hard-to-work alloys, polymers, and composites. Consequently, different concepts have recently been developed for warm SPIF to enhance a material’s formability and to improve geometrical accuracy. A review and analysis of the state-of-the-art research on hot incremental sheet forming has been conducted by Liu [279] and by Zhu et al. [280]. This hybrid forming technology has first been applied to metal sheets [281–287] and later to polymer sheets [267,288–294].

Within that framework, Al-Obaidi et al. [271] devoted their research to investigating the effectiveness of such process variants for glass fibre reinforced polymer (PA6GF47) sheets and to shorten the manufacturing process for orthotics using SPIF assisted by hot air heating (Figure 23). The PA6GF47 sheets were sandwiched between two Teflon layers and two metal sheets. Conical parts were shaped with a variety of wall angles. It is found that samples formed with a wall angle greater than 50° were distinguished by wrinkling, folding, internal cracks, and voids.

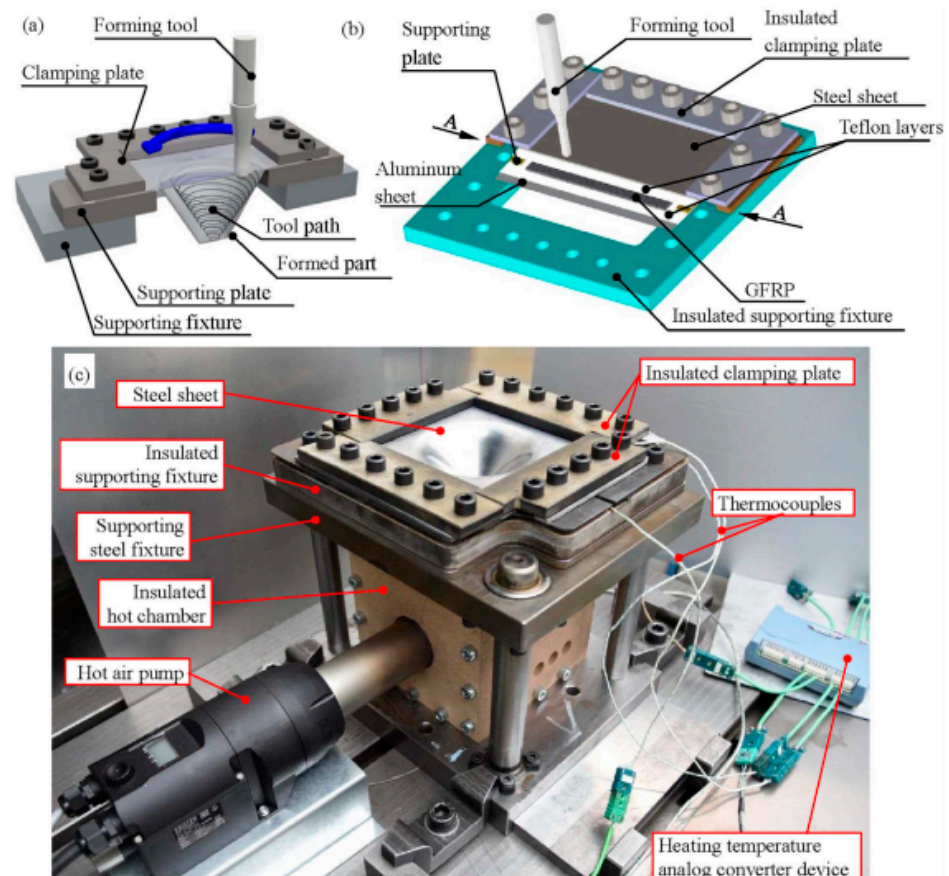


Figure 23. Principle of hot SPIF: (a) workpiece combination, (b) clamping fixture, and (c) setup assembly (reproduced with permission from [271]; copyright© 2021 The Society of Manufacturing Engineers. Published by Elsevier Ltd.).

In another study, Al-Obaidi et al. [295] continue with the same hot SPIF technology to form a basalt fibre reinforced thermoplastic polymer (BFRTTP).

As shown in Figure 24, two laminate types were considered during the forming of conical shapes: the first consists of BFRTTP incorporated between two aluminium sheets, and the second consisted of only one aluminium sheet inserted between two layers of BFRTTP. The Teflon layers were utilised to enhance the sliding of the laminate during hot SPIF. In addition, the metal sheets were employed to protect the BFRTTP from excessive heating effects and punch friction. Conical shapes were formed with several wall angles. It was noted that parts with a wall angle $\geq 50^\circ$ were suffering from delamination and void initiation. Owing to the large difference between the plastic properties of the aluminium sheet and the behaviour of the thermoplastic laminate during hot SPIF, the second type of laminate has a much greater percentage delamination than the first one.

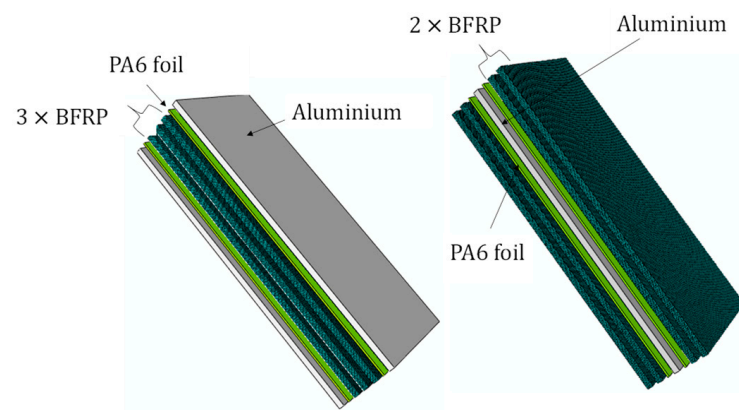


Figure 24. The BFRTP laminate structures utilised in the experiments (reproduced with permission from [295]; copyright© 2021 The Author(s). Published by Elsevier B.V.).

Based on existing knowledge of SPIF for sheet metals, the economic benefits were the same when addressing hybrid metal–polymer composites, but product formability must still be enhanced. Therefore, use of the process with its different variants and conditions needs an extensive investigation in relation to these materials.

Up to now, numerical simulations and optimisation techniques have greatly contributed to the development of SPIF [296–300], especially for metallic components with complex geometries. Therefore, the application of such techniques should be extended to FMLs.

7. Lay-Up Technique

The lay-up technique is the oldest and simplest manual method of producing open-mould laminates. During lamination, the reinforcing component is placed in the mould in the form of layers with a filling (resin). The reinforcement layers can be in the form of unidirectional continuous filament roving and in the form of staple fibre fabrics or mats. The strength and stiffness of the laminate is directly dependent on the production method and the direction of the fibres [301,302]. Components made of laminates have lower weight and greater strength than the majority of structures made of homogeneous materials. The selection of the lamination method depends on the type of materials used, the desired shape and dimensions of the product, as well as the specific utility requirements [303,304].

For this reason, the following methods of obtaining laminates can be distinguished:

- hand lay-up,
- spray lay-up,
- compression moulding,
- pultrusion,
- resin transfer moulding (RTM), and
- filament winding.

The types of laminating forms can be either internal or external. A geometrical outline of the product is formed on the required forming surface. The next stage of the lamination process is the curing of the individual layers of laminate, which can take place both at ambient and elevated temperatures with the use of infrared heaters. The conditions and time for curing of laminate largely depend on its type, shape and dimensions.

Spray lay-up technique involves applying both resin and fibre as a liquid suspension using a special spray nozzle (Figure 25). The fibres in the form of roving are continuously fed to the spray nozzle, and, in the nozzle, they are cut into fibres with a length between 0.3 mm and 13 mm. As a result, the air stream “imposes” the fibres and the resin on the mould surface [17,305,306].

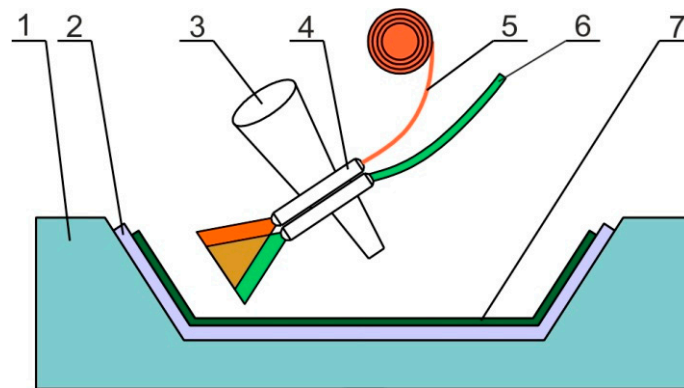


Figure 25. Scheme of spray lay-up technique: 1—mould, 2—gel coat, 3—pot of resin catalyst pot, 4—chopper gun, 5—fibre, 6—air pressurised resin, 7—laminates.

RTM is a method of manufacturing laminates in closed forms, which consists of forcing catalysed resin into a tightly closed mould, previously filled with reinforcing fibres and/or sandwich material [307–309]. The counter-mould is made similarly to the main mould. It consists of steel stiffeners and reinforcements, which allows the use of high injection pressure [310,311]. Light resin transfer moulding (LRTM) is a variation of the RTM method that uses a light, semi-flexible counter-mould that is clamped by applying a vacuum between the seals placed around the perimeter of the mould (Figure 26) [312,313]. The resin injection pressure is relatively low, and the entire process is supported by negative pressure [314–316]. The RTM/LRTM method allows the share of reinforcement in the total mass of the composite (over 60%) to be increased compared to, for example, hand lay-up lamination [317]. RTM and LRTM technologies are mainly used in the construction of boats and water equipment [318–320] and in aircraft construction [321] as well as automotive and medical composite moulding applications [322–326]. After the impregnation, the laminate component can cure, usually at room temperature [56,57]. The most important parameters determining the effective preforming saturation in the RTM process are [327]:

- an appropriate injection pressure gradient,
- good wettability in the fibre–resin system, and
- good tightness of the impregnation system.

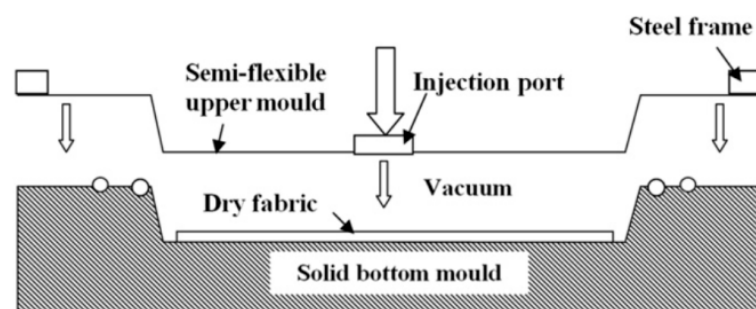


Figure 26. Schematic diagram of light resin transfer moulding (reproduced with permission from [312]; copyright© 2021 Elsevier Ltd.).

In the case of very high-quality requirements regarding the moulded parts and the use of prepregates made from composites reinforced with high-modulus fibres and resins hardened at an elevated temperature, it is necessary to cure the laminates in an autoclave (Figure 27). An autoclave is a furnace that allows both heating and pressure to be applied to a material [328]. Several single prepregate/prepreg layers stacked on top of each other are covered with a high temperature resistant foil, sealed, and connected to the vacuum lines. Negative pressure and multiplied overpressure consolidate the prepregate layers

and squeeze excess resin from the layers of fibres; the increased temperature causes the laminate to be cured [213,329]. Only single or shallow double curvature panels with relatively large radii can be formed with this technique [78,213]. However, it is an expensive process, especially when it comes to large parts [200,330,331]. In order to reduce production costs, out-of-autoclave techniques can be used that allow localised curing and/or bonding of thermosets [200,332]. Induction heating [333–335] and microwave radiation [336–338] have been proposed to cure fibre reinforced thermoset composites.

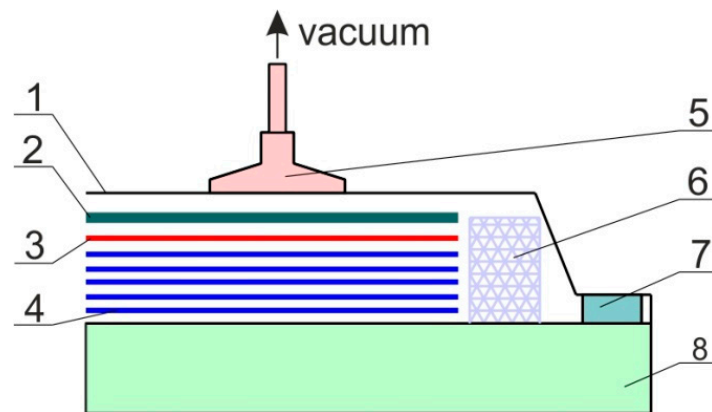


Figure 27. Schematic diagram of the autoclave setup: 1—vacuum bag, 2—breather cloth, 3—release film, 4—prepreg plies, 5—valve, 6—edge bleeder, 7—sealant, 8—tool.

Bars and profiles can be produced by the pultrusion method. Fibre is pulled through a bath of resin, and then the fibre passes through dies forming and squeezing the excess resin and the heating zones of the mould, where it is hardened [47,339,340]. The technology is intended for the production of profiles with a constant cross-section. Reinforcement, and, at a later stage, the finished elements, are pulled through successive devices shown schematically in Figure 28 [341–344]. Several works have reported using the pultrusion process for various types of fibre, e.g., kenaf fibre [345–347], kenaf–glass fibre [348–350], and jute–glass fibre [351–353].

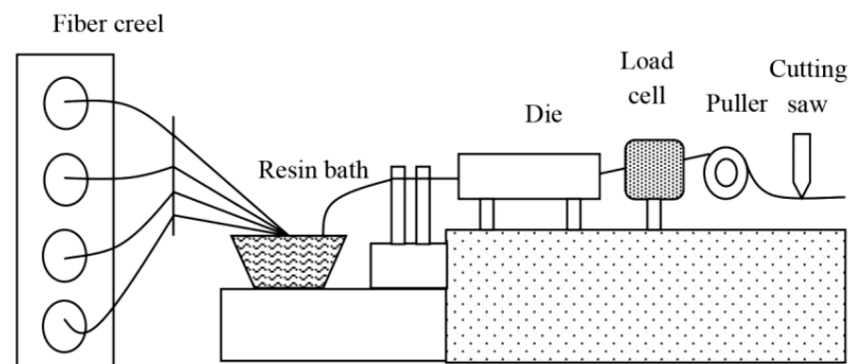


Figure 28. Schematic diagram of a pultrusion process line (reproduced with permission from [354]; copyright© 2021 Taylor & Francis).

Filament winding (Figure 29) involves the continuous winding of fibres on a rotating core with the shape of a rotational solid (cylinder, cone, etc.) [355–357]. Circumferential, helical and planetary winding [358–361] can be performed depending on the direction of rotation of the core and the way the carriage is moved. The design of the carriage with roving and the core turning device enables both the carriage speed and rotational speed of the core to be changed, so that the winding angle can be adjusted. The roving tapes used in the filament winding process may be preimpregnated with resin. Before winding on the core, they must be heated so that the resin becomes liquid [362].

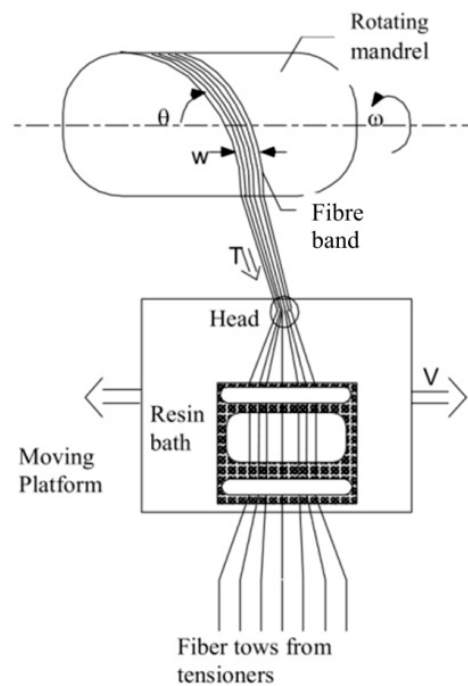


Figure 29. Schematic diagram of the filament winding process (reproduced with permission from [363]; copyright© 2021 Elsevier Science Ltd.).

From the literature review, the reader should note that there remain two different approaches to obtaining the complicated shape of the FML part (Figure 30). In the first approach, the component layers of the material are first deformed, and then a laminate is fabricated based on the deformed layers. Forming single thin layers is costly and extremely demanding. A less costly alternative is to form the FMLs to be fabricated directly. In a later part of the article, methods of plastic working and laser forming for FML panels will be presented. Table 4 summarises the main advantages and disadvantages of lay-up techniques of FML fabrication.

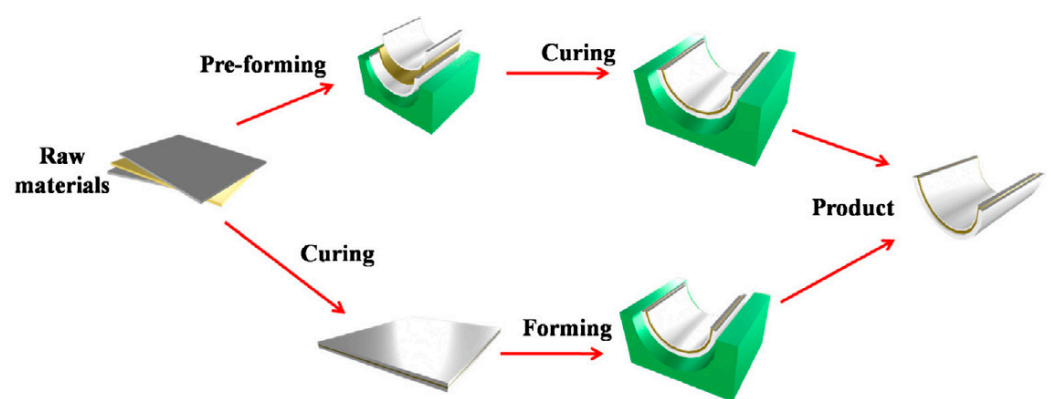


Figure 30. The routes to create a HMPC (reproduced with permission from [230]; copyright© 2021 Elsevier Ltd.).

Table 4. Main advantages and disadvantages of selected methods of fabricating HMPC components.

Method	Advantage	Disadvantage
Hand lay-up	<p>Low cost of tooling [364,365] The process is simple [364] Large, complex parts can be formed [365] Flexible design [364] Production technology is easy to master [365] Any combination of fibres and matrix materials can be used [364]</p>	<p>The process is time-consuming [364] Powder and bad smells are involved in the production environment [365] Quality of the final product depends on highly skilled manpower [364] The process is labour intensive [366]</p>
Spray lay-up	<p>Suitable for small- to medium-volume parts [364] Low-cost tooling [364]</p>	<p>It is difficult to control the fibre volume fraction [364] There is difficulty in removing trapped air from the moulding [365] The process does not provide a good surface finish [364]</p>
RTM	<p>Complex parts can be fabricated [307,309,366] Higher volume outputs and much lower cycle times than other methods [308,366] Production of smooth-surfaced parts on both inner and outer surfaces of the mould [307,308,366]. Components can be produced up to 5–20 times faster compared with open moulding techniques [367]</p>	<p>High production volumes require offset high tooling costs [307,308,367] Difficult to effectively improve the fibre volume content of the product [367] The size of the part is limited by the mould [308,367].</p>
LRTM	<p>Produces finished surfaces on both sides of the part [318,368] Improved process control enhance of dimensional stability [319,368] Significant saving in tooling costs as it only requires a single-piece mould [318,368] Cost-effective to manufacture large panels such as ship's hulls [368,369] Fabrication of large composite panels takes place at room temperature [319,370] Scalability for large structures [320,371] Toughened infusion resins can be used [371]</p>	<p>Compared with conventional RTM, LRTM is characterised by limited compaction of the reinforcement, a limited injection pressure, and lower dimensional accuracy [318–320,372] Trial and error development can prove costly and ineffective [313,373]</p>
Autoclave process	<p>Large components can be fabricated [364] Good surface finish [364]</p>	<p>High initial cost of equipment [364] High cost of maintenance [364] Not suitable for small products [364]</p>
Pultrusion	<p>Requires low labour [348–350,364] Good surface finish [348,364] Process is economical [364]</p>	<p>High cost of heated die [346,350,353,364] Limited to constant or near-constant cross-section components [346,349,364]</p>
Filament winding	<p>Complex fibre patterns can be used [355,356,364] Good resin distribution in products [364] A favourable fibre orientation can be obtained [358,359] Process can be highly automated [355–358]</p>	<p>Process is limited to convex shaped components [358,359] The external surface of the component is not smoothly finished [360,361,364] High cost of mandrell [355,356,364]</p>

8. Die Forming

In the die forming technique, sheet blanks obtain the desired shape according to the die configuration [372,373]. The energy required to cause the deformation can be applied from different sources: mechanical, hydromechanical, electromagnetic (Figure 31), by laser beam, etc. Recently, these forming methods were utilised to form steel-based FMLs, but the latest research papers have been focused mainly on aluminium-based composites. Researchers consider the configuration of the material layers [374–377] or the process parameter setup [86,378–386] to reduce material defects and go beyond the

current forming limits caused mainly by breakage and wrinkling. In order to improve the formability of the layers of FRP, many studies are focused on die forming at elevated temperatures [387–389]. The forming process can be isothermal or non-isothermal [390]. The comparison of the forming behaviour of FMLs with the conventional deep drawing process leads to the conclusion that early fracture of the laminate arises without achieving a significant depth [391–394]. FMLs must usually undergo preprocessing in terms of heating and stacking before being properly formed.

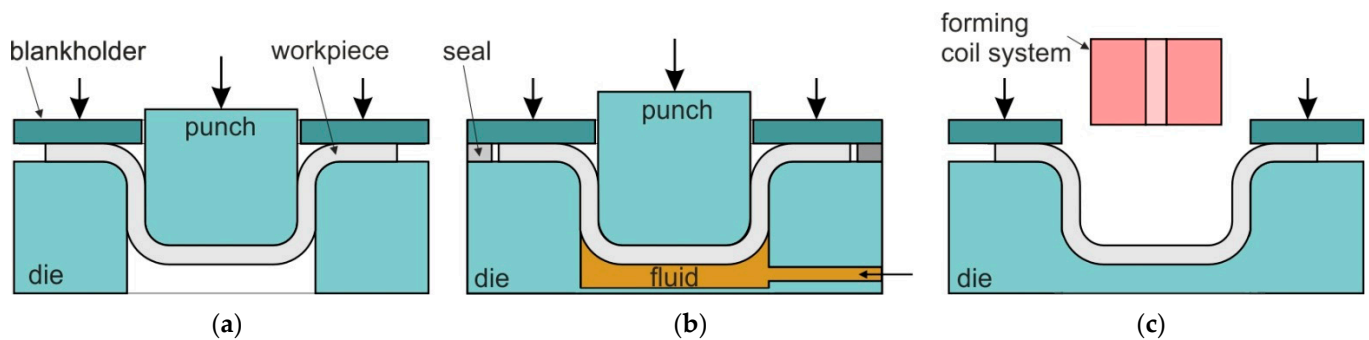


Figure 31. Variants of die forming methods: (a) stamping, (b) hydroforming, and (c) electromagnetic forming.

8.1. Stamping

Stamping is the most common method of die forming, in which the desired shape is achieved with tool sets (a blank holder and dies). To increase the forming ability of FMLs, elevated temperatures are required. Rahiminejad and Compston [9] determined the forming limit curve for FMLs in the stamping process for blanks in configuration 2:1 made of 0.45 mm thick steel and 1 mm 0/90° weaved GFPP and heated at 140 °C (above the polypropylene crystallisation temperature) and 170 °C (polypropylene melt temperature). At a temperature of 170 °C, composite flow out of the bond and in thickness reduction were observed. Better strain results were obtained for the temperature 140 °C where the middle layer softened, allowing for better slip. Nam et al. [162] investigated stamping behaviour of steel–SRPP laminate in open die configuration at room temperature, applying various values of blank holder force (2 kN, 7 kN, and 14 kN). It was found that better strain distribution was obtained for FML than for sheet steel. Furthermore, a significant effect of blank holder force was noted, in that the selection of the higher forces (7 kN and 14 kN) affects wrinkling reduction, but a delamination effect was also observed. Additionally, Blala et al. [378,379] performed drawing tests on 2/1 GLARE (0.5/0.2/0.5 mm) composite. Different blank holder forces, gaps, and cure states were considered. Deep forming cured GLARE seems not to be possible because of composite low elongation rate (5% compared to 20% Al 2024-T3 sheet) and its high coefficient of friction between Al sheets. An optimal blank holder gap (1.1 mm), 0.1 mm lower than the blank thickness (1.2 mm), and a blank holder force in the range from 3 to 6 kN was selected, achieving 31mm forming depth of semi-cured GLARE. Liu et al. [374] focused on the effect of fibre orientation on the stamp forming process of GLARE composites. FML blank containing multi-directional fibre layers (0/45–45/90°) achieved better formability depth (42 mm) than unidirectional ones (35 mm). In 2020, Blala et al. [308] improved the drawability of semi-cured Glare sheets in the deep drawing of cylindrical cups using a variable blank holder force (VBHF). Variation in the friction force of the holder and the laminate on contact surfaces varied as a function of the position of the outer flange edge (Figure 32). When there is constant blank holder force (BHF), the FML fails at the beginning of the forming process due to the fibre’s limited strain at rupture. When the BHF is too low, wrinkles occur at the flange of the drawpiece. The results of experimental tests and numerical modelling revealed that wrinkles can be eliminated with a decreased BHF trajectory.

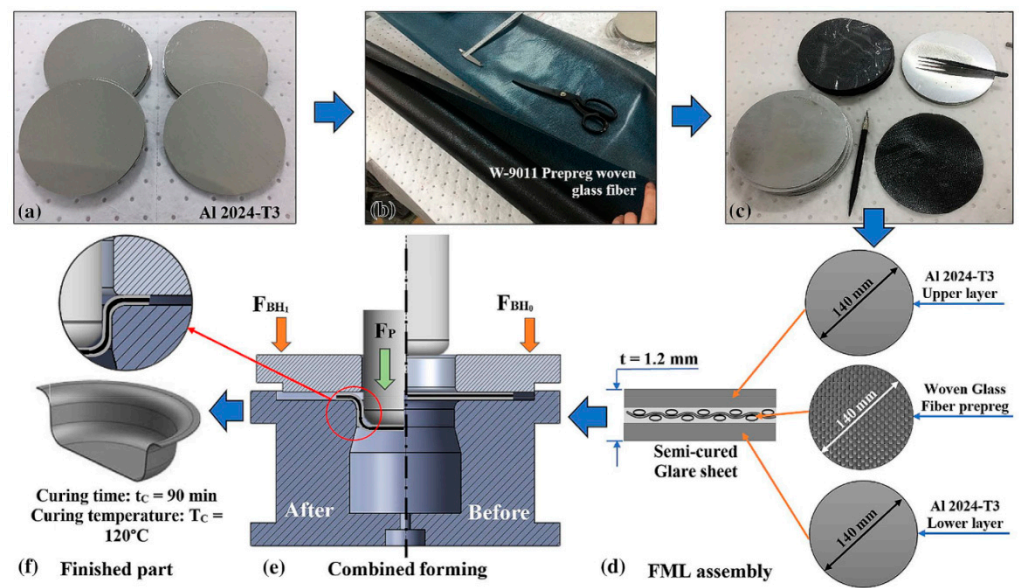


Figure 32. (a) 2024-T3 blanks, (b) W-9011 glass fibre, (c) 2/1 GLARE assembly, (d) semi-cured GLARE blank, (e) combined forming, and (f) curing of formed components (reprinted with permission from [308]; copyright© 2021, German Academic Society for Production Engineering (WGP)).

In 2021, Blala et al. [86] proposed a novel approach to stamping automated small FML parts by hot-pressing non-cured FMLs (Figure 33), which was compared with the conventional forming method (Figure 34). A significant increase in formability was observed by this process, from the 13 mm drawing depth conventionally obtained compared to the 38 mm with an improved wall thickness homogeneity produced by hot-pressing (Figure 35). The thickness reduction values achieved were 11.66% for the top and 14.30% for the bottom aluminium sheet and 6.6% for the fibre layers. It was also concluded that the lower aluminium sheet is subjected to more thinning than the upper sheet. To eliminate defects in the FML during stamp forming, Blala et al. [22] developed a new method consisting of forming non-cured laminate followed by hot-pressing. The conventional process of forming autoclave-cured 2.1 GLARE specimens leads to the formation of typical failure modes during stamping, i.e., failure by tearing, sidewall wrinkling and excessive thinning, delamination, and fracture (Figure 36a–f). The results of numerical computations and experimental tests show that the approach developed can improve the stamping process of 2/1 GLARE parts, which translates into obtaining products without the defects typical of FMLs (Figure 37g).

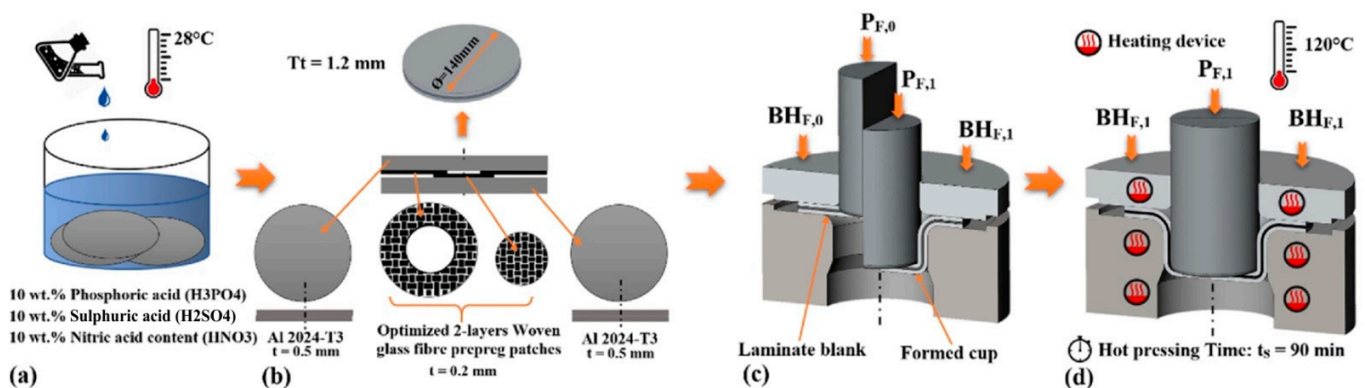


Figure 33. Preparation and forming of GLARE 2/1 using the new optimised process: (a) surface treatment of 2024-T3 sheets, (b) optimised 2/1 laminate assembly, (c) combined forming, and (d) hot pressing (reproduced with permission from [86]; copyright© 2021 Elsevier Ltd.).

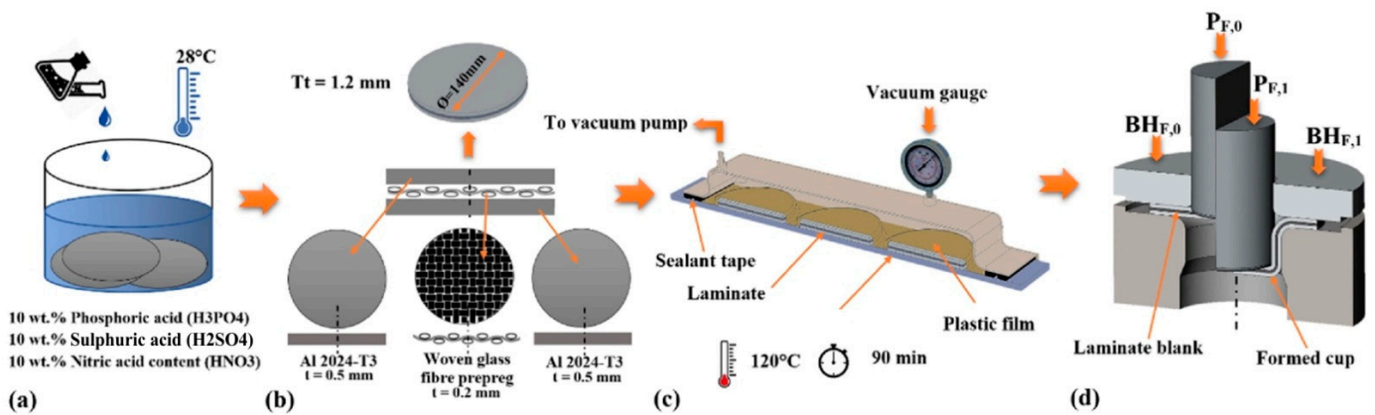


Figure 34. Preparation and forming of GLARE 2/1 using the conventional process: (a) surface treatment of 2024-T3 sheets, (b) 2/1 laminate assembly, (c) vacuum curing of blanks, and (d) forming (reproduced with permission from [86]; copyright© 2021 Elsevier Ltd.).

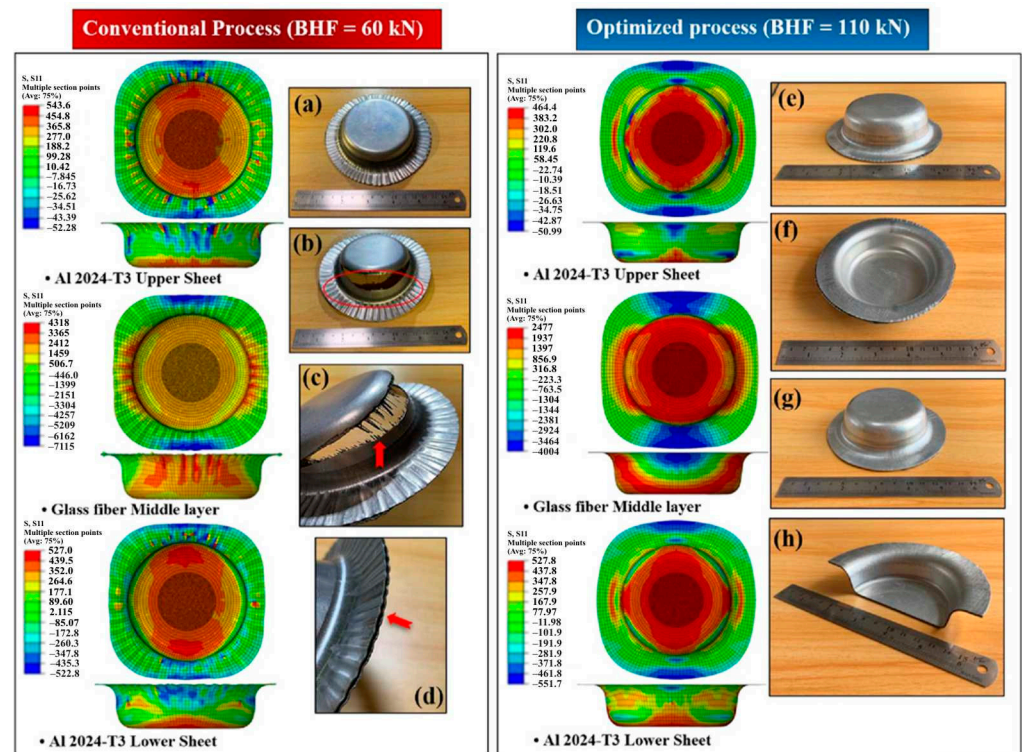


Figure 35. Comparison of deformations between (left) the conventional process and (right) the optimised process: (a) wrinkling, (b,c) the failure of the aluminium alloy, (d) delamination failure of the laminate, (e,f) drawpieces free of wrinkles and delamination, (g,h) cross section of the final drawpiece (reproduced with permission from [86]; copyright© 2021 Elsevier Ltd.).

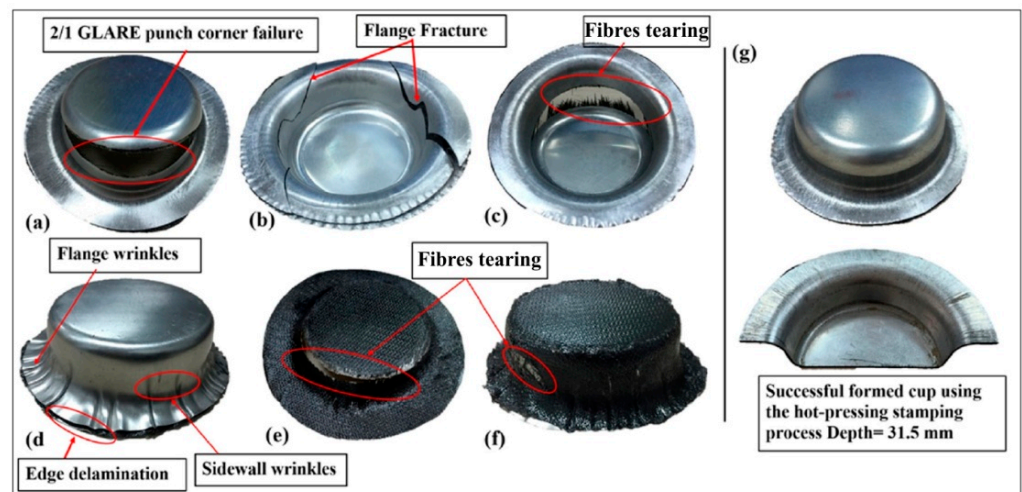


Figure 36. Failure types and locations: (a) punch corner fracture, (b) flange fracture, (c) fibre tearing and aluminium fracture, (d) sidewall and flange wrinkles, edge delamination, (e,f) tearing of glass fibre, (g) successfully formed cup using the new process proposed by Bala et al. [22] (reprinted with permission from [22]; copyright© 2021, The Author(s), under exclusive licence to Springer-Verlag London Ltd., part of Springer Nature).

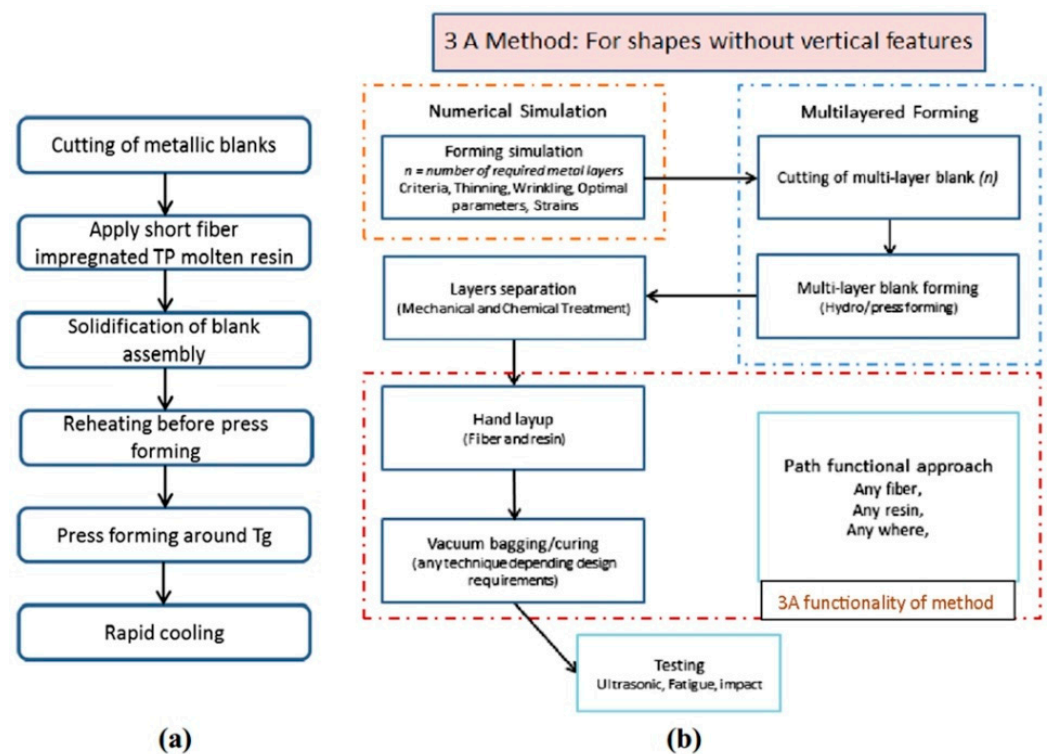


Figure 37. (a) Existing and (b) novel 3A method (reprinted with permission from [383]; copyright© 2021, Springer-Verlag France).

8.2. Hydroforming

Hydroforming is a technology for shaping tube profiles, shells, and flat sheets using fluid pressure. Elements made using this method have superior surface quality and dimensional accuracy. The main obstacle preventing the popularisation of this method is the high cost of the machines and the process, compared with conventional stamping [375]. Fibre orientation has a significant impact on FML performance; Sumana et al. [375] produced hydroformed cylindrically shaped FMLs made of 1 mm thick 6061-T6 aluminium alloy

and three alternative FRP thicknesses: 1 mm, 2 mm, and 3 mm. The lowest buckling deformation and highest buckling strength were observed during hydroforming of a cylinder shape consisting of 0/90° woven fibre, and 60/30°, $\pm 45^\circ$, and $\pm 55^\circ$ fibre orientation samples. An increase in the FRP layer thickness increases circumferential pressure causing initial buckling. Zafar et al. [382] presented an alternative method of hydromechanical deep drawing to produce FML blanks. Stacks of three Al 2024-O discs, each 0.5 mm thick, were used in the experiment at room temperature. The influence of input parameters blank holder force (7.8–14.9 kN) and cavity pressure (25–55 MPa) on wrinkles and failure were examined. As a result, lower wrinkling was observed for a 11 kN blank holder force and 42 MPa cavity pressure. The hydromechanical deep drawing process seems to be more effective than the conventional stamping process in terms of cost, productivity, and complexity. Using this approach, any type of composite bonding layer can be applied after forming and reheating and solidification treatments can be eliminated. As an extension, in their work, Zafar et al. [383] called this new approach the “3A method”, the use of which permits multiple metal blanks to be formed at once. Figure 37 shows a comparison between a forming method that is well known and thoroughly studied in the literature [395–399] (Figure 37a) and the novel “3A method” (Figure 37b). Three types of thickness of Al2024-O blanks were tested using this method: 0.5 mm, 1.5 mm, and 3×0.5 mm. The respective cavity pressures of 15, 20, and 40 MPa were established as optimal for the blanks. An elevated punching force was observed for $3 \text{ mm} \times 0.5 \text{ mm}$ during forming and explained by additional friction between the layers. The proposed forming method eliminates the need to reheat and re-solidify the thermoplastic-based composite resin system at controlled forming pressures.

Additionally, Zhang et al. [376] analysed the springback and thinning effects using the “3A method” for stacked triple aluminium sheets with a thickness of $3 \text{ mm} \times 0.5 \text{ mm}$ to form a hemispherical radius. A maximum reduction in thickness of the lower layer to 0.43 mm and successful 36 mm forming depth were noted. Liu et al. [400] compared different FMLs, ARALL, CARALL, GLARE, and the effect of their fibre layer type on the forming limit when a standard blank holding force was applied. The GLARE formability limit seems to be higher than the others while CARALL’s was the lowest—lower than for the $3 \times \text{Al}$ stack. It was noted that fibre strain damage and thinning rate of the aluminium sheet are important factors in manufacturing this type of FML.

Numerical and experimental investigations of the effect of the blank holder gap on the hydromechanical deep drawing of FMLs made with 2024-T3 aluminium alloy sheet and W-9011 prepreg woven glass fibre sheets were conducted by Blala et al. [384]. Due to applying the BHF and cavity pressure in the laminate system, the resin plays the role of rubber, which decreases the thickness of the FMLs (Figure 38). Although the value of this reduction is very small, it plays an important role in the available formability of material. Cavity pressure higher than optimal causes the formation of wrinkling starting from the 2024-T3 layer, which is directly in contact with fluid pressure. By contrast, a cavity pressure lower than optimal causes fracture of the FML. FML parts manufactured by considering the optimal value of the blank holding gap (BHG) lead to a reduction in time and effort spent in mass production [401]. An appropriate setting of the BHF, BHG, and cavity pressure ensures the achievement of higher degrees of deformation and the forming of drawpieces with a more complex shape.

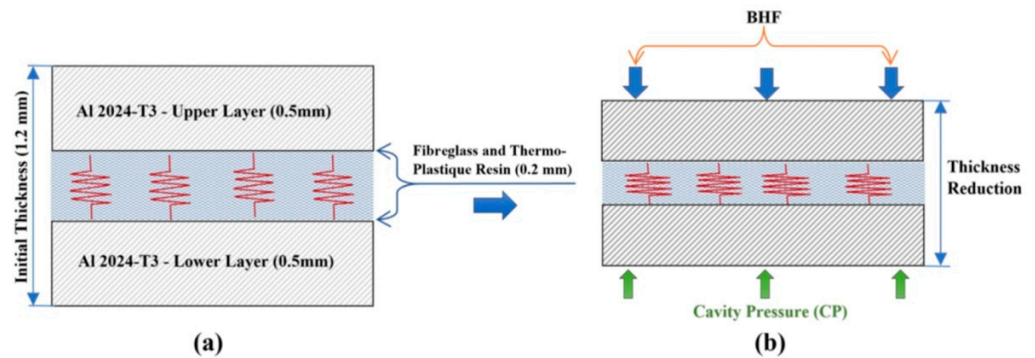


Figure 38. Effect of clamping force on the reduction in FML thickness (reprinted with permission from [384]; copyright© 2021, Springer-Verlag London Ltd., part of Springer Nature).

8.3. Electromagnetic Forming

Electromagnetic forming (EMF) is a contactless and high-speed technology dedicated to form flat and hollow components. A pulsed magnetic field is used to apply Lorentz force to the workpiece, which causes deformation. The EMF process influences such properties as residual stresses, impact toughness, and durability, and its major advantage is that it increases the formability of materials [380,402]. Chernikov et al. [127] compared the electromagnetic forming of five-layer fibre reinforced metal polymer laminates with forming using a rubber pad. The formation of rifts (Figure 39) eliminates the high-velocity impact of the material with the die and the resulting delamination of the blank. It was found that the rift zone was dominated by compressive circumferential strains, rather than tensile radial strains as during conventional rubber pad forming.

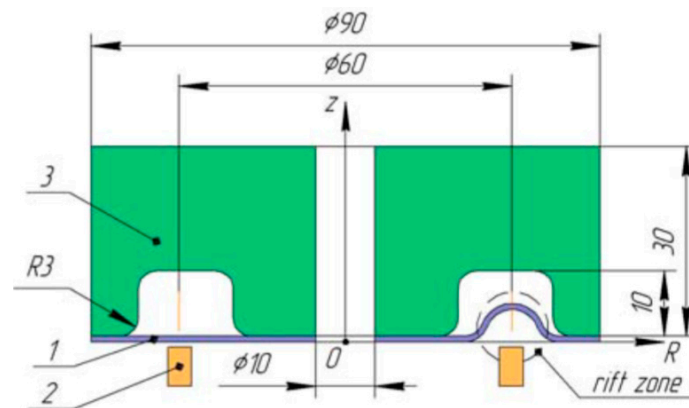


Figure 39. Schematic diagram of free electromagnetic forming: 1—workpiece, 2—coil, 3—die (reprinted with permission from [127]; copyright© 2021, KSAE/112-11).

Glushchenkov et al. [380] applied EMF to a five-layer metal–polymer composite fabricated with a 0.3 mm thickness commercial aluminium with carbon fibre interlayers bounded with two-way reinforced epoxy laminate. The strains have been analysed using the Vic-3D system, before and after deformation, and the results were compared to the rubber pad forming method. The specimens achieved a rift depth of 4.5, 5.15, and 5.35 mm, which equalled an energy charge of 2.49, 2.86, and 3.25 kJ, respectively, compared to the 4.06 mm obtained by rubber pad forming. Compressive circumferential, radial, and equivalent strains on the convex side and lower radial strains were observed and compared to rubber stamping in which there appear circumferential and tensile radial strains. On the concave side, strains were similar in both methods. The occurrence of compressive strains in EMF of the bottom side could increase formability but, on the other hand, could initiate wrinkling. Khardin et al. [381] investigated an Al–polymer–Al (0.3 mm + 0.6 mm + 0.3 mm) sandwich using the electromagnetic bending method. Blanks were made of

two AW-Al Mn1Mg0.5 sheets and a thermoplastic polyolefin middle layer. The authors stated that higher strain values cause an increase in energy level of the electromagnetic field. Part melting of the aluminium sheet was found, which set one of the forming limits. By applying the EMF method, a higher profile height was achieved than with conventional stretching without cracking (>30%).

8.4. Laser Forming

Laser forming technology applies photon irradiation to heat the component surface, which leads to deformation by thermal stress. This forming method is used to produce rapid prototypes, aligning and adjusting the FMLs. The surface of the composite, heated locally along the assumed path, undergoes elastic–plastic deformation as a result of thermal stresses.

Hu et al. [377] investigated laser peen forming (Figure 40) in the manufacture of large size, complex shape FMLs. GLARE 2–0°, GLARE 2–90°, and GLARE 3 specimens were each prepared with a 0.3 mm layer thickness to analyse the effect of fibre orientation on the process. Fibre orientation was a significant factor in the anisotropic properties of FMLs, bending being more advantageous in a perpendicular direction to fibres oriented unidirectionally. It was confirmed that, by this method, a small forming radius could be obtained with an increase in laser scanning time; GLARE 2–0°, GLARE 2–90°, and GLARE 3 specimens gained a 221.8, 91, and 177.3 mm radius concave curvature, respectively. Using this method, the creation of convex bending for different GLARE stacks was obtained with better results of deformation in the perpendicular direction to that of the fibres oriented unidirectionally.

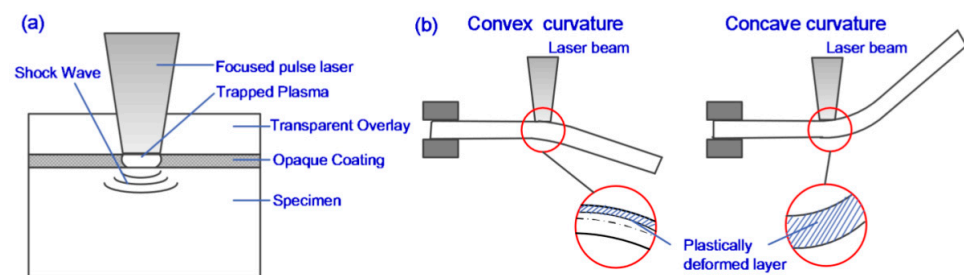


Figure 40. (a) Schematic diagram of laser peening and (b) bending out of plane with concave and convex curvatures (reproduced with permission from [377]; copyright© 2021 Elsevier B.V.).

Gisario and Barletta [385] have studied the impact of laser beam power of the operating parameters (power, scanning speed, and number of passes) on final GLARE 1 and GLARE 2 shape. The range of applicable parameters allowing the achievement of high-quality results and a precise bending angle without thermal effects has been identified. Applying a set of scans at steadily increasing distances can decrease the delamination effect, allowing more deformed profiles to be obtained. For aluminium layers, the occurrence of the tempering phenomenon caused by repeated laser irradiation should be considered in process design. In work by Gisario et al. [386], GLARE 1 and GLARE 2 FMLs were used in research and a multi-layer perceptron artificial neural network (ANN) while a Levenberg–Marquardt algorithm was employed to analyse the data. The artificial neural networks that were developed predicted the temperature and bending angle by a power set and velocity laser beam. The coefficient of determination for temperature $R^2 = 0.978$ and bending angle $R^2 = 0.963$ indicates that ANNs can be an excellent alternative to numerical and analytical models. Gisario and Barletta [385] developed two-stage laser forming of FMLs (Figure 41) to obtain components with precisely controlled bending radii.

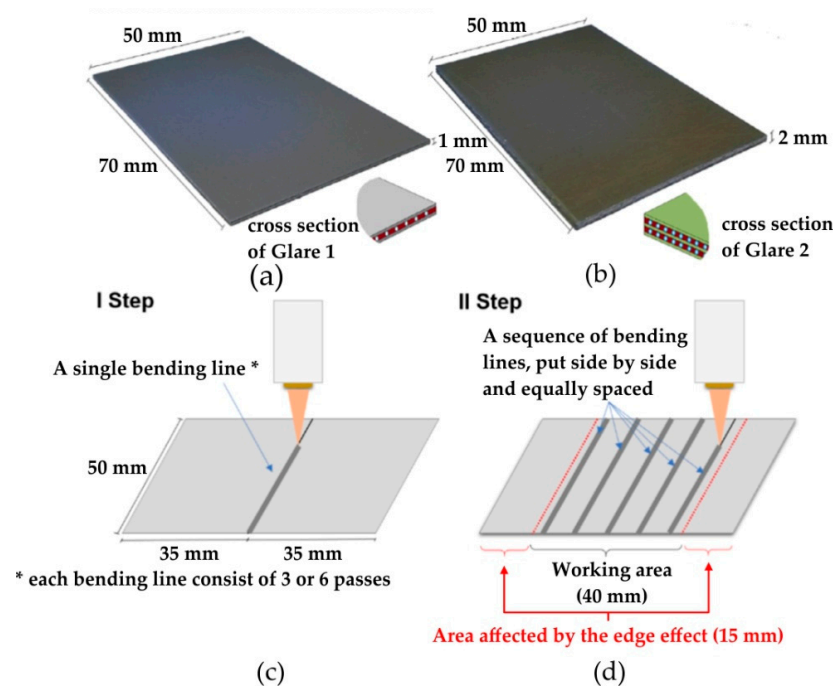


Figure 41. Visual appearance and cross-section of (a) GLARE 1 and (b) GLARE 2, and the experimental set-up of the (c) first and (d) second investigation (reproduced with permission from [385]; copyright© 2021 Elsevier Ltd.).

9. Summary and Future Trends

Plastic working technologies allow material to be given appropriate functional properties, which depend on the rheological conditions of the forming process. Metal processing and manufacturing is one of the most important segments of the industrial processing sector. In addition to the continuous improvement of the existing methods of plastic forming, new technologies are also being brought into use, the purpose of which is to reduce the energy consumption of processing, modernise technological machines, tools, and create environmentally friendly forming conditions in line with the climate policy of the European Union countries.

The review of the literature on the methods of forming of hybrid metal–polymer composites presented here triggered the following conclusions in the minds of the authors:

- Up to now, the target industry associated with FMLs has been the aviation industry focused on the use of lightweight components with relatively high strength. Progress in plastic forming technologies is also stimulated by developments in the automotive industry, which are full of exogenous innovations, primarily new production technologies and a new machine park. In the context of the Industry 4.0 concept, the development of the technology of plastic processing of aluminium alloy-based FMLs can be a stimulus for the introduction of innovative materials in the shipbuilding industry, in the production of yachts, autonomous vehicles, and light personal air land vehicles.
- Research on forming aluminium alloy-based FMLs commonly used in aerospace applications has been extended to other materials such as titanium and steel. The latter material, when used as a component of composites, can lower manufacturing costs in the automotive industry. Pressure from governments to reduce CO₂ emissions from transport will increase. In this context, weight reduction will continue to be the focus of vehicle manufacturers, and composites and other lightweight construction materials will play an increasingly important role.
- Press-brake bending of single curvature components is being replaced by alternative laser bending technologies and the formation of shot peening. Existing research confirms their high efficiency when bending plates with large curvatures and in many

planes at the same time. However, due to the longer processing time, these methods are most productive in small lot production.

- The growing interest of industry in lightweight and high strength composite structures brings the need to solve the problem of ensuring subsequent ecological recycling. It is necessary to develop new technologies for the management of post-consumer waste or to modify the current technology of producing FMLs. Thermoplastics have lower strength and a lower modulus of elasticity than epoxy or polyester resins, but show better recyclability.
- The new opportunities created by material engineering allow the fabrication of new FMLs with previously unknown properties, as well as modifying those already known in order to adapt them to new applications and reduce production and material costs. Currently, investigations are conducted on the use of nanofillers, such as single-walled or multi-walled nanotubes, to strengthen and stiffen composites.
- One of the ways to increase the deformability of composites using plastic working methods is to perform the forming process at an elevated temperature. Although an increase in temperature improved the formability of composites, the forming temperature is limited by the melting temperature of the polymer matrix and the glass transition temperature of HMPC. The temperature windows for HMPC forming are not well understood because most of the industrially used composites are still being shaped in cold forming conditions.
- Increasing the productivity and lowering the cost of producing composites is possible through the use of optimal material combinations of layers of thin metal sheets and composite. The introduction of cheap, high strength steel sheets and new thermoplastic polymers may open new windows for the use of composites that are cheap to produce and easy to recycle.
- Reducing the prices of components for the production of composites, as well as the dissemination of automated manufacturing methods, such as filament winding and RTM, have led to the development of 3D reinforcement-based spatial laminates. Designers show greater confidence in such composites than in classic composites due to the elimination of the risk of delamination.
- A critical failure phenomenon in metal–fibre laminates, in addition to poor adhesion at the metal–composite interface, is poor adhesion at the reinforcing fibre–matrix interface, leading to delamination. In order to achieve the desired shape-dimensional quality of FML elements and optimal formability, an in-depth understanding of the mechanisms of their forming, including the use of non-destructive methods of defect detection, is required.

Author Contributions: Conceptualization, T.T.; methodology, T.T., S.M.N., M.S. (Manel Sbayti), H.B., M.S. (Marcin Szpunar) and H.G.L.; validation, T.T., S.M.N., M.S. (Manel Sbayti), H.B., M.S. (Marcin Szpunar) and H.G.L.; investigation, T.T., S.M.N., M.S. (Manel Sbayti), H.B., M.S. (Marcin Szpunar) and H.G.L.; resources, T.T., S.M.N., M.S. (Manel Sbayti), H.B., M.S. (Marcin Szpunar) and H.G.L.; data curation, T.T., S.M.N., M.S. (Manel Sbayti), H.B., M.S. (Marcin Szpunar) and H.G.L.; writing—original draft preparation, T.T., S.M.N., M.S. (Manel Sbayti), H.B., M.S. (Marcin Szpunar) and H.G.L.; writing—review and editing, T.T. All authors have read and agreed to the published version of the manuscript.

Funding: This research received no external funding.

Institutional Review Board Statement: Not applicable.

Informed Consent Statement: Not applicable.

Data Availability Statement: The data presented in this study are available on request from the corresponding author.

Conflicts of Interest: The authors declare no conflict of interest.

References

1. Yamada, K.; Kötter, B.; Nishikawa, M.; Fukudome, S.; Matsuda, N.; Kawabe, K.; Fiedler, B.; Hojo, M. Mechanical Properties and Failure Mode of Thin-Ply Fiber Metal Laminates under out-of-Plane Loading. *Compos. Part A Appl. Sci. Manuf.* **2021**, *143*, 106267. [[CrossRef](#)]
2. Rao, N.N.; Rao, P.M.V.; Kumar, S. A Numerical Approach to Estimate First Ply Failure of Fibre Metal Laminate. *Rev. Compos. Matériaux Av.* **2021**, *31*, 33–39. [[CrossRef](#)]
3. Fraçz, W.; Janowski, G. Predicting effect of fiber orientation on chosen strength properties of wood-polymer composites. *Compos. Theory Pract.* **2019**, *19*, 56–63.
4. Mottaghian, F.; Yaghoobi, H.; Taheri, F. Numerical and Experimental Investigations into Post-Buckling Responses of Stainless Steel- and Magnesium-Based 3D-Fiber Metal Laminates Reinforced by Basalt and Glass Fabrics. *Compos. Part B Eng.* **2020**, *200*, 108300. [[CrossRef](#)]
5. Cortés, P.; Cantwell, W.J. The Fracture Properties of a Fibre–Metal Laminate Based on Magnesium Alloy. *Compos. Part B Eng.* **2005**, *37*, 163–170. [[CrossRef](#)]
6. Alderliesten, R.; Rans, C.; Benedictus, R. The Applicability of Magnesium Based Fibre Metal Laminates in Aerospace Structures. *Compos. Sci. Technol.* **2008**, *68*, 2983–2993. [[CrossRef](#)]
7. Sharma, A.P.; Velmurugan, R.; Shankar, K.; Ha, S. High-Velocity Impact Response of Titanium-Based Fiber Metal Laminates. Part II: Analytical Modeling. *Int. J. Impact Eng.* **2021**, *152*, 103853. [[CrossRef](#)]
8. Sharma, A.P.; Velmurugan, R. Uni-Axial Tensile Response and Failure of Glass Fiber Reinforced Titanium Laminates. *Thin-Walled Struct.* **2020**, *154*, 106859. [[CrossRef](#)]
9. Rahiminejad, D.; Compston, P. The Effect of Pre-Heat Temperature on the Formability of a Glass-Fibre/Polypropylene and Steel-Based Fibre–Metal Laminate. *Int. J. Mater. Form.* **2021**, *14*, 715–727. [[CrossRef](#)]
10. van Rooijen, R.G.J.; Sinke, J.; van der Zwaag, S. Improving the Adhesion of Thin Stainless Steel Sheets for Fibre Metal Laminate (FML) Applications. *J. Adhes. Sci. Technol.* **2005**, *19*, 1387–1396. [[CrossRef](#)]
11. Dreaves, A. Potential Use of Fibre-Steel Laminates in Hybrid Deck Systems. Master’s Thesis, Delft University of Technology, Delft, The Netherlands, 2018.
12. Park, S.Y.; Choi, W.J. The Guidelines of Material Design and Process Control on Hybrid Fiber Metal Laminate for Aircraft Structures. In *Optimum Composite Structures*; Maalawi, J., Ed.; IntechOpen: London, UK, 2019; pp. 125–168.
13. Monsalve, A.; Parra, L.; Baeza, D.; Solís, R.; Palza, H. Mechanical Properties and Morphological Characteristics of ARALL Reinforced with TRGO Doped Epoxy Resin. *Matéria* **2018**, *23*. [[CrossRef](#)]
14. Jerome, J.; Hynes, N.R.J.; Sankaranarayanan, R. Mechanical Behavioural Testing of Fibre Metal Laminate Composites. *AIP Conf. Proc.* **2020**, *2220*, 140035. [[CrossRef](#)]
15. Chen, Y.; Wang, Y.; Wang, H. Research Progress on Interlaminar Failure Behavior of Fiber Metal Laminates. *Adv. Polym. Technol.* **2020**, *2020*, 3097839. [[CrossRef](#)]
16. Asghar, W.; Nasir, M.A.; Qayyum, F.; Shah, M.; Azeem, M.; Nauman, S.; Khushnood, S. Investigation of Fatigue Crack Growth Rate in CARALL, ARALL and GLARE. *Fatigue Fract. Eng. Mater. Struct.* **2017**, *40*, 1086–1100. [[CrossRef](#)]
17. Sinmazçelik, T.; Avcu, E.; Bora, M.Ö.; Çoban, O. A Review: Fibre Metal Laminates, Background, Bonding Types and Applied Test Methods. *Mater. Des.* **2011**, *32*, 3671–3685. [[CrossRef](#)]
18. Lin, Y.; Huang, Y.; Huang, T.; Liao, B.; Zhang, D.; Li, C. Characterization of Progressive Damage Behaviour and Failure Mechanisms of Carbon Fibre Reinforced Aluminium Laminates under Three-Point Bending. *Thin-Walled Struct.* **2019**, *135*, 494–506. [[CrossRef](#)]
19. Vermeeren, C.A.J.R. *The Application of Carbon Fibres in ARALL Laminates*; Report LR-658; Delft University of Technology, Faculty of Aerospace Engineering: Delft, The Netherlands, 1991.
20. Shi, Y.; Pinna, C.; Soutis, C. Impact Damage Characteristics of Carbon Fibre Metal Laminates: Experiments and Simulation. *Appl. Compos. Mater.* **2020**, *27*, 511–531. [[CrossRef](#)]
21. Kubit, A.; Trzepieciński, T.; Krasowski, B.; Slota, J.; Spišák, E. Strength Analysis of a Rib-Stiffened GLARE-Based Thin-Walled Structure. *Materials* **2020**, *13*, 2929. [[CrossRef](#)]
22. Blala, H.; Lang, L.; Khan, S.; Li, L. A Comparative Study on the GLARE Stamp Forming Behavior Using Cured and Non-Cured Preparation Followed by Hot-Pressing. *Int. J. Adv. Manuf. Technol.* **2021**, *115*, 1461–1473. [[CrossRef](#)]
23. Abouhamzeh, M.; Smyth, N.; Sinke, J. On the Measurement of Residual Stresses in Fibre Metal Laminates. *Int. J. Adv. Manuf. Technol.* **2021**, *113*, 1663–1671. [[CrossRef](#)]
24. Giurgiutiu, V. Chapter 1—Introduction. In *Structural Health Monitoring of Aerospace Composites*; Giurgiutiu, V., Ed.; Academic Press: Oxford, UK, 2016; pp. 1–23.
25. Teresko, J. Boeing 787: A Matter of Materials—Special Report: Anatomy of a Supply Chain. Available online: <https://www.industryweek.com/leadership/companies-executives/article/21942033/boeing-787-a-matter-of-materials-special-report-anatomy-of-a-supply-chain> (accessed on 15 June 2021).
26. Ucan, H.; Scheller, J.; Nguyen, C.; Nieberl, D.; Beumler, T.; Haschenburger, A.; Meister, S.; Kappel, E.; Prussak, R.; Deden, D.; et al. Automated, Quality Assured and High Volume Oriented Production of Fiber Metal Laminates (FML) for the Next Generation of Passenger Aircraft Fuselage Shells. *Sci. Eng. Compos. Mater.* **2019**, *26*, 502–508. [[CrossRef](#)]

27. Bachmann, J.; Hidalgo, C.; Bricout, S. Environmental Analysis of Innovative Sustainable Composites with Potential Use in Aviation Sector—A Life Cycle Assessment Review. *Sci. China Technol. Sci.* **2017**, *60*, 1301–1317. [[CrossRef](#)]
28. Tadini, P.; Grange, N.; Chetehouna, K.; Gascoin, N.; Senave, S.; Reynaud, I. Thermal Degradation Analysis of Innovative PEKK-Based Carbon Composites for High-Temperature Aeronautical Components. *Aerosp. Sci. Technol.* **2017**, *65*, 106–116. [[CrossRef](#)]
29. Aamir, M.; Tolouei-Rad, M.; Giasin, K.; Nosrati, A. Recent Advances in Drilling of Carbon Fiber-Reinforced Polymers for Aerospace Applications: A Review. *Int. J. Adv. Manuf. Technol.* **2019**, *105*, 2289–2308. [[CrossRef](#)]
30. Hassanalain, M.; Abdelkefi, A. Classifications, Applications, and Design Challenges of Drones: A Review. *Prog. Aerosp. Sci.* **2017**, *91*, 99–131. [[CrossRef](#)]
31. Hassanalain, M.; Rice, D.; Abdelkefi, A. Evolution of Space Drones for Planetary Exploration: A Review. *Prog. Aerosp. Sci.* **2018**, *97*, 61–105. [[CrossRef](#)]
32. Xu, Y.; Zhu, J.; Wu, Z.; Cao, Y.; Zhao, Y.; Zhang, W. A Review on the Design of Laminated Composite Structures: Constant and Variable Stiffness Design and Topology Optimization. *Adv. Compos. Hybrid Mater.* **2018**, *1*, 460–477. [[CrossRef](#)]
33. Ye, J.; Wang, H.; Dong, J.; Liu, C.; Gao, Y.; Gong, B.; Su, B.; Peng, H.-X. Metal Surface Nanopatterning for Enhanced Interfacial Adhesion in Fiber Metal Laminates. *Compos. Sci. Technol.* **2021**, *205*, 108651. [[CrossRef](#)]
34. Rubio-González, C.; Chávez, F.; José-Trujillo, E.; Rodríguez-González, J.A.; Ruiz, A. Impact Behavior of Carbon Fiber/Epoxy Composites and Fiber Metal Laminates with Open Holes. *Fibers Polym.* **2021**, *22*, 772–785. [[CrossRef](#)]
35. Wu, X.; Zhan, L.; Huang, M.; Zhao, X.; Wang, X.; Zhao, G. Corrosion Damage Evolution and Mechanical Properties of Carbon Fiber Reinforced Aluminum Laminate. *J. Cent. South Univ.* **2021**, *28*, 657–668. [[CrossRef](#)]
36. Wang, C.; Yao, L.; He, W.; Cui, X.; Wu, J.; Xie, D. Effect of Elliptical Notches on Mechanical Response and Progressive Damage of FMLs under Tensile Loading. *Thin-Walled Struct.* **2020**, *154*, 106866. [[CrossRef](#)]
37. Pan, L.; Wang, Y.; Hu, Y.; Lv, Y.; Ali, A.; Roy, N.; Ma, W.; Tao, J. Investigation on the Effect of Configuration on Tensile and Flexural Properties of Aluminum/Self-Reinforced Polypropylene Fiber Metal Laminates. *J. Sandw. Struct. Mater.* **2020**, *22*, 1770–1785. [[CrossRef](#)]
38. Logesh, K.; Hariharasakthisudhan, P.; Rajan, B.S.; Moshi, A.A.M.; Khalkar, V. Effect of Multi-Walled Carbon Nano-Tube on Mechanical Behavior of Glass Laminate Aluminum Reinforced Epoxy Composites. *Polym. Compos.* **2020**, *41*, 4849–4860. [[CrossRef](#)]
39. Zhu, W.; Xiao, H.; Wang, J.; Li, X. Effect of Coupling Agent Quantity on Composite Interface Structure and Properties of Fiber Metal Laminates. *Polym. Compos.* **2021**, *42*, 3195–3205. [[CrossRef](#)]
40. Zhou, X.; Zhao, Y.; Chen, X.; Liu, Z.; Li, J.; Fan, Y. Fabrication and Mechanical Properties of Novel CFRP/Mg Alloy Hybrid Laminates with Enhanced Interface Adhesion. *Mater. Des.* **2021**, *197*, 109251. [[CrossRef](#)]
41. Li, L.; Lang, L.; Hamza, B.; Zhang, Q. Effect of Hydroforming Process on the Formability of Fiber Metal Laminates Using Semi-Cured Preparation. *Int. J. Adv. Manuf. Technol.* **2020**, *107*, 3909–3920. [[CrossRef](#)]
42. Morgado, M.A.; Carbas, R.J.C.; Marques, E.A.S.; da Silva, L.F.M. Reinforcement of CFRP Single Lap Joints Using Metal Laminates. *Compos. Struct.* **2019**, *230*, 111492. [[CrossRef](#)]
43. Nassir, N.A.; Birch, R.S.; Cantwell, W.J.; Al Teneiji, M.; Guan, Z.W. The Perforation Resistance of Aluminum-Based Thermoplastic FMLs. *Appl. Compos. Mater.* **2021**, *28*, 587–605. [[CrossRef](#)]
44. Bikakis, G.S.; Kalfountzos, C.D.; Theotokoglou, E.E. Elastic Buckling of Rectangular Fiber-Metal Laminated Plates under Uniaxial Compression. *J. Thermoplast. Compos. Mater.* **2020**, *33*, 1629–1651. [[CrossRef](#)]
45. Zhang, X.; Meng, W.; Zhang, T.; Huang, X.; Hou, S. Analysis and Research on Solution Method of Metal Layer Stress in Fiber Metal Laminates. *Mater. Res. Express* **2020**, *7*, 116514. [[CrossRef](#)]
46. Yelamanchi, B.; MacDonald, E.; Gonzalez-Canche, N.G.; Carrillo, J.G.; Cortes, P. The Mechanical Properties of Fiber Metal Laminates Based on 3D Printed Composites. *Materials* **2020**, *13*, 5264. [[CrossRef](#)]
47. Minchenkov, K.; Vedernikov, A.; Safonov, A.; Akhatov, I. Thermoplastic Pultrusion: A Review. *Polymers* **2021**, *13*, 180. [[CrossRef](#)] [[PubMed](#)]
48. Park, S.Y.; Choi, W.J.; Choi, H.S. A Comparative Study on the Properties of GLARE Laminates Cured by Autoclave and Autoclave Consolidation Followed by Oven Postcuring. *Int. J. Adv. Manuf. Technol.* **2010**, *49*, 605–613. [[CrossRef](#)]
49. Poodts, E.; Ghelli, D.; Brugo, T.; Panciroli, R.; Minak, G. Experimental Characterization of a Fiber Metal Laminate for Underwater Applications. *Compos. Struct.* **2015**, *129*, 36–46. [[CrossRef](#)]
50. Keshavarz, R.; Aghamohammadi, H.; Eslami-Farsani, R. The Effect of Graphene Nanoplatelets on the Flexural Properties of Fiber Metal Laminates under Marine Environmental Conditions. *Int. J. Adhes. Adhes.* **2020**, *103*, 102709. [[CrossRef](#)]
51. Li, H.; Hu, Y.; Xu, Y.; Wang, W.; Zheng, X.; Liu, H.; Tao, J. Reinforcement Effects of Aluminum-Lithium Alloy on the Mechanical Properties of Novel Fiber Metal Laminate. *Compos. Part B Eng.* **2015**, *82*, 72–77. [[CrossRef](#)]
52. Ding, Z.; Wang, H.; Luo, J.; Li, N. A Review on Forming Technologies of Fibre Metal Laminates. *Int. J. Lightweight Mater. Manuf.* **2021**, *4*, 110–126. [[CrossRef](#)]
53. Wang, H.; Tao, J.; Jin, K. The Effect of MWCNTs with Different Diameters on the Interface Properties of Ti/CFRP Fiber Metal Laminates. *Compos. Struct.* **2021**, *266*, 113818. [[CrossRef](#)]
54. Kiss, P.; Glinz, J.; Stadlbauer, W.; Burgstaller, C.; Archodoulaki, V.-M. The Effect of Thermally Desized Carbon Fibre Reinforcement on the Flexural and Impact Properties of PA6, PPS and PEEK Composite Laminates: A Comparative Study. *Compos. Part B Eng.* **2021**, *215*, 108844. [[CrossRef](#)]

55. Lin, L.; Schlarb, A.K. Development and Optimization of High-Performance PEEK/CF/Nanosilica Hybrid Composites. *Polym. Adv. Technol.* **2021**, *32*, 3150–3159. [CrossRef]
56. Reyes, G.; Gupta, S. Manufacturing and Mechanical Properties of Thermoplastic Hybrid Laminates Based on DP500 Steel. *Compos. Part A Appl. Sci. Manuf.* **2009**, *40*, 176–183. [CrossRef]
57. Iriondo, J.; Aretxabaleta, L.; Aizpuru, A. Characterisation of the Elastic and Damping Properties of Traditional FML and FML Based on a Self-Reinforced Polypropylene. *Compos. Struct.* **2015**, *131*, 47–54. [CrossRef]
58. Prasad, E.V.; Sivateja, C.; Sahu, S.K. Effect of Nanoalumina on Fatigue Characteristics of Fiber Metal Laminates. *Polym. Test.* **2020**, *85*, 106441. [CrossRef]
59. Meng, X.; Yao, L.; Wang, C.; He, W.; Xie, L.; Zhang, H. Investigation on the Low-Velocity Impact Behaviour of Non-Symmetric FMLs—Experimental and Numerical Methods. *Int. J. Crashworthiness* **2020**, 1–19. [CrossRef]
60. Muthukumar, C.; Ishak, M.; Sapuan, S.; Leman, Z.; Jawaid, M.; Jesuarockiam, N. Mechanical Properties of a Novel Fibre Metal Laminate Reinforced with the Carbon, Flax, and Sugar Palm Fibres. *Bioresources* **2018**, *13*, 5725–5739. [CrossRef]
61. Ebrahimnezhad-Khaljiri, H.; Eslami-Farsani, R.; Talebi, S. Investigating the High Velocity Impact Behavior of the Laminated Composites of Aluminum/Jute Fibers- Epoxy Containing Nanoclay Particles. *Fibers Polym.* **2020**, *21*, 2607–2613. [CrossRef]
62. Abd El-baky, M.; Alshorbagy, A.; Alsaedy, A.; Megahed, M. Fabrication of Cost Effective Fiber Metal Laminates Based on Jute and Glass Fabrics for Enhanced Mechanical Properties. *J. Nat. Fibers* **2020**, 1–16. [CrossRef]
63. Hussain, M.; Imad, A.; Saouab, A.; Nawab, Y.; Kanit, T.; Herbelot, C.; Muhammad, K. Properties and Characterization of Novel 3D Jute Reinforced Natural Fibre Aluminium Laminates. *J. Compos. Mater.* **2020**, *55*, 1879–1891. [CrossRef]
64. Mohammed, I.; Abu Talib, A.R.; Sultan, M.T.H.; Jawaid, M.; Ariffin, A.H.; Saadon, S. Mechanical Properties of Fibre-Metal Laminates Made of Natural/Synthetic Fibre Composites. *BioResources* **2018**, *13*, 2022–2034. [CrossRef]
65. Aghamohammadi, H.; Eslami-Farsani, R.; Tcharkhtchi, A. The Effect of Multi-Walled Carbon Nanotubes on the Mechanical Behavior of Basalt Fibers Metal Laminates: An Experimental Study. *Int. J. Adhes. Adhes.* **2020**, *98*, 102538. [CrossRef]
66. Abbandanak, S.; Azghan, M.; Zamani, A.; Fallahnejad, M.; Farsani, R.; Siadati, M.H. Effect of Graphene on the Interfacial and Mechanical Properties of Hybrid Glass/Kevlar Fiber Metal Laminates. *J. Ind. Text.* **2020**, 1528083720932222. [CrossRef]
67. Eslami-Farsani, R.; Aghamohammadi, H.; Khalili, S.M.R.; Ebrahimnezhad-Khaljiri, H.; Jalali, H. Recent Trend in Developing Advanced Fiber Metal Laminates Reinforced with Nanoparticles: A Review Study. *J. Ind. Text.* **2020**, 1528083720947106. [CrossRef]
68. PRISMA. Available online: <http://www.prisma-statement.org/> (accessed on 25 June 2021).
69. Sinke, J. Development of Fibre Metal Laminates: Concurrent Multi-Scale Modeling and Testing. *J. Mater. Sci.* **2006**, *41*, 6777–6788. [CrossRef]
70. Vlot, A.; Vogelesang, L.B.; de Vries, T.J. Towards Application of Fibre Metal Laminates in Large Aircraft. *Aircr. Eng. Aerosp. Technol.* **1999**, *71*, 558–570. [CrossRef]
71. Vlot, A. *Glare: History of the Development of a New Aircraft Material*; Springer: Dordrecht, The Netherlands, 2001.
72. Vermeeren, C.A.J.R. An Historic Overview of the Development of Fibre Metal Laminates. *Appl. Compos. Mater.* **2003**, *10*, 189–205. [CrossRef]
73. Alderliesten, R.C.; Schut, J.E. Delamination Growth Rate at Low and Elevated Temperatures in GLARE. In Proceedings of the 25th International Congress on the Aeronautical Sciences, Hamburg, Germany, 3–8 September 2006; Available online: http://www.icas.org/ICAS_ARCHIVE/ICAS2006/PAPERS/148.PDF (accessed on 12 July 2021).
74. Vogelesang, L.B.; Gunnink, J.W. Arall: A Materials Challenge for the next Generation of Aircraft. *Mater. Des.* **1986**, *7*, 287–300. [CrossRef]
75. Vogelesang, L.B.; Gunnink, J.W.; Chen, D.; Roebroeks, G.H.J.J.; Vlot, A. New Developments in ARALL Laminates. In Proceedings of the International Council of the Aeronautical Sciences (ICAS) Conference, Jerusalem, Israel, 28 August 1988; pp. 1615–1633.
76. Vogelesang, L.B.; Vlot, A. Development of Fibre Metal Laminates for Advanced Aerospace Structures. *J. Mater. Process. Technol.* **2000**, *103*, 1–5. [CrossRef]
77. Moussavi-Torshizi, S.E.; Dariushi, S.; Sadighi, M.; Safarpour, P. A Study on Tensile Properties of a Novel Fiber/Metal Laminates. *Mater. Sci. Eng. A* **2010**, *527*, 4920–4925. [CrossRef]
78. Sinke, J. Manufacturing Principles for Fiber Metal Laminates. Available online: <https://www.semanticscholar.org/paper/MANUFACTURING-PRINCIPLES-FOR-FIBER-METAL-LAMINATES-Sinke/0895984469cc00f46aca4267b31e61329c27a8eb> (accessed on 26 June 2021).
79. Kaleeswaran, P.; KiranBabu, K.M.; Kumar, B.S. Fabrication of Fibre Metal Laminate (FML) and Evaluation of Its Mechanical Properties. *Int. J. Appl. Eng. Res.* **2014**, *9*, 8872–8874.
80. de Boer, T. Next Generation Fibre Metal Laminates. In *Fibre Metal Laminates: An Introduction*; Vlot, A., Gunnink, J.W., Eds.; Springer: Dordrecht, The Netherlands, 2001; pp. 39–51.
81. Kuznetsova, R.; Ergun, H.; Liaw, B. Acoustic Emission of Failure in Fiber-Metal Laminates. In *Nondestructive Testing of Materials and Structures*; Büyüköztürk, O., Taşdemir, M.A., Güneş, O., Akkaya, Y., Eds.; Springer: Dordrecht, The Netherlands, 2013; pp. 619–625.
82. Mohamed, G.F.A.; Soutis, C.; Hodzic, A. Blast Resistance and Damage Modelling of Fibre Metal Laminates to Blast Loads. *Appl. Compos. Mater.* **2012**, *19*, 619–636. [CrossRef]
83. Carey, C.; Cantwell, W.J.; Dearden, G.; Edwards, K.R.; Edwardson, S.P.; Watkins, K.G. Towards a Rapid, Non-Contact Shaping Method for Fibre Metal Laminates Using a Laser Source. *Int. J. Adv. Manuf. Technol.* **2010**, *47*, 557–565. [CrossRef]

84. Tarpani, A.C.S.P.; Barreto, T.A.; Tarpani, J.R. Fatigue Failure Analysis of Riveted Fibre-Metal Laminate Lap Joints. *Eng. Fract. Mech.* **2020**, *239*, 107275. [[CrossRef](#)]
85. Kashfi, M.; Majzoubi, G.H.; Bonora, N.; Iannitti, G.; Ruggiero, A.; Khademi, E. A New Overall Nonlinear Damage Model for Fiber Metal Laminates Based on Continuum Damage Mechanics. *Eng. Fract. Mech.* **2019**, *206*, 21–33. [[CrossRef](#)]
86. Blala, H.; Lang, L.; Li, L.; Alexandrov, S. Deep Drawing of Fiber Metal Laminates Using an Innovative Material Design and Manufacturing Process. *Compos. Commun.* **2021**, *23*, 100590. [[CrossRef](#)]
87. Xu, P.; Zhou, Z.; Liu, T.; Mal, A. Determination of Geometric Role and Damage Assessment in Hybrid Fiber Metal Laminate (FML) Joints Based on Acoustic Emission. *Compos. Struct.* **2021**, *270*, 114068. [[CrossRef](#)]
88. Frizzell, R.M.; McCarthy, C.T.; McCarthy, M.A. A Comparative Study of the Pin-Bearing Responses of Two Glass-Based Fibre Metal Laminates. *Compos. Sci. Technol.* **2008**, *68*, 3314–3321. [[CrossRef](#)]
89. McCarthy, M.A.; Xiao, J.R.; Petrinic, N.; Kamoulakos, A.; Melito, V. Modelling of Bird Strike on an Aircraft Wing Leading Edge Made from Fibre Metal Laminates—Part 1: Material Modelling. *Appl. Compos. Mater.* **2004**, *11*, 295–315. [[CrossRef](#)]
90. Wilk, M.S.; Śliwa, R.E. The influence of features of aluminium alloys 2024, 6061 and 7075 on the properties of Glare-type composites. *Arch. Metall. Mater.* **2015**, *60*, 3101–3108. [[CrossRef](#)]
91. Figueroa, J.G.M.; Llanas, P.I.A. Fracture Toughness of Fiber Metal Laminates through the Concepts of Stiffness and Strain-Intensity-Factor. In Proceedings of the 17th International Conference on New Trends in Fatigue and Fracture, Cancun, Mexico, 25–27 October 2017; Ambriz, R.R., Jaramillo, D., Plascencia, G., Nait Abdelaziz, M., Eds.; Springer International Publishing: Cham, Germany, 2018; pp. 313–328.
92. Backman, D.; Patterson, E.A. Effect of Cold Working on Crack Growth from Holes in Fiber Metal Laminates. *Exp. Mech.* **2012**, *52*, 1033–1045. [[CrossRef](#)]
93. Khan, S.H.; Sharma, A.P. Failure Assessment of Fiber Metal Laminates Based on Metal Layer Dispersion under Dynamic Loading Scenario. *Eng. Fail. Anal.* **2019**, *106*, 104182. [[CrossRef](#)]
94. Merzuki, M.N.M.; Ma, Q.; Rejab, M.R.M.; Sani, M.S.M.; Zhang, B. Experimental and Numerical Investigation of Fibre-Metal-Laminates (FMLs) under Free Vibration Analysis. *Mater. Today Proc.* **2021**, S2214785321015297. [[CrossRef](#)]
95. Keipour, S.; Gerdooei, M. Springback Behavior of Fiber Metal Laminates in Hat-Shaped Draw Bending Process: Experimental and Numerical Evaluation. *Int. J. Adv. Manuf. Technol.* **2019**, *100*, 1755–1765. [[CrossRef](#)]
96. Taheri-Behrooz, F.; Shokrieh, M.M.; Yahyapour, I. Effect of Stacking Sequence on Failure Mode of Fiber Metal Laminates under Low-Velocity Impact. *Iran Polym. J.* **2014**, *23*, 147–152. [[CrossRef](#)]
97. Wang, J.; Li, J.; Fu, C.; Zhang, G.; Zhu, W.; Li, X.; Yanagimoto, J. Study on Influencing Factors of Bending Springback for Metal Fiber Laminates. *Compos. Struct.* **2021**, *261*, 113558. [[CrossRef](#)]
98. Mahendrarajah, G.; Kandare, E.; Khatibi, A.A. Enhancing the Fracture Toughness Properties by Introducing Anchored Nano-Architectures at the Metal–FRP Composite Interface. *J. Compos. Sci.* **2019**, *3*, 17. [[CrossRef](#)]
99. Sadighi, M.; Pärnänen, T.; Alderliesten, R.C.; Sayeafabi, M.; Benedictus, R. Experimental and Numerical Investigation of Metal Type and Thickness Effects on the Impact Resistance of Fiber Metal Laminates. *Appl. Compos. Mater.* **2012**, *19*, 545–559. [[CrossRef](#)]
100. Russig, C.; Bambach, M.; Hirt, G.; Holtmann, N. Shot Peen Forming of Fiber Metal Laminates on the Example of GLARE®. *Int. J. Mater. Form.* **2014**, *7*, 425–438. [[CrossRef](#)]
101. Reyes, G.; Cantwell, W.J. The Effect of Strain Rate on the Interfacial Fracture Properties of Carbon Fiber-Metal Laminates. *J. Mater. Sci. Lett.* **1998**, *17*, 1953–1955. [[CrossRef](#)]
102. Li, L.; Lang, L.; Khan, S.; Wang, Y. Investigation into Effect of the Graphene Oxide Addition on the Mechanical Properties of the Fiber Metal Laminates. *Polym. Test.* **2020**, *91*, 106766. [[CrossRef](#)]
103. Cepeda-Jiménez, C.M.; Alderliesten, R.C.; Ruano, O.A.; Carreño, F. Damage Tolerance Assessment by Bend and Shear Tests of Two Multilayer Composites: Glass Fibre Reinforced Metal Laminate and Aluminium Roll-Bonded Laminate. *Compos. Sci. Technol.* **2009**, *69*, 343–348. [[CrossRef](#)]
104. Kuang, K.S.C.; Cantwell, W.J.; Zhang, L.; Bennion, I.; Maalej, M.; Quek, S.T. Damage Monitoring in Aluminum-Foam Sandwich Structures Based on Thermoplastic Fibre-Metal Laminates Using Fibre Bragg Gratings. *Compos. Sci. Technol.* **2005**, *65*, 1800–1807. [[CrossRef](#)]
105. Langdon, G.; Nurick, G.; Lemanski, S.; Simmons, M.; Cantwell, W.; Schleyer, G. Failure Characterisation of Blast-Loaded Fibre-Metal Laminate Panels Based on Aluminium and Glass–Fibre Reinforced Polypropylene. *Compos. Sci. Technol.* **2007**, *67*, 1385–1405. [[CrossRef](#)]
106. Abdullah, M.R.; Prawoto, Y.; Cantwell, W.J. Interfacial Fracture of the Fibre-Metal Laminates Based on Fibre Reinforced Thermoplastics. *Mater. Des.* **2015**, *66*, 446–452. [[CrossRef](#)]
107. Vo, T.P.; Guan, Z.W.; Cantwell, W.J.; Schleyer, G.K. Modelling of the Low-Impulse Blast Behaviour of Fibre–Metal Laminates Based on Different Aluminium Alloys. *Compos. Part B Eng.* **2013**, *44*, 141–151. [[CrossRef](#)]
108. Abdullah, M.; Cantwell, W. The Impact Resistance of Polypropylene-Based Fibre–Metal Laminates. *Compos. Sci. Technol.* **2006**, *66*, 1682–1693. [[CrossRef](#)]
109. Kulkarni, R.R.; Chawla, K.K.; Vaidya, U.K.; Koopman, M.C.; Eberhardt, A.W. Characterization of Long Fiber Thermoplastic/Metal Laminates. *J. Mater. Sci.* **2008**, *43*, 4391–4398. [[CrossRef](#)]
110. Najafi, M.; Darvizeh, A.; Ansari, R. Effect of Nanoclay Addition on the Hygrothermal Durability of Glass/Epoxy and Fiber Metal Laminates. *Fibers Polym.* **2018**, *19*, 1956–1969. [[CrossRef](#)]

111. Múgica, J.I.; Aretxabaleta, L.; Ulacia, I.; Aurrekoetxea, J. Impact Characterization of Thermoformable Fibre Metal Laminates of 2024-T3 Aluminium and AZ31B-H24 Magnesium Based on Self-Reinforced Polypropylene. *Compos. Part A Appl. Sci. Manuf.* **2014**, *61*, 67–75. [[CrossRef](#)]
112. Carrillo, J.G.; Cantwell, W.J. Mechanical Properties of a Novel Fiber–Metal Laminate Based on a Polypropylene Composite. *Mech. Mater.* **2009**, *41*, 828–838. [[CrossRef](#)]
113. Akula, S.; Bolar, G. Comparative Evaluation of Machining Processes for Making Holes in GLARE Fiber Metal Laminates. *Mater. Today Proc.* **2021**, S2214785321040116. [[CrossRef](#)]
114. Kaboglu, C.; Mohagheghian, I.; Zhou, J.; Guan, Z.; Cantwell, W.; John, S.; Blackman, B.R.K.; Kinloch, A.J.; Dear, J.P. High-Velocity Impact Deformation and Perforation of Fibre Metal Laminates. *J. Mater. Sci.* **2018**, *53*, 4209–4228. [[CrossRef](#)]
115. Teply, J.L. Mechanics of Metal Matrix Laminates. *MRS Proc.* **1996**, *434*, 15–25. [[CrossRef](#)]
116. Gonzalez-Canche, N.G.; Flores-Johnson, E.A.; Carrillo, J.G. Mechanical Characterization of Fiber Metal Laminate Based on Aramid Fiber Reinforced Polypropylene. *Compos. Struct.* **2017**, *172*, 259–266. [[CrossRef](#)]
117. Gonzalez-Canche, N.G.; Flores-Johnson, E.A.; Cortes, P.; Carrillo, J.G. Evaluation of Surface Treatments on 5052-H32 Aluminum Alloy for Enhancing the Interfacial Adhesion of Thermoplastic-Based Fiber Metal Laminates. *Int. J. Adhes. Adhes.* **2018**, *82*, 90–99. [[CrossRef](#)]
118. Carrillo, J.G.; Gonzalez-Canche, N.G.; Flores-Johnson, E.A.; Cortes, P. Low Velocity Impact Response of Fibre Metal Laminates Based on Aramid Fibre Reinforced Polypropylene. *Compos. Struct.* **2019**, *220*, 708–716. [[CrossRef](#)]
119. Dhaliwal, G.S.; Newaz, G.M. Effect of Layer Structure on Dynamic Response and Failure Characteristics of Carbon Fiber Reinforced Aluminum Laminates (CARALL). *J. Dyn. Behav. Mater.* **2016**, *2*, 399–409. [[CrossRef](#)]
120. Dhaliwal, G.S.; Newaz, G.M. Modeling Low Velocity Impact Response of Carbon Fiber Reinforced Aluminum Laminates (CARALL). *J. Dyn. Behav. Mater.* **2016**, *2*, 181–193. [[CrossRef](#)]
121. Lee, B.-E.; Park, E.-T.; Kim, J.; Kang, B.-S.; Song, W.-J. Analytical Evaluation on Uniaxial Tensile Deformation Behavior of Fiber Metal Laminate Based on SRPP and Its Experimental Confirmation. *Compos. Part B Eng.* **2014**, *67*, 154–159. [[CrossRef](#)]
122. Sexton, A.; Cantwell, W.; Kalyanasundaram, S. Stretch Forming Studies on a Fibre Metal Laminate Based on a Self-Reinforcing Polypropylene Composite. *Compos. Struct.* **2012**, *94*, 431–437. [[CrossRef](#)]
123. Kim, H.-K.; Park, E.-T.; Song, W.-J.; Kang, B.-S.; Kim, J. Experimental and Numerical Investigation of the High-Velocity Impact Resistance of Fiber Metal Laminates and Al 6061-T6 by Using Electromagnetic Launcher. *J. Mech. Sci. Technol.* **2019**, *33*, 1219–1229. [[CrossRef](#)]
124. Najafi, M.; Ansari, R.; Darvizeh, A. Experimental Characterization of a Novel Balsa Cored Sandwich Structure with Fiber Metal Laminate Skins. *Iran Polym. J.* **2019**, *28*, 87–97. [[CrossRef](#)]
125. Zhu, W.; Xiao, H.; Wang, J.; Fu, C. Characterization and Properties of AA6061-Based Fiber Metal Laminates with Different Aluminum-Surface Pretreatments. *Compos. Struct.* **2019**, *227*, 111321. [[CrossRef](#)]
126. Rajan, B.M.C.; Kumar, A.S. The Influence of the Thickness and Areal Density on the Mechanical Properties of Carbon Fibre Reinforced Aluminium Laminates (CARAL). *Trans. Indian Inst. Met.* **2018**, *71*, 2165–2171. [[CrossRef](#)]
127. Chernikov, D.; Erisov, Y.; Petrov, I.; Alexandrov, S.; Lang, L. Research of Different Processes for Forming Fiber Metal Laminates. *Int. J. Automot. Technol.* **2019**, *20*, 89–93. [[CrossRef](#)]
128. Pan, L.; Ali, A.; Wang, Y.; Zheng, Z.; Lv, Y. Characterization of Effects of Heat Treated Anodized Film on the Properties of Hygrothermally Aged AA5083-Based Fiber-Metal Laminates. *Compos. Struct.* **2017**, *167*, 112–122. [[CrossRef](#)]
129. Woizeschke, P.; Vollertsen, F. Fracture Analysis of Competing Failure Modes of Aluminum-CFRP Joints Using Three-Layer Titanium Laminates as Transition. *J. Mater. Eng. Perform.* **2015**, *24*, 3558–3572. [[CrossRef](#)]
130. Khan, F.; Qayyum, F.; Asghar, W.; Azeem, M.; Anjum, Z.; Nasir, A.; Shah, M. Effect of Various Surface Preparation Techniques on the Delamination Properties of Vacuum Infused Carbon Fiber Reinforced Aluminum Laminates (CARALL): Experimentation and Numerical Simulation. *J. Mech. Sci. Technol.* **2017**, *31*, 5265–5272. [[CrossRef](#)]
131. Hwang, W.J.; Park, Y.T.; Hwang, W. Strength of Fiber Reinforced Metal Laminates with a Circular Hole. *Met. Mater. Int.* **2005**, *11*, 197–204. [[CrossRef](#)]
132. Boroumad, F.; Seyedkashi, S.M.H.; Pol, M.H. Experimental Study on Forming of Nanoclay-Reinforced Metal–Composite Laminates Using Deep Drawing Process. *J. Braz. Soc. Mech. Sci. Eng.* **2020**, *42*, 541. [[CrossRef](#)]
133. Song, X.; Li, Z.Y.; Shen, Y.; Chen, Y.L.; Zhang, J.Z. Comparative Analysis of Crack Resistance of Fiber-Metal Laminates with HS2 Glass/T700 Carbon Layers for Various Stress Ratios. *Strength Mater.* **2016**, *48*, 121–126. [[CrossRef](#)]
134. Fischer, T.; Grubenmann, M.; Harhash, M.; Hua, W.; Heingärtner, J.; Hora, P.; Palkowski, H.; Ziegmann, G. Experimental and Numerical Investigations on the Quasi-Static Structural Properties of Fibre Metal Laminates Processed by Thermoforming. *Compos. Struct.* **2021**, *258*, 113418. [[CrossRef](#)]
135. Li, H.; Hu, Y.; Fu, X.; Zheng, X.; Liu, H.; Tao, J. Effect of Adhesive Quantity on Failure Behavior and Mechanical Properties of Fiber Metal Laminates Based on the Aluminum–Lithium Alloy. *Compos. Struct.* **2016**, *152*, 687–692. [[CrossRef](#)]
136. Li, H.; Zhang, W.; Jiang, W.; Hua, X.; Guo, X.; Fu, X.; Tao, J. The Feasibility Research on Shot-Peen Forming of the Novel Fiber Metal Laminates Based on Aluminum–Lithium Alloy. *Int. J. Adv. Manuf. Technol.* **2018**, *96*, 587–596. [[CrossRef](#)]
137. Li, H.; Hu, Y.; Liu, C.; Zheng, X.; Liu, H.; Tao, J. The Effect of Thermal Fatigue on the Mechanical Properties of the Novel Fiber Metal Laminates Based on Aluminum–Lithium Alloy. *Compos. Part A Appl. Sci. Manuf.* **2016**, *84*, 36–42. [[CrossRef](#)]

138. Li, H.; Lu, Y.; Han, Z.; Guo, X.; Xu, Y.; Xu, X.; Tao, J. The Shot Peen Forming of Fiber Metal Laminates Based on the Aluminum-Lithium Alloy: Deformation Characteristics. *Compos. Part B Eng.* **2019**, *158*, 279–285. [CrossRef]
139. Kablov, E.N.; Antipov, V.V.; Girsh, R.I.; Serebrennikova, N.Y.; Konovalov, A.N. Fiber Metal Laminates Based on Aluminum-Lithium Alloy Sheets in New-Generation Aircraft. *Russ. Eng. Res.* **2021**, *41*, 215–221. [CrossRef]
140. Li, H.; Wang, H.; Alderliesten, R.; Xiang, J.; Lin, Y.; Xu, Y.; Zhao, H.; Tao, J. The Residual Stress Characteristics and Mechanical Behavior of Shot Peened Fiber Metal Laminates Based on the Aluminium-Lithium Alloy. *Compos. Struct.* **2020**, *254*, 112858. [CrossRef]
141. Cortés, P.; Cantwell, W.J. Fracture Properties of a Fiber-Metal Laminates Based on Magnesium Alloy. *J. Mater. Sci.* **2004**, *39*, 1081–1083. [CrossRef]
142. Zhang, X.; Ma, Q.; Dai, Y.; Hu, F.; Liu, G.; Xu, Z.; Wei, G.; Xu, T.; Zeng, Q.; Xie, W. Effects of Surface Treatments and Bonding Types on the Interfacial Behavior of Fiber Metal Laminate Based on Magnesium Alloy. *Appl. Surf. Sci.* **2018**, *427*, 897–906. [CrossRef]
143. Zhang, X.; Zhang, Y.; Ma, Q.Y.; Dai, Y.; Hu, F.P.; Wei, G.B.; Xu, T.C.; Zeng, Q.W.; Wang, S.Z.; Xie, W.D. Effect of Surface Treatment on the Corrosion Properties of Magnesium-Based Fibre Metal Laminate. *Appl. Surf. Sci.* **2017**, *396*, 1264–1272. [CrossRef]
144. Okumus, F. An Elastic-Plastic Stress Analysis in Silicon Carbide Fiber Reinforced Magnesium Metal Matrix Composite Beam Having Rectangular Cross Section under Transverse Loading. *KSME Int. J.* **2004**, *18*, 221–229. [CrossRef]
145. Cortés, P.; Cantwell, W.J. The Prediction of Tensile Failure in Titanium-Based Thermoplastic Fibre–Metal Laminates. *Compos. Sci. Technol.* **2006**, *66*, 2306–2316. [CrossRef]
146. Nassir, N.A.; Birch, R.S.; Cantwell, W.J.; Sierra, D.R.; Edwardson, S.P.; Dearden, G.; Guan, Z.W. Experimental and Numerical Characterization of Titanium-Based Fibre Metal Laminates. *Compos. Struct.* **2020**, *245*, 112398. [CrossRef]
147. Suresh Kumar, S.; Shankar, P.A.; Lalith Kumar, K. Failure Investigation on High Velocity Impact Deformation of Boron Carbide (B4C) Reinforced Fiber Metal Laminates of Titanium/Glass Fiber Reinforced Polymer. *Def. Technol.* **2021**, S2214914721000684. [CrossRef]
148. Ali, A.; Pan, L.; Duan, L.; Zheng, Z.; Sapkota, B. Characterization of Seawater Hygrothermal Conditioning Effects on the Properties of Titanium-Based Fiber-Metal Laminates for Marine Applications. *Compos. Struct.* **2016**, *158*, 199–207. [CrossRef]
149. Sun, J.; Daliri, A.; Lu, G.; Liu, D.; Xia, F.; Gong, A. Tensile Behaviour of Titanium-Based Carbon-Fibre/Epoxy Laminate. *Constr. Build. Mater.* **2021**, *281*, 122633. [CrossRef]
150. Sharma, A.P.; Velmurugan, R.; Shankar, K.; Ha, S. High-Velocity Impact Response of Titanium-Based Fiber Metal Laminates. Part I: Experimental Investigations. *Int. J. Impact Eng.* **2021**, *152*, 103845. [CrossRef]
151. Miller, J.L.; Progar, D.J.; Johnson, W.S.; St. Clair, T.S.L. Preliminary Evaluation of Hybrid Titanium Composite Laminates. *J. Adhes.* **1995**, *54*, 223–240. [CrossRef]
152. Chamis, C.C.; Lark, R.F.; Sullivan, T.L. *Boron/Aluminum-Graphite/Resin Advanced Fiber Composite Hybrids*; National Aeronautics and Space Administration: Washington, DC, USA, 1975. Available online: <https://ntrs.nasa.gov/api/citations/19750007005/downloads/19750007005.pdf> (accessed on 19 July 2021).
153. Shanmugam, L.; Kazemi, M.E.; Qiu, C.; Rui, M.; Yang, L.; Yang, J. Influence of UHMWPE Fiber and Ti6Al4V Metal Surface Treatments on the Low-Velocity Impact Behavior of Thermoplastic Fiber Metal Laminates. *Adv. Compos. Hybrid Mater.* **2020**, *3*, 508–521. [CrossRef]
154. Bernd-Arno, B.; Dilger, K.; Lippky, K.; Kaempf, L.; Hübner, S.; Hartwig, S.; Altun, Y.; Gabriel, M.; Farahmand, E.; Micke-Camuz, M. Combined Deep Drawing and Fusion Bonding of Structural FRP-Metal Hybrid Parts. *Procedia Manuf.* **2019**, *29*, 296–304. [CrossRef]
155. Karunakaran, N.; Rajadurai, A. Effect of Surface Treatment on Mechanical Properties of Glass Fiber/Stainless Steel Wire Mesh Reinforced Epoxy Hybrid Composites. *J. Mech. Sci. Technol.* **2016**, *30*, 2475–2482. [CrossRef]
156. Pärnänen, T.; Vääntinen, A.; Kanerva, M.; Jokinen, J.; Saarela, O. The Effects of Debonding on the Low-Velocity Impact Response of Steel-CFRP Fibre Metal Laminates. *Appl. Compos. Mater.* **2016**, *23*, 1151–1166. [CrossRef]
157. Patnaik, A.K.; Bauer, C.L.; Srivatsan, T.S. The Extrinsic Influence of Carbon Fibre Reinforced Plastic Laminates to Strengthen Steel Structures. *Sadhana* **2008**, *33*, 261–272. [CrossRef]
158. Schmidt, H.C.; Damerow, U.; Lauter, C.; Gorny, B.; Hankeln, F.; Homberg, W.; Troester, T.; Maier, H.J.; Mahnken, R. Manufacturing Processes for Combined Forming of Multi-Material Structures Consisting of Sheet Metal and Local CFRP Reinforcements. In *Key Engineering Materials*; Trans Tech Publications Ltd.: Aedermannsdorf, Switzerland, 2012; Volume 504–506, pp. 295–300. [CrossRef]
159. Aiello, M.A.; Valente, L.; Rizzo, A. Moment Redistribution in Continuous Reinforced Concrete Beams Strengthened with Carbon-Fiber-Reinforced Polymer Laminates. *Mech. Compos. Mater.* **2007**, *43*, 453–466. [CrossRef]
160. Engelkemeier, K.; Mücke, C.; Hoyer, K.P.; Schaper, M. Anodizing of Electrolytically Galvanized Steel Surfaces for Improved Interface Properties in Fiber Metal Laminates. *Adv. Compos. Hybrid Mater.* **2019**, *2*, 189–199. [CrossRef]
161. Guo, Y.; Zhai, C.; Li, F.; Zhu, X.; Xu, F.; Wu, X. Formability, Defects and Strengthening Effect of Steel/CFRP Structures Fabricated by Using the Differential Temperature Forming Process. *Compos. Struct.* **2019**, *216*, 32–38. [CrossRef]
162. Nam, J.; Cantwell, W.; Das, R.; Lowe, A.; Kalyanasundaram, S. Deformation Behaviour of Steel/SRPP Fibre Metal Laminate Characterised by Evolution of Surface Strains. *Adv. Aircr. Spacecr. Sci.* **2016**, *3*, 61–75. [CrossRef]
163. Bernd-Arno, B.; Sven, H.; Nenad, G.; Moritz, M.-C.; Tim, W.; André, N. Forming and Joining of Carbon-Fiber-Reinforced Thermoplastics and Sheet Metal in One Step. *Procedia Eng.* **2017**, *183*, 227–232. [CrossRef]

164. Wollmann, T.; Hahn, M.; Wiedemann, S.; Zeiser, A.; Jaschinski, J.; Modler, N.; Ben Khalifa, N.; Meißen, F.; Paul, C. Thermoplastic Fibre Metal Laminates: Stiffness Properties and Forming Behaviour by Means of Deep Drawing. *Arch. Civ. Mech. Eng.* **2018**, *18*, 442–450. [[CrossRef](#)]
165. Gerstenberger, C.; Osiecki, T.; Kroll, L.; Scholz, P.; Seidlitz, H. Processing and Characterization of Cathodic Dip Coated Metal/Composite-Laminates. *Arch. Civ. Mech. Eng.* **2016**, *16*, 467–472. [[CrossRef](#)]
166. Martins, J.L.C.H. CFRP Joints with Hybrid Laminates Metal-Carbon Fibre. Master's Thesis, Universidade do Porto, Porto, Portugal, 2018.
167. Voswinkel, D.; Kloidt, D.; Grydin, O.; Schaper, M. Time Efficient Laser Modification of Steel Surfaces for Advanced Bonding in Hybrid Materials. *Prod. Eng.* **2021**, *15*, 263–270. [[CrossRef](#)]
168. Ebnesaajad, S.; Ebnesaajad, C.F. *Surface Treatment of Materials for Adhesive Bonding*, 2nd ed.; William Andrew Applied Science Publishers: Norwich, NY, USA, 2014.
169. Shanmugam, L.; Kazemi, M.E.; Yang, J. Improved Bonding Strength between Thermoplastic Resin and Ti Alloy with Surface Treatments by Multi-step Anodization and Single-step Micro-arc Oxidation Method: A Comparative Study. *ES Mater. Manuf.* **2019**, *3*, 57–65. [[CrossRef](#)]
170. Shang, X.; Marques, E.A.S.; Machado, J.J.M.; Carbas, R.J.C.; Jiang, D.; da Silva, L.F.M. Review on Techniques to Improve the Strength of Adhesive Joints with Composite Adherends. *Compos. Part B Eng.* **2019**, *177*, 107363. [[CrossRef](#)]
171. dos Santos, D.G.; Carbas, R.J.C.; Marques, E.A.S.; da Silva, L.F.M. Reinforcement of CFRP Joints with Fibre Metal Laminates and Additional Adhesive Layers. *Compos. Part B Eng.* **2019**, *165*, 386–396. [[CrossRef](#)]
172. Mosse, L.; Cantwell, W.J.; Cardew-Hall, M.J.; Compston, P.; Kalyanasundaram, S.A. Study of the Effect of Process Variables on the Stamp Forming of Rectangular Cups Using Fibre-Metal Laminate Systems. *Adv. Mater. Res.* **2005**, *6–8*, 649–656. [[CrossRef](#)]
173. Kim, S.Y.; Choi, W.J.; Park, S.Y. Spring-Back Characteristics of Fiber Metal Laminate (GLARE) in Brake Forming Process. *Int. J. Adv. Manuf. Technol.* **2007**, *32*, 445–451. [[CrossRef](#)]
174. Benedict, A.V. An Experimental Investigation of GLARE and Restructured Fiber Metal Laminates Metal Laminates. Master's Thesis, Embry-Riddle Aeronautical University, Daytona Beach, FL, USA, 2012.
175. Suigman, S.; Crocombe, A.D. The static and fatigue response of metal laminate and hybrid fibre-metal laminate doublers joints under tension loading. *Compos. Struct.* **2012**, *94*, 2937–2951. [[CrossRef](#)]
176. Lee, D.-W.; Park, B.-J.; Park, S.-Y.; Choi, C.-H.; Song, J.-I. Fabrication of High-Stiffness Fiber-Metal Laminates and Study of Their Behavior under Low-Velocity Impact Loadings. *Compos. Struct.* **2018**, *189*, 61–69. [[CrossRef](#)]
177. Sun, J.; Daliri, A.; Lu, G.; Ruan, D.; Lv, Y. Tensile Failure of Fibre-Metal-Laminates Made of Titanium and Carbon-Fibre/Epoxy Laminates. *Mater. Des.* **2019**, *183*, 108139. [[CrossRef](#)]
178. Cortés, P.; Cantwell, W.J. Structure–Properties Relations in Titanium-Based Thermoplastic Fiber–Metal Laminates. *Polym. Compos.* **2006**, *27*, 264–270. [[CrossRef](#)]
179. Hu, Y.; Li, H.; Fu, X.; Zhang, X.; Tao, J.; Xu, J. Hygrothermal Characterization of Polyimide–Titanium-Based Fibre Metal Laminate. *Polym. Compos.* **2018**, *39*, 2819–2825. [[CrossRef](#)]
180. Pan, Y.; Wu, G.; Cheng, X.; Zhang, Z.; Li, M.; Ji, S.; Huang, Z. Mode I and Mode II Interlaminar Fracture Toughness of CFRP/Magnesium Alloys Hybrid Laminates. *Compos. Interfaces* **2016**, *23*, 453–465. [[CrossRef](#)]
181. Zhou, P.; Wu, X.; Pan, Y.; Tao, Y.; Wu, G.; Huang, Z. Mechanical Properties of Carbon Fibre-Reinforced Polymer/Magnesium Alloy Hybrid Laminates. *Mater. Res. Express* **2018**, *5*, 046523. [[CrossRef](#)]
182. Zhu, G.Z.; Zheng, C.L.; Lu, X.F. The Influence of Loading Rate on the Interfacial Fracture Toughness of Carbon Fiber-Metal Laminates Based on Magnesium Alloy. *Adv. Mater. Res.* **2011**, *328–330*, 1373–1376. [[CrossRef](#)]
183. Harris, A.F.; Beevers, A. The Effects of Grit-Blasting on Surface Properties for Adhesion. *Int. J. Adhes. Adhes.* **1999**, *19*, 445–452. [[CrossRef](#)]
184. Critchlow, G.W.; Brewis, D.M. Review of Surface Pre-treatments for Aluminium Alloys. *Int. J. Adhes. Adhes.* **1996**, *16*, 255–275. [[CrossRef](#)]
185. Cognard, P. *Handbook of Adhesives and Sealants*, 1st ed.; Elsevier: Amsterdam, The Netherlands, 2005.
186. Park, S.Y.; Choi, W.J.; Choi, H.S.; Kwon, H.; Kim, S.H. Recent Trends in Surface Treatment Technologies for Airframe Adhesive Bonding Processing: A Review (1995–2008). *J. Adhes.* **2010**, *86*, 192–221. [[CrossRef](#)]
187. Park, S.Y.; Choi, W.J.; Choi, H.S.; Kwon, H. Effects of Surface Pre-Treatment and Void Content on GLARE Laminate Process Characteristics. *J. Mater. Process. Technol.* **2010**, *210*, 1008–1016. [[CrossRef](#)]
188. Kinloch, A.J.; Little, M.S.G.; Watts, J.F. The Role of the Interphase in the Environmental Failure of Adhesive Joints. *Acta Mater.* **2000**, *48*, 4543–4553. [[CrossRef](#)]
189. Sheasby, P.G.; Pinner, R. *The Surface Treatment and Finishing of Aluminium and Its Alloys*, 6th ed.; ASM International: Materials Park, OH, USA, 2001.
190. Zucchi, F.; TrabANELLI, G.; Grassi, V.; Frignani, A. Protective Treatments of a Magnesium Alloy with Silanes. In Proceedings of the EUROCORR 2001, Riva del Garda, Italy, 30 September–4 October 2001. paper no. 72.
191. Hobbs, P.M.; Kinloch, A.J. The Computational Molecular Modelling of Organosilane Primers. *J. Adhes.* **1998**, *66*, 203–228. [[CrossRef](#)]
192. Anagreh, N.; Dorn, L.; Bilke-Krause, C. Low-Pressure Plasma Pretreatment of Polyphenylene Sulfide (PPS) Surfaces for Adhesive Bonding. *Int. J. Adhes. Adhes.* **2008**, *28*, 16–22. [[CrossRef](#)]

193. Polini, W.; Sorrentino, L. Improving the Wettability of 2024 Aluminium Alloy by Means of Cold Plasma Treatment. *Appl. Surf. Sci.* **2003**, *214*, 232–242. [CrossRef]
194. Spadaro, C.; Dispenza, C.; Sunseri, C. The Influence of the Nature of the Surface Oxide on the Adhesive Fracture Energy of Aluminium-Bonded Joints as Measured by T-Peel Tests. *Int. J. Adhes. Adhes.* **2008**, *28*, 211–221. [CrossRef]
195. Walters, C.T. *Laser Surface Preparation for Adhesive Bonding II*; AFRL Wright-Patterson AFB: Dublin, OH, USA, 2004; pp. 1–69.
196. Zhu, J.; Hu, Y.; Xu, M.; Yang, W.; Fu, L.; Li, D.; Zhou, L. Enhancement of the Adhesive Strength between Ag Films and Mo Substrate by Ag Implanted via Ion Beam-Assisted Deposition. *Materials* **2018**, *11*, 762. [CrossRef] [PubMed]
197. Loh, I.-H.; Hirvone, J.K.; Martin, J.R.; Revesz, P.; Boyd, C. The Promotion of Metal/Polymer Adhesion by Ion Beam Enhanced Deposition. *MRS Online Proc. Libr.* **1987**, *108*, 241–246. [CrossRef]
198. Molitor, P.; Barron, V.; Young, T. Surface Treatment of Titanium for Adhesive Bonding to Polymer Composites: A Review. *Int. J. Adhes. Adhes.* **2001**, *21*, 129–136. [CrossRef]
199. Hahn, M.; Ben Khalifa, N.; Paul, C.; Lehmann, B.; Breidenbach, A.; Reisewitz, S.; Rogner, I.; Vogt, H.-P.; Vogt, O.; Cuong, N.; et al. *LEIKA Abschlussbericht (Final Project Report)*; Forel: Dresden, Germany, 2017.
200. Müller, B.; Palardy, G.; Teixeira De Freitas, S.; Sinke, J. Out-of-Autoclave Manufacturing of GLARE Panels Using Resistance Heating. *J. Compos. Mater.* **2018**, *52*, 1661–1675. [CrossRef] [PubMed]
201. Drakonakis, V.M.; Seferis, J.C.; Domanidis, C.C. Curing Pressure Influence of Out-of-Autoclave Processing on Structural Composites for Commercial Aviation. *Adv. Mater. Sci. Eng.* **2013**, *2013*, 356824. [CrossRef]
202. Rajkumar, G.R.; Krishna, M.; Narasimhamurthy, H.N.; Keshavamurthy, Y.C.; Nataraj, J.R. Investigation of Tensile and Bending Behavior of Aluminum Based Hybrid Fiber Metal Laminates. *Procedia Mater. Sci.* **2014**, *5*, 60–68. [CrossRef]
203. Yu, G.-C.; Wu, L.-Z.; Ma, L.; Xiong, J. Low Velocity Impact of Carbon Fiber Aluminum Laminates. *Compos. Struct.* **2015**, *119*, 757–766. [CrossRef]
204. Christke, S.; Gibson, A.G.; Grigoriou, K.; Mouritz, A.P. Multi-Layer Polymer Metal Laminates for the Fire Protection of Lightweight Structures. *Mater. Des.* **2016**, *97*, 349–356. [CrossRef]
205. Zu, S.; Zhou, Z.; Zhang, J. Numerical Simulation of Pin-Loaded Joints of Fiber Metal Laminate. *Iran Polym. J.* **2019**, *28*, 145–155. [CrossRef]
206. Mohammed, I.; Abu Talib, A.R.; Sultan, M.T.H.; Saadon, S. Fire Behavioural and Mechanical Properties of Carbon Fibre Reinforced Aluminium Laminate Composites for Aero-Engine. *Int. J. Eng. Technol.* **2018**, *7*, 22–27. [CrossRef]
207. Wu, G.; Yang, J.-M. The Mechanical Behavior of GLARE Laminates for Aircraft Structures. *JOM* **2005**, *57*, 72–79. [CrossRef]
208. Vlot, A.; Kroon, E.; La Rocca, G. Impact Response of Fiber Metal Laminates. *Key Eng. Mater.* **1998**, *141–143*, 235–276. [CrossRef]
209. Ardakani, M.A.; Khatibi, A.A.; Parsaiyan, H. An Experimental Study on the Impact Resistance of Glass-Fiber-Reinforced Aluminum (Glare) Laminates. Available online: <https://www.iccm-central.org/Proceedings/ICCM17proceedings/Themes/Behaviour/DAMAGE%20TOLERANCE%20&%20IMPACT/INT%20-%20DAMAGE%20TOLER%20&%20IMPACT/IF7.4%20Ardakani.pdf> (accessed on 12 July 2021).
210. Wang, W.X.; Takao, Y.; Matsubara, T. Galvanic Corrosion-Resistant Carbon Fiber Metal Laminates. In Proceedings of the 16th International Conference on Composite Materials, ICCM-16—“A Giant Step Towards Environmental Awareness: From Green Composites to Aerospace”, Kyoto, Japan, 8–13 July 2007; pp. 1–10.
211. Mukesh, A.M.; Hynes, N.R.J. Corrosion Behaviour of Fibre Metal Laminates and Control by Inhibitors. *AIP Conf. Proc.* **2019**, *2142*, 070008. [CrossRef]
212. Hagenbeek, M.; van Hengel, C.; Bosker, O.J.; Vermeeren, C.A.J.R. Static Properties of Fibre Metal Laminates. *Appl. Compos. Mater.* **2003**, *10*, 207–222. [CrossRef]
213. Sinke, J. Forming technology for composite/metal hybrids. In *Composites Forming Technologies*; Long, A.C., Ed.; Woodhead Publishing Series in Textiles; Woodhead Publishing: Sawston, UK, 2007; pp. 197–219.
214. Holleman, E.; van Praag, R. *On the Minimum Bend Radius of Some GLARE 2 and GLARE 3 Grades (BE2040 Subtask 3.1-g)*; Delft University of Technology: Delft, The Netherlands, 1995.
215. Vlot, A.; Gunnink, J.W. *Fibre Metal Laminates: An Introduction*; Springer: Dordrecht, The Netherlands, 2001.
216. Isiktas, A.; Taskin, V. Springback Behavior of Fiber Metal Laminates with Carbon Fiber-Reinforced Core in V-Bending Process. *Arab. J. Sci. Eng.* **2020**, *45*, 9357–9366. [CrossRef]
217. Bellini, C.; Di Cocco, V.; Iacoviello, F.; Sorrentino, L. Influence of Structural Characteristics on the Interlaminar Shear Strength of CFRP/Al Fibre Metal Laminates. *Procedia Struct. Integr.* **2019**, *18*, 373–378. [CrossRef]
218. Bellini, C.; Di Cocco, V.; Iacoviello, F.; Sorrentino, L. Performance Evaluation of CFRP/Al Fibre Metal Laminates with Different Structural Characteristics. *Compos. Struct.* **2019**, *225*, 111117. [CrossRef]
219. Pärnänen, T.; Alderliesten, R.; Rans, C.; Brander, T.; Saarela, O. Applicability of AZ31B-H24 Magnesium in Fibre Metal Laminates—An Experimental Impact Research. *Compos. Part A Appl. Sci. Manuf.* **2012**, *43*, 1578–1586. [CrossRef]
220. Bellini, C.; Di Cocco, V.; Iacoviello, F.; Sorrentino, L. Experimental Analysis of Aluminium/Carbon Epoxy Hybrid Laminates under Flexural Load. *Frat. Integrità Strutt.* **2019**, *13*, 739–747. [CrossRef]
221. Ahmadi, H.; Sabouri, H.; Liaghat, G.; Bidkhorri, E. Experimental and Numerical Investigation on the High Velocity Impact Response of GLARE with Different Thickness Ratio. *Procedia Eng.* **2011**, *10*, 869–874. [CrossRef]
222. Chen, F.-K.; Huang, T.-B. Formability of Stamping Magnesium-Alloy AZ31 Sheets. *J. Mater. Process. Technol.* **2003**, *142*, 643–647. [CrossRef]

223. Moon, Y.H.; Kang, S.S.; Cho, J.R.; Kim, T.G. Effect of Tool Temperature on the Reduction of the Springback of Aluminum Sheets. *J. Mater. Process. Technol.* **2003**, *132*, 365–368. [CrossRef]
224. Li, H.; Tian, J.; Fei, W.; Han, Z.; Tao, G.; Xu, Y.; Xu, X.; Tao, J. Spring-Back and Failure Characteristics of Roll Bending of GLARE Laminates. *Mater. Res. Express* **2019**, *6*, 0865b2. [CrossRef]
225. Kulkarni, K.M.; Schey, J.A.; Badger, D.V. Investigation of Shot Peening as a Forming Process for Aircraft Wing Skins. *J. Appl. Metalwork.* **1981**, *1*, 34–44. [CrossRef]
226. Friese, A.; Lohmar, J.; Wüstefeld, F. Current Applications of Advanced Peen Forming Implementation. In *Shot Peening*; Wagner, L., Ed.; John Wiley & Sons, Ltd.: New York, NY, USA, 2003; pp. 53–61.
227. Zweschper, T.; Riegert, G.; Dillenz, A.; Busse, G. Ultraschallangeregte Thermografie Mittels Frequenzmodulierterelastischer Wellen. In *Thermografie-Kolloquium*; 2003; pp. 45–52. Available online: https://www.dgzfp.de/Portals/24/PDFs/Bbonline/BB_86-CD/pdfs/V05Zweschper.pdf (accessed on 4 July 2021).
228. Bisle, W.; Meier, T.; Mueller, S.; Airbus, S.; Bremen. In-Service Inspection Concept for GLARE®—An Example for the Use of New UT Array In-Spection Systems. Available online: <https://www.ndt.net/article/ecndt2006/doc/Tu.2.1.1.pdf> (accessed on 11 July 2021).
229. Naresh, K.; Khan, K.A.; Umer, R.; Cantwell, W.J. The Use of X-ray Computed Tomography for Design and Process Modeling of Aerospace Composites: A Review. *Mater. Des.* **2020**, *190*, 108553. [CrossRef]
230. Hu, Y.; Zhang, W.; Jiang, W.; Cao, L.; Shen, Y.; Li, H.; Guan, Z.; Tao, J.; Xu, J. Effects of Exposure Time and Intensity on the Shot Peen Forming Characteristics of Ti/CFRP Laminates. *Compos. Part A Appl. Sci. Manuf.* **2016**, *91*, 96–104. [CrossRef]
231. Unal, O.; Varol, R. Almen Intensity Effect on Microstructure and Mechanical Properties of Low Carbon Steel Subjected to Severe Shot Peening. *Appl. Surf. Sci.* **2014**, *290*, 40–47. [CrossRef]
232. Russig, C.; Bambach, M.; Gottschalk, M.; Hirt, G. Recent Investigations on Shot Peen Forming of GLARE Sheets and Rotary Peen Forming. Available online: <https://www.shotpeener.com/library/pdf/2014115.pdf> (accessed on 30 June 2021).
233. Voss, R.F.; Winter, P.M. Peening Device for Tube Finishing. U.S. Patent US3648498A, 14 March 1972.
234. Wang, Z.-Y.; Wang, Q.-Y.; Liu, Y.-J. Evaluation of Fatigue Strength Improvement by CFRP Laminates and Shot Peening onto the Tension Flanges Joining Corrugated Steel Webs. *Materials* **2015**, *8*, 5348–5362. [CrossRef] [PubMed]
235. Jeswiet, J.; Micari, F.; Hirt, G.; Bramley, A.; Duflou, J.; Allwood, J. Asymmetric Single Point Incremental Forming of Sheet Metal. *CIRP Ann.* **2005**, *54*, 88–114. [CrossRef]
236. Lu, H.; Kearney, M.; Li, Y.; Liu, S.; Daniel, W.J.T.; Meehan, P.A. Model Predictive Control of Incremental Sheet Forming for Geometric Accuracy Improvement. *Int. J. Adv. Manuf. Technol.* **2016**, *82*, 1781–1794. [CrossRef]
237. Li, Y.; Chen, X.; Liu, Z.; Sun, J.; Li, F.; Li, J.; Zhao, G. A Review on the Recent Development of Incremental Sheet-Forming Process. *Int. J. Adv. Manuf. Technol.* **2017**, *92*, 2439–2462. [CrossRef]
238. Skjødt, M. Rapid Prototyping by Single Point Incremental Forming of Sheet Metal. Ph.D. Thesis, Technical University of Denmark, Lyngby, Denmark, 2008.
239. Peter, I.; Fracchia, E.; Canale, I.; Maiorano, R. Incremental Sheet Forming for Prototyping Automotive Modules. *Procedia Manuf.* **2019**, *32*, 50–58. [CrossRef]
240. Trzepieciński, T. Recent Developments and Trends in Sheet Metal Forming. *Metals* **2020**, *10*, 779. [CrossRef]
241. Afonso, D. Forming without a Die—Fundamentals and Applications of Single Point Incremental Forming. Ph.D. Thesis, Universidade de Aveiro, Aveiro, Portugal, 2016.
242. Duflou, J.R.; Habraken, A.-M.; Cao, J.; Malhotra, R.; Bambach, M.; Adams, D.; Vanhove, H.; Mohammadi, A.; Jeswiet, J. Single Point Incremental Forming: State-of-the-Art and Prospects. *Int. J. Mater. Form.* **2018**, *11*, 743–773. [CrossRef]
243. Eksteen, P.D.W. Development of Incrementally Formed Patient-Specific Titanium Knee Prosthesis. Master’s Thesis, Stellenbosch University, Stellenbosch, Africa, 2013.
244. Vanhove, H.; Carette, Y.; Vancleef, S.; Duflou, J.R. Production of Thin Shell Clavicle Implants through Single Point Incremental Forming. *Procedia Eng.* **2017**, *183*, 174–179. [CrossRef]
245. Sbayti, M.; Bahloul, R.; Belhadjsalah, H. Efficiency of Optimization Algorithms on the Adjustment of Process Parameters for Geometric Accuracy Enhancement of Denture Plate in Single Point Incremental Sheet Forming. *Neural Comput. Applic.* **2020**, *32*, 8829–8846. [CrossRef]
246. Cheng, Z.; Li, Y.; Xu, C.; Liu, Y.; Ghafoor, S.; Li, F. Incremental Sheet Forming towards Biomedical Implants: A Review. *J. Mater. Res. Technol.* **2020**, *9*, 7225–7251. [CrossRef]
247. Kalo, A.; Newsum, M.J. An Investigation of Robotic Incremental Sheet Metal Forming as a Method for Prototyping Parametric Architectural Skins. In *Robotic Fabrication in Architecture, Art and Design 2014*; McGee, W., Ponce de Leon, M., Eds.; Springer International Publishing: Cham, Germany, 2014; pp. 33–49.
248. Lublasser, E.I.; Braumann, J.; Goldbach, B.D.; Brell-Çokcan, S. Robotic Forming: Rapidly Generating 3D Forms and Structures through Incremental Forming. In *Proceedings of the 21st International Conference of the Association for Computer-Aided Architectural Design Research in Asia CAADRIA, Melbourne, Australia, 30 March–2 April 2016*; pp. 539–548.
249. Trzepieciński, T.; Krasowski, B.; Kubit, A.; Wydrzyński, D. Possibilities of Application of Incremental Sheet-Forming Technique in Aircraft Industry. *ZN PRz Mech.* **2018**, 87–100. [CrossRef]
250. Gupta, P.; Jeswiet, J. Manufacture of an Aerospace Component by Single Point Incremental Forming. *Procedia Manuf.* **2019**, *29*, 112–119. [CrossRef]

251. Gupta, P.; Szekeres, A.; Jeswiet, J. Design and Development of an Aerospace Component with Single-Point Incremental Forming. *Int. J. Adv. Manuf. Technol.* **2019**, *103*, 3683–3702. [\[CrossRef\]](#)
252. Amino, M.; Mizoguchi, M.; Terauchi, Y.; Maki, T. Current Status of “Dieless” Amino’s Incremental Forming. *Procedia Eng.* **2014**, *81*, 54–62. [\[CrossRef\]](#)
253. Vanhove, H.; Mohammadi, A.; Guo, Y.S.; Duflou, J.R. High-Speed Single Point Incremental Forming of an Automotive Aluminium Alloy. In *Key Engineering Materials*; Trans Tech Publications Ltd.: Aedermannsdorf, Switzerland, 2014; Volume 622–623, pp. 433–439. [\[CrossRef\]](#)
254. Oleksik, V. Influence of Geometrical Parameters, Wall Angle and Part Shape on Thickness Reduction of Single Point Incremental Forming. *Procedia Eng.* **2014**, *81*, 2280–2285. [\[CrossRef\]](#)
255. Liu, F.; Li, X.; Li, Y.; Wang, Z.; Zhai, W.; Li, F.; Li, J. Modelling of the Effects of Process Parameters on Energy Consumption for Incremental Sheet Forming Process. *J. Clean. Prod.* **2020**, *250*, 119456. [\[CrossRef\]](#)
256. Gohil, A.; Modi, B. Review of the Effect of Process Parameters on Performance Measures in the Incremental Sheet Forming Process. *Proc. Inst. Mech. Eng. Part B J. Eng. Manuf.* **2021**, *235*, 303–332. [\[CrossRef\]](#)
257. Benedetti, M.; Fontanari, V.; Monelli, B.; Tassan, M. Single-Point Incremental Forming of Sheet Metals: Experimental Study and Numerical Simulation. *Proc. Inst. Mech. Eng. Part B J. Eng. Manuf.* **2017**, *231*, 301–312. [\[CrossRef\]](#)
258. Centeno, G.; Martínez-Donaire, A.; Bagudanch, I.; Morales-Palma, D.; Garcia-Romeu, M.; Vallesano, C. Revisiting Formability and Failure of AISI304 Sheets in SPIF: Experimental Approach and Numerical Validation. *Metals* **2017**, *7*, 531. [\[CrossRef\]](#)
259. Ambrogio, G.; Palumbo, G.; Sgambitterra, E.; Guglielmi, P.; Piccininni, A.; De Napoli, L.; Villa, T.; Fragomeni, G. Experimental Investigation of the Mechanical Performances of Titanium Cranial Prostheses Manufactured by Super Plastic Forming and Single-Point Incremental Forming. *Int. J. Adv. Manuf. Technol.* **2018**, *98*, 1489–1503. [\[CrossRef\]](#)
260. Liu, Z.; Li, G. Single Point Incremental Forming of Cu-Al Composite Sheets: A Comprehensive Study on Deformation Behaviors. *Arch. Civ. Mech. Eng.* **2019**, *19*, 484–502. [\[CrossRef\]](#)
261. Abdelkader, W.B.; Bahloul, R.; Arfa, H. Numerical Investigation of the Influence of Some Parameters in SPIF Process on the Forming Forces and Thickness Distributions of a Bimetallic Sheet CP-Titanium/Low-Carbon Steel Compared to an Individual Layer. *Procedia Manuf.* **2020**, *47*, 1319–1327. [\[CrossRef\]](#)
262. Franzen, V.; Kwiatkowski, L.; Martins, P.A.F.; Tekkaya, A.E. Single Point Incremental Forming of PVC. *J. Mater. Process. Technol.* **2009**, *209*, 462–469. [\[CrossRef\]](#)
263. Mohammadi, A.; Vanhove, H.; Attisano, M.; Ambrogio, G.; Duflou, J.R. Single Point Incremental Forming of Shape Memory Polymer Foam. *MATEC Web Conf.* **2015**, *21*, 04007. [\[CrossRef\]](#)
264. Hernández-Ávila, M.; Lozano-Sánchez, L.M.; Perales-Martínez, I.A.; Elías-Zúñiga, A.; Bagudanch, I.; García-Romeu, M.L.; Elizalde, L.E.; Barrera, E.V. Single Point Incremental Forming of Bilayer Sheets Made of Two Different Thermoplastics. *J. Appl. Polym. Sci.* **2019**, *136*, 47093. [\[CrossRef\]](#)
265. Fiorotto, M.; Sorgente, M.; Luchetta, G. Preliminary Studies on Single Point Incremental Forming for Composite Materials. *Int. J. Mater. Form.* **2010**, *3*, 951–954. [\[CrossRef\]](#)
266. Lozano-Sánchez, L.M.; Sustaita, A.O.; Soto, M.; Biradar, S.; Ge, L.; Segura-Cárdenas, E.; Diabb, J.; Elizalde, L.E.; Barrera, E.V.; Elías-Zúñiga, A. Mechanical and Structural Studies on Single Point Incremental Forming of Polypropylene-MWCNTs Composite Sheets. *J. Mater. Process. Technol.* **2017**, *242*, 218–227. [\[CrossRef\]](#)
267. Conte, R.; Ambrogio, G.; Pulice, D.; Gagliardi, F.; Filice, L. Incremental Sheet Forming of a Composite Made of Thermoplastic Matrix and Glass-Fiber Reinforcement. *Procedia Eng.* **2017**, *207*, 819–824. [\[CrossRef\]](#)
268. Clavijo-Chaparro, S.L.; Iturbe-Ek, J.; Lozano-Sánchez, L.M.; Sustaita, A.O.; Elías-Zúñiga, A. Plasticized and Reinforced Poly(Methyl Methacrylate) Obtained by a Dissolution-Dispersion Process for Single Point Incremental Forming: Enhanced Formability towards the Fabrication of Cranial Implants. *Polym. Test.* **2018**, *68*, 39–45. [\[CrossRef\]](#)
269. Okada, M.; Kato, T.; Otsu, M.; Tanaka, H.; Miura, T. Development of Optical-Heating-Assisted Incremental Forming Method for Carbon Fiber Reinforced Thermoplastic Sheet—Forming Characteristics in Simple Spot-Forming and Two-Dimensional Sheet-Fed Forming. *J. Mater. Process. Technol.* **2018**, *256*, 145–153. [\[CrossRef\]](#)
270. Borić, A.; Kalendová, A.; Urbanek, M.; Pepelnjak, T. Characterisation of Polyamide (PA)12 Nanocomposites with Montmorillonite (MMT) Filler Clay Used for the Incremental Forming of Sheets. *Polymers* **2019**, *11*, 1248. [\[CrossRef\]](#)
271. Al-Obaidi, A.; Kunke, A.; Kräusel, V. Hot Single-Point Incremental Forming of Glass-Fiber-Reinforced Polymer (PA6GF47) Supported by Hot Air. *J. Manuf. Process.* **2019**, *43*, 17–25. [\[CrossRef\]](#)
272. Jackson, K.P.; Allwood, J.M.; Landert, M. Incremental Forming of Sandwich Panels. *J. Mater. Process. Technol.* **2008**, *204*, 290–303. [\[CrossRef\]](#)
273. Kumar, A.; Gulati, V.; Kumar, P.; Singh, V.; Kumar, B.; Singh, H. Parametric Effects on Formability of AA2024-O Aluminum Alloy Sheets in Single Point Incremental Forming. *J. Mater. Res. Technol.* **2019**, *8*, 1461–1469. [\[CrossRef\]](#)
274. Kurra, S.; Regalla, S.P. Experimental and Numerical Studies on Formability of Extra-Deep Drawing Steel in Incremental Sheet Metal Forming. *J. Mater. Res. Technol.* **2014**, *3*, 158–171. [\[CrossRef\]](#)
275. Gatea, S.; Ou, H.; McCartney, G. Review on the Influence of Process Parameters in Incremental Sheet Forming. *Int. J. Adv. Manuf. Technol.* **2016**, *87*, 479–499. [\[CrossRef\]](#)
276. Girjob, C.; Racz, G. Study of the Formability of Laminated Lightweight Metallic Materials. *MATEC Web Conf.* **2017**, *121*, 03008. [\[CrossRef\]](#)

277. Davarpanah, M.A.; Malhotra, R. Formability and Failure Modes in Single Point Incremental Forming of Metal-Polymer Laminates. *Procedia Manuf.* **2018**, *26*, 343–348. [[CrossRef](#)]
278. Harhash, M.; Palkowski, H. Incremental Sheet Forming of Steel/Polymer/Steel Sandwich Composites. *J. Mater. Res. Technol.* **2021**, *13*, 417–430. [[CrossRef](#)]
279. Liu, Z. Heat-Assisted Incremental Sheet Forming: A State-of-the-Art Review. *Int. J. Adv. Manuf. Technol.* **2018**, *98*, 2987–3003. [[CrossRef](#)]
280. Zhu, H.; Ou, H.; Popov, A. Incremental Sheet Forming of Thermoplastics: A Review. *Int. J. Adv. Manuf. Technol.* **2020**, *111*, 565–587. [[CrossRef](#)]
281. Fan, G.; Sun, F.; Meng, X.; Gao, L.; Tong, G. Electric Hot Incremental Forming of Ti-6Al-4V Titanium Sheet. *Int. J. Adv. Manuf. Technol.* **2010**, *49*, 941–947. [[CrossRef](#)]
282. Göttmann, A.; Diettrich, J.; Bergweiler, G.; Bambach, M.; Hirt, G.; Loosen, P.; Poprawe, R. Laser-Assisted Asymmetric Incremental Sheet Forming of Titanium Sheet Metal Parts. *Prod. Eng.* **2011**, *5*, 263–271. [[CrossRef](#)]
283. Amini, S.; Hosseinpour Gollo, A.; Paktinat, H. An Investigation of Conventional and Ultrasonic-Assisted Incremental Forming of Annealed AA1050 Sheet. *Int. J. Adv. Manuf. Technol.* **2017**, *90*, 1569–1578. [[CrossRef](#)]
284. Mohammadi, A.; Vanhove, H.; Van Bael, A.; Duflou, J.R. Towards Accuracy Improvement in Single Point Incremental Forming of Shallow Parts Formed under Laser Assisted Conditions. *Int. J. Mater. Form.* **2016**, *9*, 339–351. [[CrossRef](#)]
285. Ambrogio, G.; Gagliardi, F. Temperature Variation during High Speed Incremental Forming on Different Lightweight Alloys. *Int. J. Adv. Manuf. Technol.* **2015**, *76*, 1819–1825. [[CrossRef](#)]
286. Al-Obaidi, A.; Kräusel, V.; Landgrebe, D. Induction Heating Validation of Dieless Single-Point Incremental Forming of AHSS. *J. Manuf. Mater. Process.* **2017**, *1*, 5. [[CrossRef](#)]
287. Vahdani, M.; Mirnia, M.J.; Bakhshi-Jooybari, M.; Gorji, H. Electric Hot Incremental Sheet Forming of Ti-6Al-4V Titanium, AA6061 Aluminum, and DC01 Steel Sheets. *Int. J. Adv. Manuf. Technol.* **2019**, *103*, 1199–1209. [[CrossRef](#)]
288. Bagudanch, I.; Vives-Mestres, M.; Sabater, M.; Garcia-Romeu, M.L. Polymer Incremental Sheet Forming Process: Temperature Analysis Using Response Surface Methodology. *Mater. Manuf. Process.* **2017**, *32*, 44–53. [[CrossRef](#)]
289. Bagudanch, I.; Garcia-Romeu, M.L.; Centeno, G.; Elías-Zúñiga, A.; Ciurana, J. Forming Force and Temperature Effects on Single Point Incremental Forming of Polyvinylchloride. *J. Mater. Process. Technol.* **2015**, *219*, 221–229. [[CrossRef](#)]
290. Ambrogio, G.; Gagliardi, F.; Conte, R.; Russo, P. Feasibility Analysis of Hot Incremental Sheet Forming Process on Thermoplastics. *Int. J. Adv. Manuf. Technol.* **2019**, *102*, 937–947. [[CrossRef](#)]
291. Conte, R.; Gagliardi, F.; Ambrogio, G.; Filice, F.; Russo, P. Performance Analysis of the Incremental Sheet Forming on PMMA Using a Combined Chemical and Mechanical Approach. *AIP Conf. Proc.* **2017**, *1896*, 080026. [[CrossRef](#)]
292. Sridhar, R.; Rajenthirakumar, D. Polymer Sheet Hot Incremental Forming—An Innovative Polymer Forming Approach. *Polym. Polym. Compos.* **2016**, *24*, 447–454. [[CrossRef](#)]
293. Kulkarni, S.; Sreedhara, V.S.M.; Mocko, G. Heat Assisted Single Point Incremental Forming of Polymer Sheets. In Proceedings of the ASME 2016 International Design Engineering Technical Conferences and Computers and Information in Engineering Conference, Charlotte, NC, USA, 21–24 August 2016; pp. 1–9.
294. Formisano, A.; Durante, M.; Langella, A.; Minutolo, F.M.C. Localized Heat Assisted Incremental Forming of Polycarbonate Sheets by Tool Rotation. In Proceedings of the AIP Conference Proceedings, Vitoria-Gasteiz, Spain, 8–10 May 2019; Volume 2113, p. 110002. [[CrossRef](#)]
295. Al-Obaidi, A.; Graf, A.; Kräusel, V.; Trautmann, M. Heat Supported Single Point Incremental Forming of Hybrid Laminates for Orthopedic Applications. *Procedia Manuf.* **2019**, *29*, 21–27. [[CrossRef](#)]
296. Kurra, S.; Hifzur Rahman, N.; Regalla, S.P.; Gupta, A.K. Modeling and Optimization of Surface Roughness in Single Point Incremental Forming Process. *J. Mater. Res. Technol.* **2015**, *4*, 304–313. [[CrossRef](#)]
297. Sbayti, M.; Bahloul, R.; Belhadjsalah, H. Numerical Modeling of Hot Incremental Forming Process for Biomedical Application. In *Proceedings of the Design and Modeling of Mechanical Systems—III*; Haddar, M., Chaari, F., Benamara, A., Chouchane, M., Karra, C., Aifaoui, N., Eds.; Springer International Publishing: Cham, Germany, 2018; pp. 881–891.
298. Sbayti, M.; Bahloul, R.; BelHadjsalah, H.; Zemzemi, F. Optimization Techniques Applied to Single Point Incremental Forming Process for Biomedical Application. *Int. J. Adv. Manuf. Technol.* **2018**, *95*, 1789–1804. [[CrossRef](#)]
299. Sbayti, M.; Bahloul, R.; Belhadjsalah, H. Simulation of the Local Heating Effect on Incremental Sheet Forming Process. In Proceedings of the Advances in Mechanical Engineering, Materials and Mechanics, Cham, Germany, 26–27 August 2021; Kharrat, M., Baccar, M., Dammak, F., Eds.; Springer International Publishing: Cham, Germany, 2021; pp. 144–151.
300. Mulay, A.; Ben, B.S.; Ismail, S.; Kocanda, A. Prediction of Average Surface Roughness and Formability in Single Point Incremental Forming Using Artificial Neural Network. *Arch. Civ. Mech. Eng.* **2019**, *19*, 1135–1149. [[CrossRef](#)]
301. Şen, I. Lay-Up Optimisation of Fibre Metal Laminates: Development of a Design Methodology for Wing Structures. Ph.D. Thesis, Delft University of Technology, Delft, The Netherlands, 22 October 2015.
302. Razali, N.; Sapuan, S.M.; Razali, N. Mechanical Properties and Morphological Analysis of Roselle/Sugar Palm Fiber Reinforced Vinyl Ester Hybrid Composites. In *Natural Fibre Reinforced Vinyl Ester and Vinyl Polymer Composites*; Sapuan, S.M., Ismail, H., Zainudin, E.S., Eds.; Woodhead Publishing: Sawston, UK, 2018; pp. 169–180.
303. Seretis, G.V.; Kouzilos, G.; Manolakos, D.E.; Provatidis, C.G. On the Graphene Nanoplatelets Reinforcement of Hand Lay-up Glass Fabric/Epoxy Laminated Composites. *Compos. Part B Eng.* **2017**, *118*, 26–32. [[CrossRef](#)]

304. Sinke, J. Manufacturing of GLARE Parts and Structures. *Appl. Compos. Mater.* **2003**, *10*, 293–305. [CrossRef]
305. Patel, P.; Chokshi, S. A review of fabrication methods and stacking sequence arrangements of fiber for composite material. *Int. J. Curr. Eng. Sci. Res.* **2018**, *5*, 13–20.
306. Balasubramanian, K.; Sultan, M.T.H.; Rajeswari, N. Manufacturing techniques of composites for aerospace applications. In *Sustainable Composites for Aerospace Applications*; Jawaid, M., Thariq, M., Eds.; Woodhead Publishing Series in Composites Science and Engineering; Woodhead Publishing: Sawston, UK, 2018; pp. 55–67.
307. Werner, H.O.; Dörr, D.; Henning, F.; Kärger, L. Numerical Modeling of a Hybrid Forming Process for Three-Dimensionally Curved Fiber-Metal Laminates. *AIP Conf. Proc.* **2019**, *2113*, 020019. [CrossRef]
308. Blala, H.; Lang, L.; Khan, S.; Alexandrov, S. Experimental and Numerical Investigation of Fiber Metal Laminate Forming Behavior Using a Variable Blank Holder Force. *Prod. Eng.* **2020**, *14*, 509–522. [CrossRef]
309. Kamaraj, L.; Raja, V.; Nair, V.H.; Sreerag, K.M.; Vishvesvaran, K.M.; Balaji, M. Review on Manufacturing of Fibre Metal Laminates and Its Characterization Techniques. *Int. J. Mech. Eng. Technol.* **2017**, *8*, 561–578.
310. Salve, A.; Kulkarni, R.; Mache, A. A Review: Fiber Metal Laminates (FML's)-Manufacturing, Test Methods and Numerical Modeling. *Int. J. Eng. Technol. Sci.* **2016**, *6*, 71–84. [CrossRef]
311. Subesh, T.; Yogaraj, D.; Ramesh, V. Characterization of Fiber Metal Laminates, Bonding and Manufacturing Methods. *IJITEE* **2019**, *8*, 1062–1065. [CrossRef]
312. Hutchinson, J.R.; Schubel, P.J.; Warrior, N.A. A Cost and Performance Comparison of LRTM and VI for the Manufacture of Large Scale Wind Turbine Blades. *Renew. Energy* **2011**, *36*, 866–871. [CrossRef]
313. Mendikute, J.; Plazaola, J.; Baskaran, M.; Zugasti, E.; Aretxabaleta, L.; Aurrekoetxea, J. Impregnation Quality Diagnosis in Resin Transfer Moulding by Machine Learning. *Compos. Part B Eng.* **2021**, *221*, 108973. [CrossRef]
314. Jensen, B.; Cano, R.; Hales, S.; Alexa, J.A.; Weiser, E.; Loos, A.C.; Johnson, W.S. Fiber Metal Laminates Made by the VARTM Process. Available online: <http://iccm-central.org/Proceedings/ICCM17proceedings/Themes/Manufacturing/MANUFACTURING%20TECH/C3.2%20Jensen.pdf> (accessed on 5 July 2021).
315. Shah, M.; Chaudhary, V. Flow Modeling and Simulation Study of Vacuum Assisted Resin Transfer Molding (VARTM) Process: A Review. *IOP Conf. Ser. Mater. Sci. Eng.* **2020**, *872*, 012087. [CrossRef]
316. Hancioglu, M.; Sozer, E.M.; Advani, S.G. Comparison of In-Plane Resin Transfer Molding and Vacuum-Assisted Resin Transfer Molding 'Effective' Permeabilities Based on Mold Filling Experiments and Simulations. *J. Reinf. Plast. Compos.* **2020**, *39*, 31–44. [CrossRef]
317. Technologia RTM—Buster. Available online: <http://bustergfc.pl/technologie/technologie-rtm/> (accessed on 25 June 2021).
318. Seydibeyoğlu, M.Ö.; Dođru, A.; Kandemir, M.B.; Aksoy, Ö. Lightweight Composite Materials in Transport Structures. In *Lightweight Polymer Composite Structures*; CRC Press: Boca Raton, FL, USA, 2020.
319. Brouwer, W.D.; van Herpt, E.C.F.C.; Labordus, M. Vacuum Injection Moulding for Large Structural Applications. *Compos. Part A Appl. Sci. Manuf.* **2003**, *34*, 551–558. [CrossRef]
320. Zisimopoulos, D.A. Use of Fiber Reinforced Plastics in Ship Construction: A Study of SOLAS Regulation II-2/17 on Alternative Design and Arrangements for Fire Safety. Available online: <https://core.ac.uk/reader/38467591> (accessed on 14 June 2021).
321. Laurenzi, S.; Marchetti, M. Advanced Composite Materials by Resin Transfer Molding for Aerospace Applications. In *Composites and Their Properties*; Hu, N., Ed.; IntechOpen: London, UK, 2012.
322. Light RTM Process (LRTM). Available online: <https://www.rtmcomposites.com/process/light-rtm-lrtm> (accessed on 26 June 2021).
323. Huang, Z.M.; Lee, S.Y.; Kim, H.M.; Youn, J.R.; Song, Y.S. Three-Dimensional Numerical Simulation for Resin Transfer Molding of Automotive Wheel. *Korea-Aust. Rheol. J.* **2019**, *31*, 141–147. [CrossRef]
324. Agwa, M.; Youssef, S.M.; Ali-Eldin, S.S.; Megahed, M. Integrated Vacuum Assisted Resin Infusion and Resin Transfer Molding Technique for Manufacturing of Nano-Filled Glass Fiber Reinforced Epoxy Composite. *J. Ind. Text.* **2020**. [CrossRef]
325. Hergan, P.; Li, Y.; Zaloznik, L.; Kaynak, B.; Arbeiter, F.; Fauster, E.; Schledjewski, R. Using (VA)RTM with a Rigid Mould to Produce Fibre Metal Laminates with Proven Impact Strength. *J. Manuf. Mater. Process.* **2018**, *2*, 38. [CrossRef]
326. Polowick, C. Optimizing Vacuum Assisted Resin Transfer Moulding (VARTM) Processing Parameters to Improve Part Quality. Master's Thesis, Carleton University, Ottawa, ON, Canada, 2013.
327. Kozioł, M.; Ślężiona, J. Charakterystyka płyt kompozytowych wytworzonych metodą RTM ze zszywanych preform włókna szklanego. *Inżynieria Mater.* **2008**, *29*, 109–113.
328. Pishvar, M.; Amirkhosravi, M.; Altan, M.C. Effect of autoclave cure pressure on mechanical properties and void characteristics of composite laminates. In Proceedings of the 36th Oklahoma AIAA/ASME Symposium, Norman, OK, USA, 16 April 2016.
329. Tryzna, P. Technologie Wytwarzania Kompozytów Polimerowych cz.2. Available online: http://www.baltazarkompozyty.pl/index.php?option=com_content&view=article&id=225&catid=39&Itemid=215 (accessed on 25 June 2021).
330. Bader, M.G. Selection of Composite Materials and Manufacturing Routes for Cost-Effective Performance. *Compos. Part A Appl. Sci. Manuf.* **2002**, *33*, 913–934. [CrossRef]
331. Centea, T.; Grunenfelder, L.K.; Nutt, S.R. A Review of Out-of-Autoclave Prepregs—Material Properties, Process Phenomena, and Manufacturing Considerations. *Compos. Part A Appl. Sci. Manuf.* **2015**, *70*, 132–154. [CrossRef]

332. Lee, J.; Ni, X.; Daso, F.; Xiao, X.; King, D.; Gómez, J.S.; Varela, T.B.; Kessler, S.S.; Wardle, B.L. Advanced Carbon Fiber Composite Out-of-Autoclave Laminate Manufacture via Nanostructured out-of-Oven Conductive Curing. *Compos. Sci. Technol.* **2018**, *166*, 150–159. [CrossRef]
333. Severijns, C.; de Freitas, S.T.; Poulis, J.A. Susceptor-Assisted Induction Curing Behaviour of a Two Component Epoxy Paste Adhesive for Aerospace Applications. *Int. J. Adhes. Adhes.* **2017**, *75*, 155–164. [CrossRef]
334. Mahdi, S.; Kim, H.-J.; Gama, B.A.; Yarlagadda, S.; Gillespie, J.W. A Comparison of Oven-Cured and Induction-Cured Adhesively Bonded Composite Joints. *J. Compos. Mater.* **2003**, *37*, 519–542. [CrossRef]
335. Joseph, C.; Viney, C. Electrical Resistance Curing of Carbon-Fibre/Epoxy Composites. *Compos. Sci. Technol.* **2000**, *60*, 315–319. [CrossRef]
336. Glauser, T.; Johansson, M.; Hult, A. A Comparison of Radiation and Thermal Curing of Thick Composites. *Macromol. Mater. Eng.* **2000**, *274*, 25–30. [CrossRef]
337. Tanrattanakul, V.; Jaroendee, D. Comparison between Microwave and Thermal Curing of Glass Fiber–Epoxy Composites: Effect of Microwave-Heating Cycle on Mechanical Properties. *J. Appl. Polym. Sci.* **2006**, *102*, 1059–1070. [CrossRef]
338. Nightingale, C.; Day, R.J. Flexural and Interlaminar Shear Strength Properties of Carbon Fibre/Epoxy Composites Cured Thermally and with Microwave Radiation. *Compos. Part A Appl. Sci. Manuf.* **2002**, *33*, 1021–1030. [CrossRef]
339. Li, J.; Ben, G.; Yang, J. Fabrication of Hemp Fiber-Reinforced Green Composites with Organoclay-Filled Poly(Butylene Succinate) Matrix by Pultrusion Process. *Sci. Eng. Compos. Mater.* **2014**, *21*, 289–294. [CrossRef]
340. Cui, H. Glass Fiber Reinforced Biorenewable Polymer Composites and the Fabrication with Pultrusion Process. Ph.D. Thesis, Iowa State University, Ames, IA, USA, 2013.
341. Vedernikov, A.; Safonov, A.; Tucci, F.; Carlone, P.; Akhatov, I. Pultruded Materials and Structures: A Review. *J. Compos. Mater.* **2020**, *54*, 4081–4117. [CrossRef]
342. Fairuz, A.M.; Sapuan, S.M.; Zainudin, E.S.; Jaafar, C.N.A. Polymer composite manufacturing using a pultrusion process: A review. *Am. J. Appl. Sci.* **2014**, *11*, 1798–1810. [CrossRef]
343. Sandberg, M.; Yuksel, O.; Comminal, R.B.; Sonne, M.R.; Jabbari, M.; Larsen, M.; Salling, F.B.; Baran, I.; Spangenberg, J.; Hattel, J.H. Numerical modeling of the mechanics of pultrusion. In *Mechanics of Materials in Modern Manufacturing Methods and Processing Techniques*; Silberschmidt, V.V., Ed.; Elsevier: Amsterdam, The Netherlands, 2020; pp. 173–195.
344. Biswas, B.; Bandyopadhyay, N.R.; Sinha, A. Chapter 16—Mechanical and Dynamic Mechanical Properties of Unsaturated Polyester Resin-Based Composites. In *Unsaturated Polyester Resins*; Thomas, S., Hosur, M., Chirayil, C.J., Eds.; Elsevier: Amsterdam, The Netherlands, 2019; pp. 407–434.
345. Zamri, M.H.; Osman, M.R.; Akil, H.M.; Shahidan, M.H.A.; Mohd Ishak, Z.A. Development of Green Pultruded Composites Using Kenaf Fibre: Influence of Linear Mass Density on Weathering Performance. *J. Clean. Prod.* **2016**, *125*, 320–330. [CrossRef]
346. Zamri, M.H.; Akil, H.M.; Ishak, Z.A.M.; Bakar, A.A. Effect of Different Fiber Loadings and Sizes on Pultruded Kenaf Fiber Reinforced Unsaturated Polyester Composites. *Polym. Compos.* **2015**, *36*, 1224–1229. [CrossRef]
347. Zamri, M.H.; Akil, H.M.; MohdIshak, Z.A. Pultruded Kenaf Fibre Reinforced Composites: Effect of Different Kenaf Fibre Yarn Tex. *Procedia Chem.* **2016**, *19*, 577–585. [CrossRef]
348. Hashemi, F.; Tahir, P.M.; Madsen, B.; Jawaid, M.; Majid, D.; Brancheriau, L.; Juliana, A. Volumetric Composition and Shear Strength Evaluation of Pultruded Hybrid Kenaf/Glass Fiber Composites. *J. Compos. Mater.* **2016**, *50*, 2291–2303. [CrossRef]
349. Zakaria, K.Z.; Akil, H.M.; Shamsuddin, M.S.M.; Ishak, Z.A.M. Mechanical Performance of Pultruded Kenaf/Glass Hybrid Fiber Reinforced Unsaturated Polyester under Hygrothermal Conditions. *AIP Conf. Proc.* **2020**, *2267*, 020045. [CrossRef]
350. Hashemi, F.; Brancheriau, L.; Tahir, P.M. Hybridization and Yarns Configuration Effects on Flexural Dynamic and Static Properties of Pultruded Hybrid Kenaf/Glass Fiber Composites. *Compos. Part A Appl. Sci. Manuf.* **2018**, *112*, 415–422. [CrossRef]
351. Uawongsuwan, P.; Yang, Y.; Hamada, H. Long Jute Fiber-Reinforced Polypropylene Composite: Effects of Jute Fiber Bundle and Glass Fiber Hybridization. *J. Appl. Polym. Sci.* **2015**, *132*. [CrossRef]
352. Akil, H.M.; Santulli, C.; Sarasini, F.; Tirillò, J.; Valente, T. Environmental Effects on the Mechanical Behaviour of Pultruded Jute/Glass Fibre-Reinforced Polyester Hybrid Composites. *Compos. Sci. Technol.* **2014**, *94*, 62–70. [CrossRef]
353. Zamri, M.H.; Akil, H.M.; Bakar, A.A.; Ishak, Z.A.M.; Cheng, L.W. Effect of Water Absorption on Pultruded Jute/Glass Fiber-Reinforced Unsaturated Polyester Hybrid Composites. *J. Compos. Mater.* **2012**, *46*, 51–61. [CrossRef]
354. Singh, J.; Kumar, M.; Kumar, S.; Mohapatra, S.K. Properties of Glass-Fiber Hybrid Composites: A Review. *Polym. Plast. Technol. Eng.* **2017**, *56*, 455–469. [CrossRef]
355. Aldoumani, N.; Giannetti, C.; Abdallah, Z.; Belblidia, F.; Khodaparast, H.H.; Friswell, M.I.; Sienz, J. Optimisation of the Filament Winding Approach Using a Newly Developed In-House Uncertainty Model. *Eng* **2020**, *1*, 122–136. [CrossRef]
356. Boon, Y.D.; Joshi, S.C.; Bhudolia, S.K. Review: Filament Winding and Automated Fiber Placement with In Situ Consolidation for Fiber Reinforced Thermoplastic Polymer Composites. *Polymers* **2021**, *13*, 1951. [CrossRef] [PubMed]
357. Mansour, G.; Kyratsis, P.; Korlos, A.; Tzetzis, D. Investigation into the Effect of Cutting Conditions in Turning on the Surface Properties of Filament Winding GFRP Pipe Rings. *Machines* **2021**, *9*, 16. [CrossRef]
358. Faria, H. Analytical and Numerical Modelling of the Filament Winding Process. Available online: <https://www.iccm-central.org/Proceedings/ICCM17proceedings/Themes/Manufacturing/MANUFACTURING%20TECH/C3.5%20Faria.pdf> (accessed on 8 July 2021).

359. Deng, B.; Shi, Y.; Yu, T.; Zhao, P. Influence Mechanism and Optimization Analysis of Technological Parameters for the Composite Prepreg Tape Winding Process. *Polymers* **2020**, *12*, 1843. [CrossRef] [PubMed]
360. Tele, D.; Wakhare, N.; Bhosale, R.; Bharde, P.; Nerkar, S. A Review on Design and Development of Filament Winding Machine for Composite Materials. *Int. J. Curr. Eng. Technol.* **2016**, *6*, 74–77.
361. Shen, C.; Han, X. Damage and Failure Analysis of Filament Wound Composite Structure Considering Fibre Crossover and Undulation. *Adv. Compos. Lett.* **2018**, *27*, 096369351802700202. [CrossRef]
362. Li, S.; Soden, P.D.; Reid, S.R.; Hinton, M.J. Indentation of Laminated Filament-Wound Composite Tubes. *Composites* **1993**, *24*, 407–421. [CrossRef]
363. Zhao, L.; Mantell, S.C.; Cohen, D.; McPeak, R. Finite element modeling of the filament winding process. *Compos. Struct.* **2001**, *52*, 499–510. [CrossRef]
364. Nptel, Online Courses and Certification. Available online: <https://nptel.ac.in/content/storage2/courses/101104010/downloads/Lecture7.pdf> (accessed on 26 June 2021).
365. Hand Lay-Up Process Advantages and Disadvantages. Available online: <https://www.unicomposite.com/hand-lay-up-process-advantages-and-disadvantages/> (accessed on 26 June 2021).
366. Shramstad, J.D. *Evaluation of Hand Lay-Up and Resin Transfer Molding in Composite Wind Turbine Blade Manufacturing*; Montana State University-Bozeman: Bozeman, MT, USA, 1999.
367. Park, S.-J.; Seo, M.-K. Element and Processing. In *Interface Science and Technology*; Park, S.-J., Seo, M.-K., Eds.; Elsevier: Amsterdam, The Netherlands, 2011; pp. 431–499.
368. Dai, J.; Pellaton, D.; Hahn, H.T. A Comparative Study of Vacuum-Assisted Resin Transfer Molding (VARTM) for Sandwich Panels. *Polym. Compos.* **2003**, *24*, 672–685. [CrossRef]
369. Dong, C.J. Development of a Process Model for the Vacuum Assisted Resin Transfer Molding Simulation by the Response Surface Method. *Compos. Part A Appl. Sci. Manuf.* **2006**, *37*, 1316–1324. [CrossRef]
370. Sun, X.; Li, S.; Lee, L.J. Mold Filling Analysis in Vacuum-Assisted Resin Transfer Molding. Part I: SCRIMP Based on a High-Permeable Medium. *Polym. Compos.* **1998**, *19*, 807–817. [CrossRef]
371. Hughes, W.J. *Overview of Vacuum-Assisted Resin Transfer Molding Processing*; U.S. Department of Transportation Federal Aviation Administration: Washington, DC, USA, 2013; p. 69.
372. Resin Transfer Moulding—Light (RTM-Light)|Sirris Leuven-Gent Composites Application Lab. Available online: <http://www.slc-lab.be/services/process-equipment/rtm-light/resin-transfer-moulding-%E2%80%93-light-rtm-light> (accessed on 26 June 2021).
373. McGrane, R.A. Vacuum Assisted Resin Transfer Molding of Foam Sandwich Composite Materials: Process Development and Model Verification. Master's Thesis, Virginia Polytechnic Institute and State University, Blacksburg, VA, USA, 2001.
374. Liu, S.; Lang, L.; Sherkatghanad, E.; Wang, Y.; Xu, W. Investigation into the Fiber Orientation Effect on the Formability of GLARE Materials in the Stamp Forming Process. *Appl. Compos. Mater.* **2018**, *25*, 255–267. [CrossRef]
375. Sumana, B.; Vidya Sagar, H.; Sharma, K.; Krishna, M. Numerical Analysis of the Effect of Fiber Orientation on Hydrostatic Buckling Behavior of Fiber Metal Composite Cylinder. *J. Reinf. Plast. Compos.* **2015**, *34*, 1422–1432. [CrossRef]
376. Zhang, R.; Lang, L.; Zafar, R.; Lin, L.; Zhang, W. Investigation into Thinning and Spring Back of Multilayer Metal Forming Using Hydro-Mechanical Deep Drawing (HMDD) for Lightweight Parts. *Int. J. Adv. Manuf. Technol.* **2016**, *82*, 817–826. [CrossRef]
377. Hu, Y.; Zheng, X.; Wang, D.; Zhang, Z.; Xie, Y.; Yao, Z. Application of Laser Peen Forming to Bend Fibre Metal Laminates by High Dynamic Loading. *J. Mater. Process. Technol.* **2015**, *226*, 32–39. [CrossRef]
378. Blala, H.; Lang, L.; Sherkatghanad, E.; Li, L. An Investigation into Process Parameters Effect on the Formability of GLARE Materials Using Stamp Forming. *Appl. Compos. Mater.* **2019**, *26*, 1423–1436. [CrossRef]
379. Blala, H.; Lang, L.; Li, L.; Khan, S.; Alexandrov, S. Process Control Improvement in Deep Drawing of Hemispherical Cups Made of GLARE Material. *MATEC Web Conf.* **2020**, *319*, 04003. [CrossRef]
380. Glushchenkov, V.; Chernikov, D.; Erisov, Y.; Petrov, I.; Alexandrov, S.; Lang, L.H. Electro-Magnetic Forming of Fiber Metal Laminates. In *Key Engineering Materials*; Trans Tech Publications Ltd.: Aedermannsdorf, Switzerland, 2019; Volume 794, pp. 107–112. [CrossRef]
381. Khardin, M.; Harhash, M.; Chernikov, D.; Glushchenkov, V.; Palkowski, H. Preliminary Studies on Electromagnetic Forming of Aluminum/Polymer/Aluminum Sandwich Sheets. *Compos. Struct.* **2020**, *252*, 112729. [CrossRef]
382. Zafar, R.; Lihui, L.; Rongjing, Z. Analysis of Hydro-Mechanical Deep Drawing and the Effects of Cavity Pressure on Quality of Simultaneously Formed Three-Layer Al Alloy Parts. *Int. J. Adv. Manuf. Technol.* **2015**, *80*, 2117–2128. [CrossRef]
383. Zafar, R.; Lang, L.; Zhang, R. Experimental and Numerical Evaluation of Multilayer Sheet Forming Process Parameters for Light Weight Structures Using Innovative Methodology. *Int. J. Mater. Form.* **2016**, *9*, 35–47. [CrossRef]
384. Blala, H.; Lang, L.; Li, L.; Sherkatghanad, E.; Alexandrov, S. Investigation on the Effect of Blank Holder Gap in the Hydroforming of Cylindrical Cups, Made of Fiber Metal Laminate. *Int. J. Adv. Manuf. Technol.* **2020**, *108*, 2727–2740. [CrossRef]
385. Gisario, A.; Barletta, M. Laser Forming of Glass Laminate Aluminium Reinforced Epoxy (GLARE): On the Role of Mechanical, Physical and Chemical Interactions in the Multi-Layers Material. *Opt. Lasers Eng.* **2018**, *110*, 364–376. [CrossRef]
386. Gisario, A.; Mehrpouya, M.; Rahimzadeh, A.; De Bartolomeis, A.; Barletta, M. Prediction Model for Determining the Optimum Operational Parameters in Laser Forming of Fiber-Reinforced Composites. *Adv. Manuf.* **2020**, *8*, 242–251. [CrossRef]

387. Land, P.; Crossley, R.; Branson, D.; Ratchev, S. Technology Review of Thermal Forming Techniques for Use in Composite Component Manufacture. *SAE Int. J. Mater. Manuf.* **2016**, *9*, 81–89. [[CrossRef](#)]
388. Tatsuno, D.; Yoneyama, T.; Kawamoto, K.; Okamoto, M. Hot Press Forming of Thermoplastic CFRP Sheets. *Procedia Manuf.* **2018**, *15*, 1730–1737. [[CrossRef](#)]
389. Chen, Y. Elevated-Temperature Deformation and Forming of Aluminum-Matrix Composites. Ph.D. Thesis, Ohio State University, Columbus, OH, USA, 1991.
390. Saraiva, F. Development of Press Forming Techniques for Thermoplastic Composites: Investigation of a Multiple Step Forming Approach. Master's Thesis, Delft University of Technology, Delft, The Netherlands, 2017.
391. Thirukumaran, M.; Siva, I.; Jappes, J.W.; Manikandan, V. Forming and Drilling of Fiber Metal Laminates—A Review. *J. Reinf. Plast. Compos.* **2018**, *37*, 981–990. [[CrossRef](#)]
392. Rajabi, A.; Kadkhodayan, M.; Manoochchri, M.; Farjadfar, R. Deep-Drawing of Thermoplastic Metal-Composite Structures: Experimental Investigations, Statistical Analyses and Finite Element Modeling. *J. Mater. Process. Technol.* **2015**, *215*, 159–170. [[CrossRef](#)]
393. Saadatfard, A.; Gerdooei, M.; Jalali Aghchai, A. Drawing Potential of Fiber Metal Laminates in Hydromechanical Forming: A Numerical and Experimental Study. *J. Sandw. Struct. Mater.* **2020**, *22*, 1386–1403. [[CrossRef](#)]
394. Mennecart, T.; Gies, S.; Ben Khalifa, N.; Tekkaya, A.E. Analysis of the Influence of Fibers on the Formability of Metal Blanks in Manufacturing Processes for Fiber Metal Laminates. *J. Manuf. Mater. Process.* **2019**, *3*, 2. [[CrossRef](#)]
395. Bell, C.; Corney, J.; Zuelli, N.; Savings, D. A State of the Art Review of Hydroforming Technology: Its Applications, Research Areas, History, and Future in Manufacturing. *Int. J. Mater. Form.* **2020**, *13*, 789–828. [[CrossRef](#)]
396. Abdullah, M.R.; Cantwell, W.J. The High-Velocity Impact Response of Thermoplastic–Matrix Fibre–Metal Laminates. *J. Strain Anal. Eng. Des.* **2012**, *47*, 432–443. [[CrossRef](#)]
397. Kalyanasundaram, S.; DharMalingam, S.; Venkatesan, S.; Sexton, A. Effect of Process Parameters during Forming of Self Reinforced—PP Based Fiber Metal Laminate. *Compos. Struct.* **2013**, *97*, 332–337. [[CrossRef](#)]
398. Mosse, L.; Compston, P.; Cantwell, W.J.; Cardew-Hall, M.; Kalyanasundaram, S. The Effect of Process Temperature on the Formability of Polypropylene Based Fibre–Metal Laminates. *Compos. Part A Appl. Sci. Manuf.* **2005**, *36*, 1158–1166. [[CrossRef](#)]
399. Mosse, L.; Compston, P.; Cantwell, W.J.; Cardew-Hall, M.; Kalyanasundaram, S. Stamp Forming of Polypropylene Based Fibre–Metal Laminates: The Effect of Process Variables on Formability. *J. Mater. Process. Technol.* **2006**, *172*, 163–168. [[CrossRef](#)]
400. Liu, S.; Lang, L.; Guan, S.; Alexandrov, S.; Zeng, Y. Investigation into Composites Property Effect on the Forming Limits of Multi-Layer Hybrid Sheets Using Hydroforming Technology. *Appl. Compos. Mater.* **2019**, *26*, 205–217. [[CrossRef](#)]
401. Blala, H.; Lang, L.; Khan, S.; Li, L.; Alexandrov, S. An Analysis of Process Parameters in the Hydroforming of a Hemispherical Dome Made of Fiber Metal Laminate. *Appl. Compos. Mater.* **2021**, *28*, 685–704. [[CrossRef](#)]
402. Glushchenkov, V. Pulse-Magnetic Processing of Materials—Development—Problems and Solution Techniques. *Key Eng. Mater.* **2016**, *684*, 511–514. [[CrossRef](#)]